Republic of Iraq
Ministry of Higher Education
and Scientific Research
Babylon University
College of Materials Engineering
Department of Metallurgical Engineering

Investigation the Corrosion and Wear Behavior of the First Generation and Second Generation of Titanium Biomaterials

A Thesis
Submitted to the Council of the College of Materials Engineering / University of Babylon in Partial Fulfillment of the Requirements for the Master Degree in Materials Engineering / Metallurgy

By
Manar Abdulameer Hussein Hassan

Supervised by
Assist. Prof. Dr. Zuheir Talib Khulief

2022 A.D **1443 A.H**

بِسْمِ اللَّهِ الرَّحْمَٰنِ الرَّحِيمِ

﴿ فَتَعَالَى اللَّهُ الْمَلِكُ الْحَقُّ وَلَا تَعْجَلْ بِالْقُرْآنِ مِنْ قَبْلِ أَنْ يُقْضَى إِلَيْكَ وَحْيُهُ وَقُلْ رَبِّ زِدْنِي عِلْمًا ﴾

صدَقَ آلله العليّ العظيم

سورة طه(114)

Supervisor Certificates

I am Certify that this thesis, entitled **(Investigation the Second Generation of Titanium Biomaterials)** was prepared by **(Manar Abdulameer AL-Musawi)** under our supervision at the department of metallurgy engineering / College of Materials Engineering / University of Babylon in Partial fulfillment of the requirements for the degree of Master in Material's Engineering/Metallurgy.

Signature :

Name of Supervisor : Asst. Prof. Dr. Zuheir Talib Khulief

Date: / / 2022

Dedication:

This study is wholeheartedly dedicated to my beloved parents, who have been my source of inspiration and gave me strength when I thought of giving up, who continually provide their moral, spiritual, emotional, and financial support.

To my brothers, sisters, friends, who shared their words of advice and encouragement to finish this study.

And lastly, I dedicated this study to Almighty God, thank you for the guidance, strength, power of mind, protection and skills.

All of these, I offer to you.

With my respect and love

Manar Abdulameer AL-Musawi

2022

Acknowledgement

In the name of Allah, the most gracious, the most merciful. First of all, great thanks are to (ALLAH his MAJESTY) for enabling me to finish this study, my sincere appreciation and deepest gratitude is to Department of Metallurgical Engineering and Asst. Prof. Dr. Zuheir Talib Khulief whom I had the honor of being under their guidance and supervision, their constructive suggestion, patience and continuous encouragement are highly acknowledged through this study. Special thanks for my family , my friends for supporting me through the time of study.

Manar Abdulameer AL-Musawi

2022

Abstract

This investigation was mainly aimed to systematic investigate the microstructure, electrochemical properties, and tribological properties of the second-generation β-titanium alloys. Three different second–generation titanium– based alloys Ti–15 Mo, Ti–13Zr–13Nb and Ti–8Mo–4Nb–2Zr were used in this investigation. In addition, traditionally used Cp-Ti with α – microstructure and the first generation Ti–6Al-4V with α+β microstructure were used for comparison.

The surface morphology, structure and mechanical behavior of the titanium alloy used in this investigation were characterized using X- ray Diffraction (XRD), Optical Microscopy (OM),Field Emission Scanning Electron Microscopy (FESEM), micro-hardness measurements and elastic modulus measurements. XRD, OM, and FESEM analysis showed that the Ti-15Mo consisted of two phases α +β known as metastable β phase, Ti-13Zr-13Nb consisted predominantly of β – phase and α – phase in some regions known as β-rich, and Ti-8Mo-4Nb-2Zr consisted of single-phase β – phase. Cp- Ti consisted of single phase α–phase and Ti-6Al-4V consisted of two phases α + β as expected. In term of mechanical properties Ti-8Mo-4Nb-2Zr alloy had the lowest elastic modulus of 102 GPa, and average Vickers micro–hardness higher than others did.

Also in term of corrosion resistance Ti-8Mo-4Nb-2Zr alloy exhibited lowest corrosion rate than others alloys.

The tribological behavior was investigated at normal loads of 10 and 20N. Generally, the total removed wear volume and coefficient of friction increased with increase the load from 10 to 20N in this investigation. However, the rate of depassivation/repassivation influenced the tribological behavior of titanium alloys. Thus, the Ti-

8Mo-4Nb-2Zr alloy exhibited decrease in total removed wear volume with increase the loads. The first generation Ti-6Al-4V alloy showed lower total removed wear volume and lower coefficient of friction during the wear test as compared to others. The tribological mechanism is a predominantly abrasive wear mechanism. However, considering the biomedical applications, the second- generation β-microstructure Ti-8Mo-4Nb-2Zr could be a good candidate with relatively good corrosion resistance, low elastic modulus, comparable wear behavior and non-toxic elements.

List of abbreviation and symbol

Abbreviations:

Abbreviation	*Expression*
ASTM	American Society for Testing and Materials
BCC	body centered cubic
CE	counter electrode
COF	coefficient of friction
EDX	energy dispersive X-ray spectrometer
ELI	Extra-Low-Interstitials
e.m.f	An electro motive force
FESEM	Field Emission Scanning Electron Microscopy
HCP	hexagonal close packed
HFT	High Field Theory
Hv	micro – Vickers hardness
OCP	open circuit potential technique
OM	optical microscopy
PD	Potentiodynamic polarization
PDM	Point Defect Model
PS	potentiostatic polarization
RE	reference electrode
SCE	standard calomel electrode
SLM	selective laser melting
THR	
UHMWPE	Ultra-high molecular weight polyethylene
UTS	ultimate tensile strength
WE	working electrode
XRD	X-ray diffraction
XRF	X-Ray fluoresce

Symbols:

Symbol	Expression	Unit
E_{corr}	Corrosion potential	V
E_{pp}	passivation potential	V
i_{pp}	passive current density	μA/ m²
Eb	potential will reach its breaking point	V
Er	re-passivation potential	V
i_{corr}	corrosion current density	μA/ m²
μ	friction coefficient between any two surfaces that come into contact	-
Ft	tangential force	N
F_n	normal applied load throughout the wear test	N
F_a	adhesive friction force	N
F_d	deformation friction force	N
V	volume loss throughout the wear test	mm^3
K	wear coefficient	-
L	overall distance of sliding throughout the wear test	mm
k′	dimensional wear coefficient	$(mm^3N^{-1}m^{-1})$
λ	severity of lubricated sliding asperity contact	mm^2
t_{min}	minimal layer thickness	mm
$\sigma*$	rubbing surface's root mean square surface roughness	μm
Rq_1^2	initial surface's mean square surface roughness value	μm
Rq_2^2	second surface's mean square surface roughness	μm
ω	relative speed of the two surfaces	mm/s
P	contact pressure inverse	N/m
η	lubricant viscosity	Pa.s
E	elastic moduli	Gpa
ρ	alloy's density	(g/cm^3)
V_L	velocity of a longitudinal	mm/s

	ultrasonic wave	
VS	velocity of a shear ultrasonic wave	mm/s
t_L	transit time of a longitudinal ultrasonic wave	sec
t_S,	transit time of a shear ultrasonic wave	sec
l	sample thickness	mm
mpy	corrosion rate	(mils per year)
E.W	equivalent weight for alloy elements	(g/eq.)
A	surface area exposed to the corrosion media	(cm^2)

Content:

Chapter One/ Introduction

1.1. General Introduction and Motivation……..……..…1

1.2. Biomedical materials:Biomedical materials……..3

1.2.1. Orthopedic Biomaterials ……4

1.3. Objectives of This Investigation:…. ……..……..……5

Chapter Two/Theoretical Part

2.1.General View……..…...…6

2.2. Biomaterials …….…...6

2.2.1.Metallic Biomaterials' Evolution Throughout History.…...…9

2.2.2.Fundamental Factors to Consider in the Selection and Metallic Implants Design…….…….12

2.2.2.1. Biocompatibility..……..……..……..…...13

2.2.2.2 Corrosion Resistance…….……....15

2.2.2.3 Mechanical Resistance……..…...16

2.2.2.4 Wear Resistance…….....…17

2.2.2.5.Osseointergration……..…….....20

2.3 Titanium.……20

2.3.1 Titanium's General Properties…….....20

2.3.2. Crystals Structure of Titanium……..…….....21

2.3.3 Titanium Alloys……....21

2.3.3.1 Near α and α- Titanium Alloys……...……..22

2.3.3.2 α-β Phase Titanium Alloys……..…….23

2.3.3.3 Second-Generation β-Titanium……..…….....23

2.3.4. Phase diagram of Titanium alloys used……..24

2.3.5. Alloying Elements Biocompatibility…….…….26
2.4 Corrosion Behavior ……..……28
2.4.1 Electrochemical Techniques for Corrosion Study……...32
2.4.1.1 Open Circuit Potential (OCP)…….33
2.4.1.2 Potentiodynamic Polarization (PD)…….…...34
2.4.1.3.Ptentistatic Polarization(PS)……..…….....35
2.4.2 Mechanisms of Corrosion…….……36
2.4.3 Corrosion of Titanium Alloys ……..37
2.5 Tribology Behavior…..……..39
2.5.1 Friction……..39
2.5.1.1.The Coefficient of Friction……..……..39
2.5.1.2 Frictional Components……..39
2.5.2 Wear Phenomenon……...…..…40
2.5.2.1.Wear Mechanisms…….…41
2.5.3 Lubrication……..…….…42
2.5.4 Techniques for Tribological Testing and Characterization...44
2.5.5 Tribology of Titanium Alloys……..……..……45
2.6 Literature Review……..46
2.6.1 Literature Review about Corrosion……,……46
2.6.2 Literature Review about Wear……..50
2.6.3 Literature Review about Elastic Modulus……53
2.6.4. Conclusion of The Peppers……..……55

Chapter Three/ Experimental Part

3.1.General View……..……....56
3.2. Used Alloys……..……....58

3.3 Titanium Alloys Characterization...……...…...59

3.3.1 Microstructural Investigation……..59

3.3.1.1 Alloys Preparation……..….59

3.3.1.2 X-Ray Diffraction Analysis (XRD)……60

3.3.1.3 Optical Microscopy Analysis (OM)..……...61

3.3.1.4. Field Emission Scanning Electron Microscopy (FESEM)……..61

3.3.2 Mechanical Properties……61

3.3.2.1 Micro-Hardness Test…….……61

3.3.2.2 Elastic Modulus by Ultrasound Technique……61

3.3.3 In Vitro Tests……..62

3.3.3.1 Electrochemical Test……..62

3.3.3.1.2 Electrochemical Media…….62

3.3.3.1.3 Electrochemical Test……63

3.3.3.1.3.1 Open Circuit Potential (OCP) Measurement……63

3.3.3.1.3.2 Potentiodynamic Measurements……64

3.3.3.1.4 Metals Ions Release Test……...64

3.3.3.1.5 Tribology Test...……65

3.3.4.1 Wear Track Analysis……66

3.3.4.1.1 Worn Surface Characterization ……66

3.3.4.1.1.1 Optical Microscopy Analysis ……...66

3.3.4.1.1.2 Surface Roughness Calculation……66

Chapter Four /Result and Discussions

4.1.General View……..…..67

4.2. Microstructure and Phase Constitution of Titanium Alloys used in this Investigation …….……..…….….67

4.3. Mechanical Characterization……73

4.3.1. Modulus of Elasticity……..…73

4.3.2. Vickers Micro-Hardness …….……...….....74

4.4 In Vitro Tests ……..……75

4.4.1 Electrochemical Test ……..…75

4.4.1.1.Open Circuit Potential Examination (OCP) and Ptentiodynamic Polarization test ……..…75

4.4.1.2 Ion Release…….....78

4.5. Tribological Behaviors……..….79

4.5.1. Lubricated Sliding Friction..……..……79

4.5.2. Wear Track Morphology and Roughness…….87

4.5.3. Total Removed Wear Volume ……..…90

Chapter Five/ Conclusions and Suggestions

5.1.Conclusions……...93

5.2.Suggestions…….…….....95

Reference……...……..…96

Appendices……118

Chapter One

Introduction

1.1. General Introduction and Motivation:

Titanium and Ti-alloys have been intensively investigated in the last few decades because of their distinctive properties, such as high biocompatibility, low density, high specific strength, excellent corrosion resistance and low Young's modulus **[1-3].** Titanium alloys are commonly used as replacements in artificial bones in the human body, dental implants and joints **[3]**.

Commercial pure titanium Cp-Ti, with α-phase type structure, was primarily used in some orthopedic and dental applications without producing toxicity during service in the human body **[1, 4-6]**. However, the mechanical properties of commercial pure titanium Cp-Ti are unsuitable for some applications that need wear resistance and high strength **[7, 8]**. Hence, to tackle this problem, Ti-alloys have been developed to increase their strength **[9].** To meet the requirements of biomaterial for biomedical applications, commercial pure titanium Cp-Ti was replaced by the first generation titanium alloys Ti-6Al-4V with β+α phases **[10]**. Nevertheless, it was reported that the release of vanadium and aluminum ions from Ti-6Al-4V alloy throughout a long time use, might causes long-term health problems. For examples osteomalacia, Alzheimer's diseases, neurological disorders, peripheral neuropath. In addition, these alloying elements can retard osseointegration after the transplant process, meaning that there is a delay in the integration of the bones **[7, 9, 11, 12]**.

While numerous investigates focused on some of the favorite properties of commercially pure Cp-Ti and first generation titanium alloys Ti-6Al-4V alloy, but there are some problems that are need to be overcome. The modern studies show that the Cp-Ti (α-phase) and Ti-6Al-4V (α+β phase) alloys have an elastic modulus of above 100 GPa which is higher than the modulus of elasticity of the bone of 20 GPa, that leads to a

stress shielding effect. This stress leads to bone and implant loss **[1, 13-16]**. Tribological properties are poor with different loads and different friction conditions [**17]**. Moreover, Ti- alloys with single phase have less corrosion rate than Ti- alloys with more than one phases **[18]**.

To tackle these issues, many studies focused on the developed different Ti-based alloys with low Yonge modulus, non-allergic and non-toxic elements, and with single phase **[19,20]**. Therefore, the second-generation titanium biomaterials β- titanium alloys with low elastic modulus and nontoxic elements including, Mo, Zr, Nb, and Ta have been extensively investigated for biomedical applications **[19,21-23]**. It was reported that the second-generation titanium alloys β or near β can offer significant advantages for biomedical applications **[24]**. However, there are different β titanium alloys compositions, with wide ranging microstructures β, β+α, β+α′, β+α″, and β+ω **[25]**. It is far from clear what microstructure is optimum. Is the β phase or β phase and a second phase (β+α, β+α′, β+α″, and β+ω) is preferable. Is a metastable β phase or rich β phase alloys better or worse than a single stable β phase alloys. Small changes in the alloy composition or the process conditions can give major changes in the microstructure. These changes will have a major effect on all properties, including elastic modulus, electrochemical resistance, and tribological resistance. However, there has been no systematic investigation that correlates microstructure with these properties.

Based on these unknowns, this investigation aims to understand a wide range of second-generation titanium alloys with systematic difference in microstructure and with difference in composition to understand the influence of these key variables on the mechanical, electrochemical, and tribological behavior, in comparison to Cp-Ti and the first generation titanium alloys Ti-6Al-4V.

1.2.Biomedical materials:

According to the European Conference on Biomaterials, a biomedical material, or biomaterial is: a material intended to interface with biological systems to evaluate, treat, augment or replace any tissue, organ or function of the body.**[26]**

Some metals are used as passive substitutes for hard tissue replacement such as total hip and knee joints, for fracture healing aids as bone plates and screws, spinal fixation devices, and dental implants because of their excellent mechanical properties and corrosion resistance. Some metallic alloys are used for more active roles in devices such as vascular stents, catheter guide wires, orthodontic archwires, and cochlea implants**.[27]**

Traditionally the study of biomaterials focuses on issues such as biocompatibility, host-tissue reaction to implants, cytotoxicity, and basic structure-property relationships [1-81. These issues are important. They provide a strong scientific basis for a clear understanding of many successful medical devices such as the mechanical heart valve. However in biomaterials engineering, the manufacturing and processing aspects emerge as a primary concern. **[28]**

Although each biomedical application possesses its own specific set of requirements, there is one requirement which all biomedical materials must fulfil, namely, biocompatibility. Biocompatibility implies that there is either no adverse reaction or else an appropriate interaction. It is required to ensure that the potential for rejection or other hostile interaction between the implant and the host is limited. In many cases, it is relatively easy to find materials that possess the physical properties required for a specific application, such as strength, elasticity, or optical transparency. The difficulty, however, is in selecting materials that react appropriately, or not at all, with the host environment while maintaining these.**[26]**

1.2.1. Orthopedic Biomaterials :

Orthopaedic injuries and pathologies are among the most common medical conditions. While fractures are no longer an anticipated part of a child's medical history, over 6.2 million fractures occur each year in the U.S. population. Osteoarthritis affects one in five individuals over the age of 70. These and other conditions—including rheumatoid arthritis, osteosarcoma, and ligament tears—often require an intervention that includes the replacement of some portion of tissue. For most of these applications, autografts and allografts have proven problematic based primarily on material availability. Artificial materials have shown tremendous success in a number of applications, particularly total-joint replacement, but are not without their downsides, including long-term biocompatibility and survivability issues. As is the case in many areas of tissue and organ replacement, the future of tissue engineering holds great promise. If orthopaedic surgeons are able to replace diseased or damaged tissue with a material that will immediately take over the original structural and mechanical function, while it becomes completely integrated with the natural tissue with time, the current gap between natural and engine.**[29]**

Titanium is generally considered a metallic material with the best biocompatibility properties and, as a consequence, it finds more and more application as a biomaterial. However, pure titanium is characterized by relatively low mechanical properties, so in many applications it is replaced. by titanium alloys, which are more expensive, less biocompatible, but with better mechanical properties.**[30]**

Titanium and titanium alloys have very good resistance to crevice corrosion; however, they are extremely sensitive to fretting corrosion. This type of corrosion may occur only when a metallic surface is in contact with another surface (metallic or not), in the presence of a compression stress

and slight reciprocal movements. This can happen, for example, in orthopedic applications, in the tape morse of joint prostheses (between the femoral head and stem), and under the heads of screws in ostheosynthesis devices. In these cases, the onset of fretting corrosion on titanium alloys has been confirmed by microscopic analyses at the damaged parts and by the presence of black titanium powder on the surrounding tissues, which seem to tolerate it. The sensitivity to fretting corrosion is the main limit of titanium and its alloys for orthopedic applications, especially because the fatigue or simply brittle fractures start very often at the corresponding sites of corrosion.**[30]**

1.3.Objectives of This Investigation:

The main objectives of this investigation are:

1- Study of three different microstracture of the second generation of the beta phase alloys, namely Ti- 13Zr-13Nb (rich beta), Ti-15Mo (metastable beta) and Ti-8Mo-4Nb-2Zr (single phase beta), in comparison to commercial pure titanium and first generation titanium alloys.

2- study the influence of the systematically different microstructures of second-generation titanium biomaterials β- titanium alloys on the electrochemical behavior of these alloys, in comparison to commercial pure titanium and first generation titanium alloys, and thereby come up with recommendation for the ideal implant microstructure.

3- study the influence of the systematically different microstructures of second-generation titanium biomaterials β- titanium alloys on the tribological behavior of these alloys, in comparison to commercial pure titanium and first generation titanium alloys, and thereby come up with recommendation for the ideal implant microstructure.

CHAPTER TWO

Theoretical Part

Theoretical Part

2.1. General View

In this chapter, the literature on this work will be reviewed. In the beginning, a detailed explanation of biomaterials will be presented, followed by an explanation of the historical developments of metallic biomaterials, these sections focusing on biomaterials definitions, biomedical materials, plus the basic considerations for selection of metallic implants and design implants. The differences in titanium alloys are discussed in the following sections in terms of general characteristics, titanium alloys as biomaterials, and biocompatibility of alloying components. The next two major parts are on corrosion and tribology in general, and specifically about titanium alloys. Finally, the last part contains a review of the literature on elastic modulus, corrosion, and wear processes of titanium alloys.

2.2. Biomaterials

Biomaterials share the advantage of being used closely with the body**.** However, various topic specialists have characterized biomaterials in slightly different ways. A biomaterial, as defined by the National Institute of Health Consensus Development Conference, is any material (other than drugs) or mixture of materials, synthetic or natural, that is used as a whole or as a part of a system to replace or promote part of an organic or tissue, and can be used for any period of time. According to Materials Science, a biomaterial is “a material that has been designed to adopt a shape that may be utilized alone or as part of a complex system in intimate touch with a living body, via regulation of interactions with components of living systems” **[3].** A biomaterial, in other terms, is "any material, artificial or natural in origin, utilized to replace or aid a portion of a tissue or organ while in intimate touch with it." As a result, the prefix "bio" in biomaterials

refers to "biocompatibility" rather than "biomedical or biological properties"**.** Furthermore, a biomaterial is defined as a component of medical devices in the legal field. Medical devices are defined as "any implement, instrument, machine, implant, apparatus, in vitro reagent or software, calibrator, material, or other similar or related articles, manufactured to be used alone or in conjunction with other articles" (combination) for one or more specific purposes such as research, prevention, monitoring, diagnosis, assisting, controlling conception, or sustaining life **[31].** Materials used for corrective eyeglasses and artificial limb prostheses, for example, are examples of biomedical devices, whereas total hip replacement (THRs) and contact lenses are instances of biomaterials, according to the legal definition. Figure 2.1 depicts the defining limits of biomedical materials, biological materials, and biomaterials **[3]**, while Figure 2.2 describes the major uses of biomaterials in the human body **[32]**, and Figure 2.3 depicts the various medical implants. **[33]**. Metals, ceramics, polymers, and composite materials are the four types of materials classified by Materials Science. Natural biomaterial groups can be combined with previous biomaterial groups**[3]**.

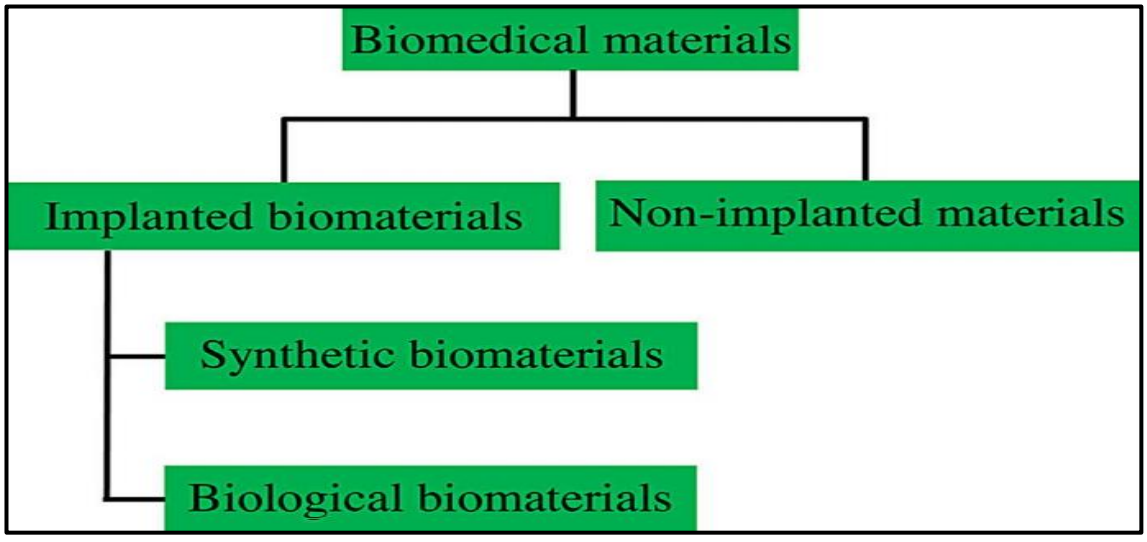

Figure 2.1 Biomedical materials, biological materials, and biomaterials all have different definitions **[3]**.

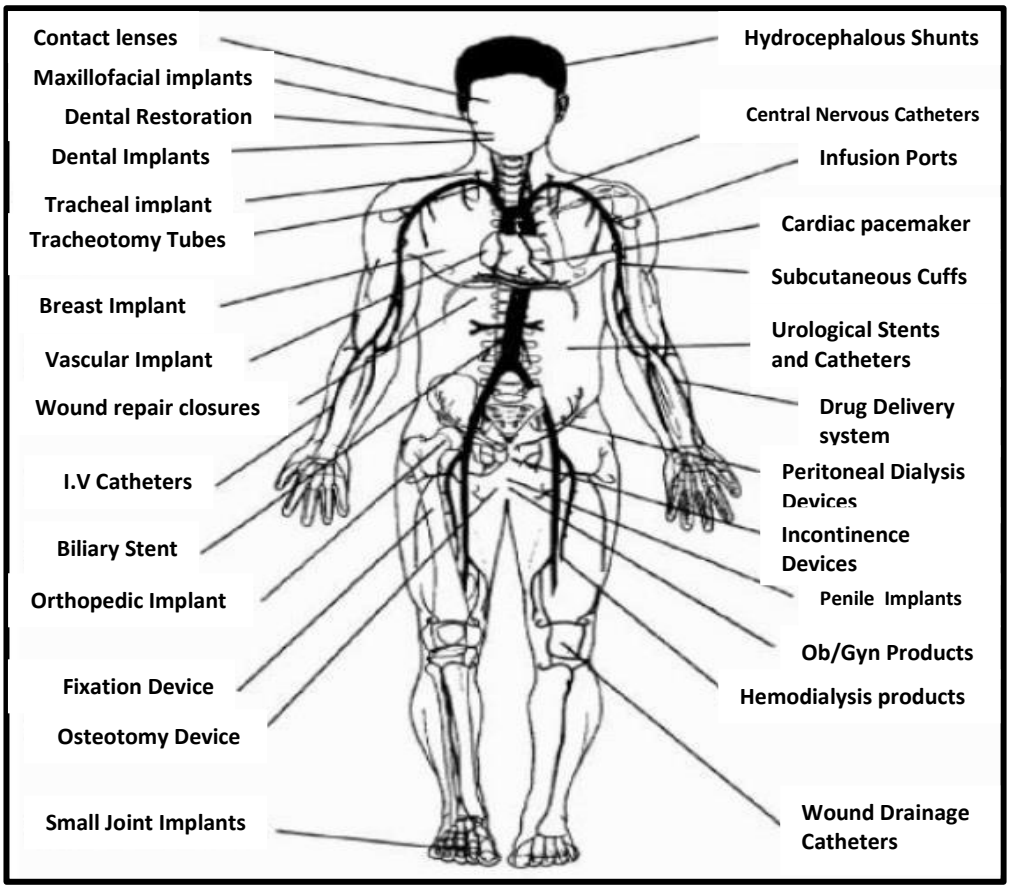

Figure2.2 The most important uses of biomaterials in the human body **[32].**

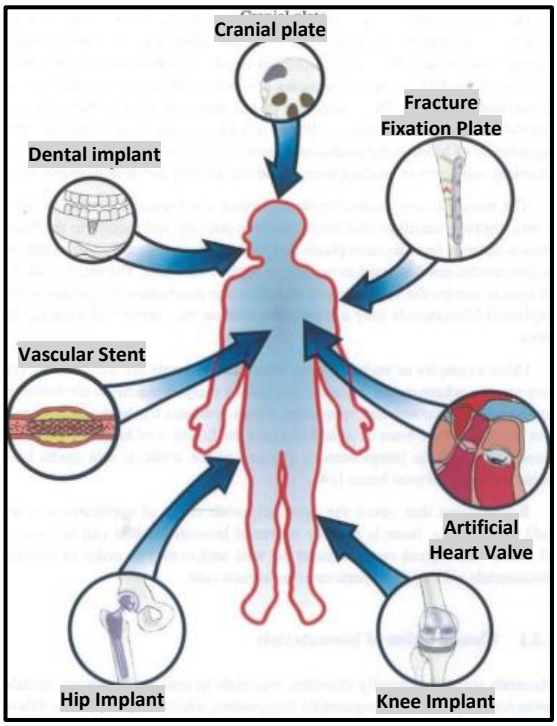

Figure 2.3 Various medical devices used in the human body **[33]**.

2.2.1 Metallic Biomaterials' Evolution throughout History

Since nineteenth century, metals and alloys have been frequently utilized as medical implants. Industry produces a large number of metals and alloys as the economy and technology develop. Only just few metals and alloys, however, are biocompatible and have a lengthy record of accomplishment of effectiveness as medical implants**.** These few metals and alloys are classified into four groups: stainless steels alloys, cobalt-based alloys, titanium-based alloys, and others not specified, these groups based on the major alloying element **[3].**

Stainless steel alloys have been used for medical implants since the 1920s **[34]**. 316L is the most often utilized biomaterial among stainless steels and has been for a long period. Stainless steel, despite its capacity to passivate and build a passive oxide layer made mainly of chromium oxide, has a tendency to corrode within the body under specific conditions in oxygen-deprived areas and highly stressed. According to reports, for stainless steel alloys the most prevalent issues that inhibit its use as implants, according to studies, include: poor osseointegration in the vicinity of granulated tissue between the surface and tissue, crevice and fretting corrosion, , and a very high Young's modulus**.** For the last fifty years, cobalt-based alloys have been employed in biomedical applications due to their better corrosion and wear resistance versus stainless steels **[34, 35].**

Commercially pure titanium and titanium alloys have been recommended as a replacement for stainless steel alloys (316L) and cobalt-based alloys since they often contain hazardous elements such as Ni, Co, and Cr. As a result, since the early 1970s, titanium and specific titanium alloys have been employed in biomedical applications **[36, 37]**.

First, because of its greater corrosion resistance and ability to spontaneously produce an inert and stable oxide coating when exposed to

an oxidizing environment, Cp-Ti was proposed for use as a biomedical material **[36, 37]**. Unalloyed Cp-Ti can be supplied; Cp-Ti grades 1–4 by the American Society for Testing and Materials (ASTM). The most common unalloyed titanium used in dental implant applications is CP-Ti grade 2**[2, 36]**. Cp-Ti has many benefits, but it also has some drawbacks. For example, in some situations, such as intense wear usage (low wear resistance) and hard tissue replacement, the mechanical characteristics of Cp-Ti cannot fulfill the criteria of biomedical applications **[2, 38, 39]**.

As a substitute for the Cp-Ti alloy, the first generation titanium alloys, a titanium-6 percent aluminum-4 percent vanadium (Ti-6Al-4V) alloy with α-β phase structure was recommended. Furthermore, there are worries regarding aluminum and vanadium toxicity, which might create significant issues once the metal ions are liberated within the live organism. New titanium alloy compositions based on V-free α-β-type titanium have been developed to address possible vanadium toxicity **[2, 38, 39]**. To address vanadium toxicity, Ti-6Al-7Nb and Ti-5Al2.5Fe alloys with high mechanical characteristics and metallurgical behavior similar to Ti-6Al4V were created **[1, 37, 40]**. Despite their numerous advantages, The elastic modulus of -α- phase type and α-β-phase type titanium-based alloys is substantially greater than that of human bone, bringing in a stress shielding influence **[37, 39, 41-43]**. As a result, low modulus β- type titanium alloys were recommended to reduce the stress shielding effect; the literature has more than one system of β-type titanium alloys **[2, 43-51]**.

Subsequently, NiTi shape memory alloys and novel magnesium-based alloys have been proposed. These minerals are currently being developed owing to their unique material characteristics, such as NiTi's shape memory and the degradability of magnesium alloys **[52-55]**. Their characteristics may be beneficial for more specific applications like regeneration (magnesium -based alloys), bone tissue creation and hard

tissues/organs non-conventional reconstructive surgery (NiTi shape memory alloys as vascular stents)**[52-55]**. Table 2.1 lists the benefits, drawbacks, and metallic implants' principal uses in the human body **[7]**. Figures 2.4 and 2.5 depict a typical clinical application of metallic materials; in figure 2.4a, the Harrington rod is an example of a stainless-steel surgical device and in figure 2.4b, the stem of a THR is typically made of stainless steel, cobalt-based alloys, or titanium-based alloys. Figure 2.5 depicts an application of a NiTi shape memory alloy. A vascular stent (a) and an aneurysm clip (b) **[3].**

Table 2.1. A comparison of metallic implants used within the body **[7]**

Metals and Alloys	Selected Examles	Advantages	Disadvantage	Principal Application
Titanium based alloys	Cp-Ti Ti-Al-V Ti-Al-Nb Ti-13Nb-13Zr Ti-Mo-Zr-Fe	High biocompatibility Low Young modulus excellent corrosion resistance low density	Poor tribological prperties toxic effect of Al and V on long term	Bone and joint replacement, fracture fixation dental implants pacemaker encapslation
Cobalt and Cr alloys	Co-Cr-Mo Cr-Ni-Cr-Mo	High wear resistance	Allergy consideration with Ni , Cr and Co much higher modulus than bone	Bone and joint replacement, dental implants, dental restorations, heart valves
Stainless Steels	316L Stainless steel	High wear resistance	Allergy consideration with Ni and Cr much higher modulus than bone	fracture fixation, stents, surgical instruments
Others	Ni-Ti	Low Young modulus	Ni cause allergy	Bone plates, stents, orthodontic wires
	Platinum and t-Ir	High corrosion resistance under extreme voltage potential and charge transfer condition		electrodes
	Hg-Ag-Sn amalgam	Easy in situ formability to a desired shape susceptible to corrotion in the oral environment	Concerns related to Hg toxity	dental restorations

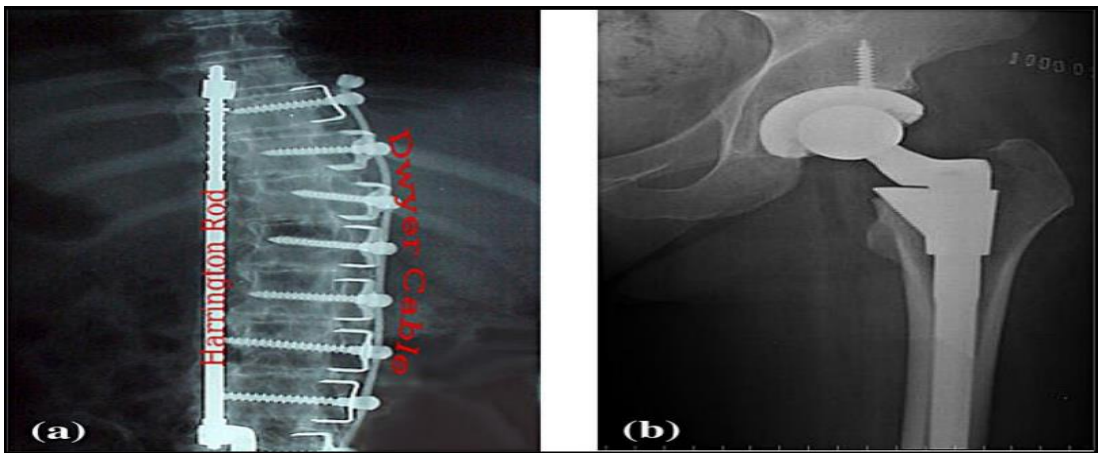

Figure.2.4: (a)The Harrington rod, and (b)the stem of a total hip replacement **[3]**.

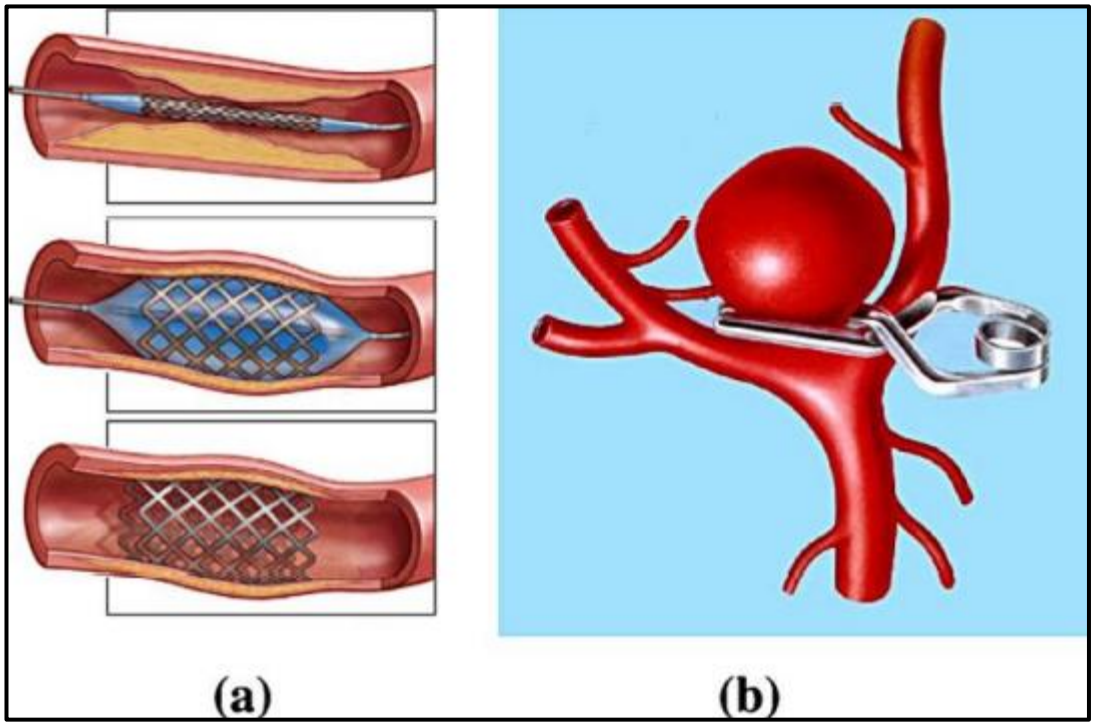

Figure 2.5:(a) a vascular stent, (b) an aneurysm clip **[3]**.

2.2.2 Fundamental Factors to Consider in the Selection and Metallic Implants Design

The selection and design of metallic biomaterials is determined in order to be used in the living body without rejection for an extended period of time, and by their specific medical application. Osseointegration, excellent biocompatibility, great corrosion resistance, appropriate

mechanical characteristics, and great wear resistance are the basic features of a metallic implant **[3]**.

2.2.2.1 biocompatibility

The substances chosen and designed for implantable devices must be compatible with the live body and therefore have no detrimental systemic or local implications on the human body. When utilized in a biological system as an implant, no substance is very inert for an extended period. The utilization of elements that already exist in the biological system is the basic assumption in the selection and design of a biomaterial, in order to avoid any detrimental consequences (systemic or local). Table 2.2 lists the public elements that found in the human body. The majority of the human body elements is nitrogen, hydrogen, carbon, and oxygen, these elements make up 96 percent of the body's mass; they provide as the foundation for water and proteins. The elements found predominantly in extracellular fluid, blood (K, Na, and Cl), or bones (P, Ca, and Mg) make up the bulk of the human body (4 percent); these elements are given in table 2.3**[56]**. Additionally, table 2.4 lists the micronutrients or roles of trace elements in the human body, all of which are toxic in high concentrations; as a result, for healthy body physiology, development, and growth, these elements must be at relatively low levels **[56, 57]**.

Table 2.5, lists the known trace or micronutrients. To conclude, several metals may be utilized in the human body, while so many of these elements are micronutrients in small quantities, they are harmful and highly poisonous at greater ones **[3]**. The biocompatibility of various alloys and pure metals that can be utilized as metallic biomaterials is depicted in Figure 2.6**[58]**. When designing and selecting biomaterials, toxic metals must not be utilized in biomaterial alloys as alloying elements. Although, as previously stated, no metal is completely non-toxic or inert; thus, alloys used in biomedical implants would be made from inert elements, elements

found as micronutrients or those elements with excellent corrosion resistance **[58]**.

Table 2.2 :Elements in the human body **[3]**

Element	O	C	H	N	Ca	P	K	S	Na	Cl	Mg	Trace element
Wt%	65.0	18.5	9.5	3.3	1.5	1.0	0.4	0.3	0.2	0.2	0.1	<0.01
At%	25.5	9.5	63.0	1.4	0.31	0.22	0.06	0.05	0.3	0.03	0.1	<0.01

Table 2.3: Macro Elements Functions in the human body **[56].**

Macro element	Roles
O,C,H,N	In water and the molecular structures of proteins
Ca	structures of bone and teeth
P	structures of bone and teeth, required for ATP, the energy carrier in animals
Mg	Important in pone structure, deficiency results in tetany(muscle spasms) and can lead t calcium deficiency
Na	Major electrolyte of blood extracellular fluid required for maintenance of pH and osmotic balance
K	Major electrolyte of blood intracellular fluid required for maintenance of pH and osmotic balance
Cl	Major electrolyte of blood extracellular and intracellular fluid, required for maintenance of pH and osmotic balance.
S	Element of the essential amino acids methionine and cysteine. Contained in the vitamins thiamin and biotin. As part of glutathione it is required for detoxification. Poor growth due to reduced protein synthesis and lower glutathione levels potentially increasing oxidative or xenobiotic damage are consequences of low sulfur and methionine and /or cysteine intake.

Table 2.4: Trace Element Functions in the Human Body **[3].**

Trace Element	Roles
Fe	Contained in heme groups of hemoglobin and myoglobin which are required for oxygen transport in the body, as well as many other metabolic enzymes and Fe-S proteins. Part of the cytochrome p450 family of enzymes. The genetic disease hemochromatosis results from excess iron absorption. Similar symptoms can be produced through excessive transfusions required for the treatment of other diseases.
Cu	Contained in enzymes of the ferroxidase system which regulates iron transport in the blood and facilitate release from storage. A structural element in the enzymes tyrosine, cytochrome c oxidase, ascorbic acid oxidase, amine oxidases, and the antioxidant enzyme copper zinc superoxide dismutase, amongst others. A copper deficiency can result in anemia from reduced ferroxidase function. Excess copper level cause liver malfunction and are associated with genetic disorder Wilsons Disease
Mn	Major component of the mitochondria antioxidant enzyme manganese superoxide dismutase. A manganese deficiency can lead to improper bone formation reproductive disorders. An excess manganese can lead to poor iron absorption.
I	Required for production of thyroxine which plays an important role in metabolic rate. Deficient or excessive iodine intake can cause goiter (an enlarged thyroid gland)
Zn	Important for productive function due to its role in FSH (follicle stimulating hormone) and LH (leutinizing hormone), required for DNA binding of zinc finger proteins which regulate a variety of activities. A component of the enzymes alcohol dehydrogenase, lactic dehydrogenase carbonic anhydrase, ribonuclease, DNA polymerase and the antioxidant copper zinc superoxide dismutase. An excess of zinc may cause anemia or reduced bone formation.
Se	Contained in the antioxidant enzyme glutathione peroxidase and heme oxidase. deficiency results in oxidative membrane damage with different effects in different species. Human deficiency causes cardiomyopathy and is known as Keshan diseases.
Co	Contained in vitamin B12. An excess may cause cardiac failure.
Mo	Contained in enzyme xanthine. Required for the excretion of nitrogen in uric acid in birds. An excess can cause diarrhea and growth reduction.
Cr	A cofactor in the regulation sugar levels. Chromium deficiency may cause hyperglycemia (elevated blood sugar) and glucosuria (glucose in the urine). Elevated level of some forms of chromium, such as Cr(VI), can be carcinogenic.

Table 2.5: The list of trace elements found in the human body**[3]**.

Barium	Chromium	Iron	Selenium
Beryllium	Cobalt	Lithium	Strontium
Boron	Copper	Molybdenum	Tungsten
Cesium	Iodine	Nickel	Zinc

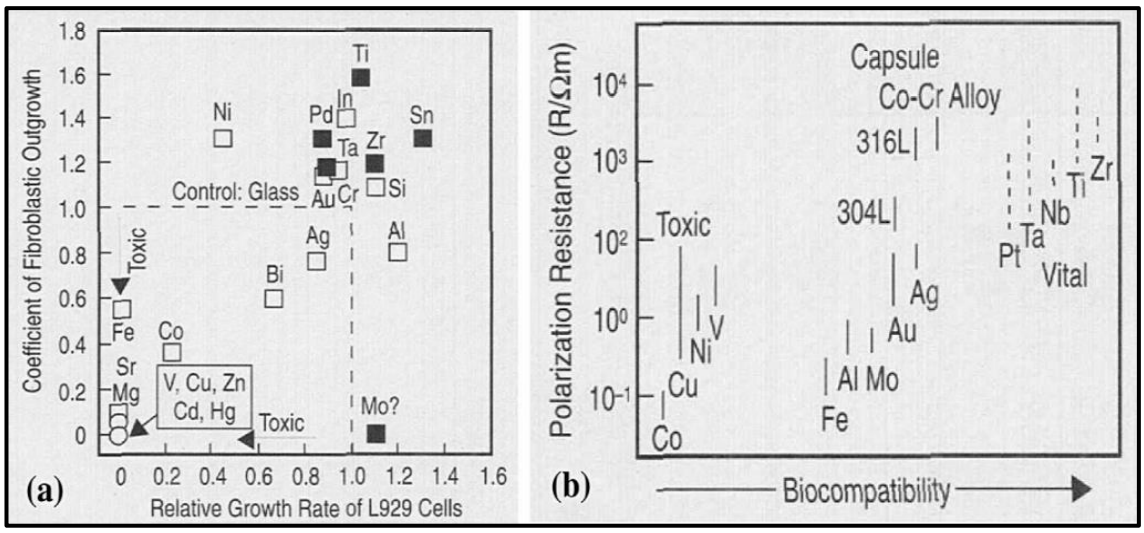

Figure 2.6: (a) Some pure metals are cytotoxic to cells, (b) the relationship between biocompatibility and polarization resistances of stainless steels, pure metals, and cobalt-chromium alloys **[58]**.

2.2.2.2 corrosion resistance

The outside environment (ambient conditions) differs chemically and physiologically from the inside the human body's environment. In usual circumstances, human body’s solutions consist primarily of Cl+, Na+, and other soluble protein, amino acids, trace ions, and approximately 9 percent brine. Table 2.6 shows human blood plasma ionic concentration **[59]**. At pressure of 1 atm and 37°C, the pH of these fluids is almost balanced, ranging from 7.2 to 7.4**[60]**. Likewise, different regions of the human body have varying amounts of oxygen and different pH levels. As a result, an implant may be corrosion

resistant in one part of the body while being poor corrosion resistant in another part **[60]**.

In reality, under specific situations, such as injury or surgery, the pH of human bodily fluid can fluctuate between 7.2 -7.4 to 3-4, causing inflammation owing to inflammatory cell discharge. Additionally, ionic strength fluctuations might occur because of high ion deposits or blood pressure. As a result, the human body will react to an implant as if it were an attack environment. Furthermore, Oxygen partial pressure in the human body raises the corrosion ratio of the implants by delaying the development of the oxide film on the surface of a broken or removed implant **[60]**. In an ideal world, a metallic implant would be corrosion resistant; as a result, metal ion release from a biomaterial metallic implant, which results in hazardous responses, under normal physiological conditions, ion release should be reduced and maintained at appropriate levels in the severe conditions and for Long-term service for more than 30 years **[3]**.

Table.2.6. Human blood plasma ionic concentrations (mM) **[49].**

Ion	Human tissue fluid	Human blood plasma
Na^+	142.0	142.0
HCO^{3-}	4.2	27.0
K^+	5.0	5.0
HPO_4^{2-}	1.0	1.0
Mg^{2+}	1.5	1.5
Cl^-	147.8	103.0
Ca^{2+}	2.5	2.5
SO_4^{2-}	0.5	0.5

2.2.2.3 mechanical resistance

The metallic implant that can be utilized to change any live body component. Bone must be capable of determining the bone's mechanical performance**.** As a result, the metallic implant's mechanical properties, such as ultimate tensile

strength (UTS), toughness, and Young's modulus, must all be taken into account when selecting and designing a metallic implant **[4]**. Table 2.7 lists the mechanical properties of the controlling metallic biomaterials. Stainless steel, cobalt alloys, and titanium-based alloys have a much higher Young's modulus (>100 GPa) than bone (10-30 GPa) **[4]**. As a result, biological reactions, notably atrophy surrounding the implant site, develop, prompting revision surgery, this is known as the "stress shielding effect". A metallic implant with a modulus of elasticity equivalent to or similar to bone must be used as a bone replacement. Strength of fatigue is defined as the number of cyclic stresses that a material can withstand, without causing it to fail under fatigue. In reality, cyclic loading can cause skeletal implant fatigue (e.g., spinal fixations, hip replacement joints, wires, knee joints, and plates). Service conditions (corrosion environment, load vectors, cycle frequency, and wearing, material microstructure, and product surface quality) are all factors that have a major effect on fatigue life **[3]**.

Table 2.7 Metallic biomaterials and cortical bone mechanical properties **[4].**

Material	**Young's modulus(Gpa)**	**Ulltimate tensile strength(Mpa)**	**Fracture Toughness(MPa√m)**
CoCrMo alloys	240	900-1540	≈100
316L stainless steel	200	540-1000	≈100
Ti-alloys	105-125	900	≈80
Mg alloys	40-45	100-250	15-40
NiTi alloy	30-50	1355	30-60
Cortical bone	10-30	130-150	2-12

2.2.2.4 wear resistance

Wear is an unavoidable issue in any joint replacement, regardless of the biological materials employed**.** The kind of joint is crucial when choosing biological material types. The elbow, shoulder, knee, ankle, and hip are examples of long bone joints, whereas the wrist, tooth, and skull are static joint

examples. The mobile joints are classified as harmonious or non-harmonious depending on the fit of the opposing bones. Congruent joints include the shoulder and hip (figure 2.8), whereas non-harmonious joints include the knee and ankle (figure 2.9)**.** As shown in figure 2.8, Brittle ceramics are used as articulating surfaces in socket joints and ball joints; a ball-shaped head is closely coupled to a cup-like socket, dispersing stress similarly. Table 2.8 shows the wear-resistance classification of articulating surfaces for joint prosthetics and orthotics. Figure 2.9 shows a contact of two non-harmonious hard surfaces, because of the very heterogeneous load, Brittle ceramic materials cannot withstand this sort of force; instead, in these circumstances, tough metallic and polymeric materials are employed **[3]**.

Currently, joint replacement may be classed as "Hard-on-Hard," in which case the joint replacement is composed of “Ceramic-on-Ceramic, CoCrMo-on-CoCrMo , or Al_2O_3-on-CoCrMo”; or “Hard-on-Soft,” in which case “Metallic-on-UHMWPE, Ceramic-on-Ultra-high molecular weight polyethylene (UHMWPE)” is used to make the joint replacement. For a metallic implant, the friction coefficient should be low, or the wear resistance should be higher. In addition, vice versa will result in the loosening of the implant and the formation of wear debris might induce inflammation comparable to pyrogens or bacteria, culminating in the destruction of the metallic implant's bone support **[65-67]**.

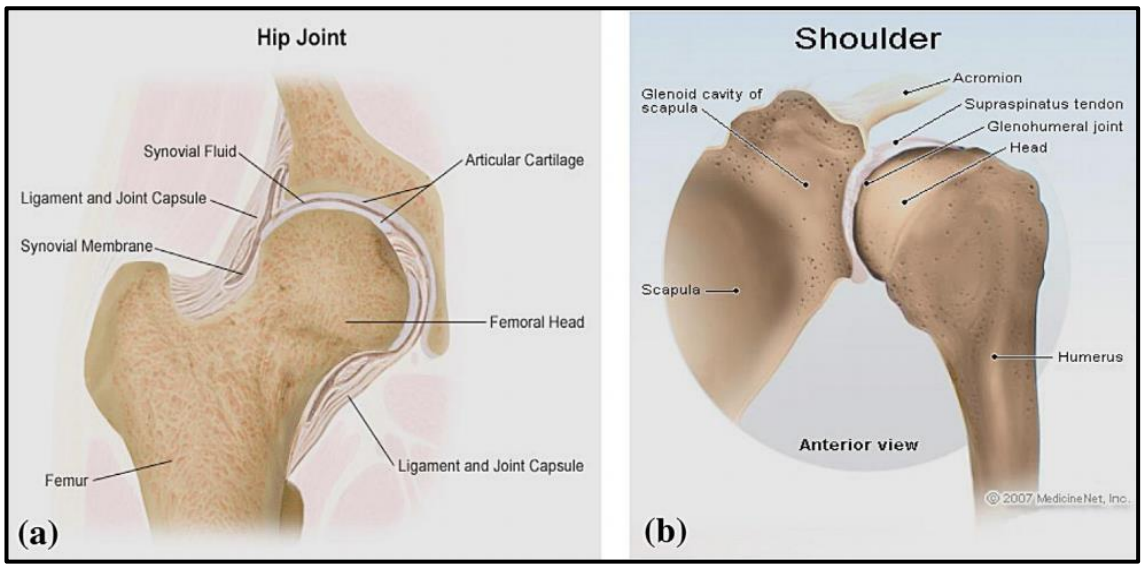

Figure 2.8. Human bodies have two congruent joints: (a) the hip joint and (b) the shoulder joint **[3].**

Table 2.8: Wear resistance of articulating surfaces for joint prostheses **[3].**

Ball and socket	Wearing resistance
Ceramic-on-Ceramic (Al_2O_3 or ZrO_2)	Superior
CoCrMo-on-CoCrMo	Excellent
Al_2O_3-on-CoCrMo	Excellent
Al_2O_3 on UHMWPE[a]	Excellent
CoCrMo on UHMWPE	Good
Ti6Al4V on UHMWPE	Good
Metal on metal (stainless steels or titanium alloys)	Poor

[a] UHMWPE, ultra-high molecular weight polyethylene.

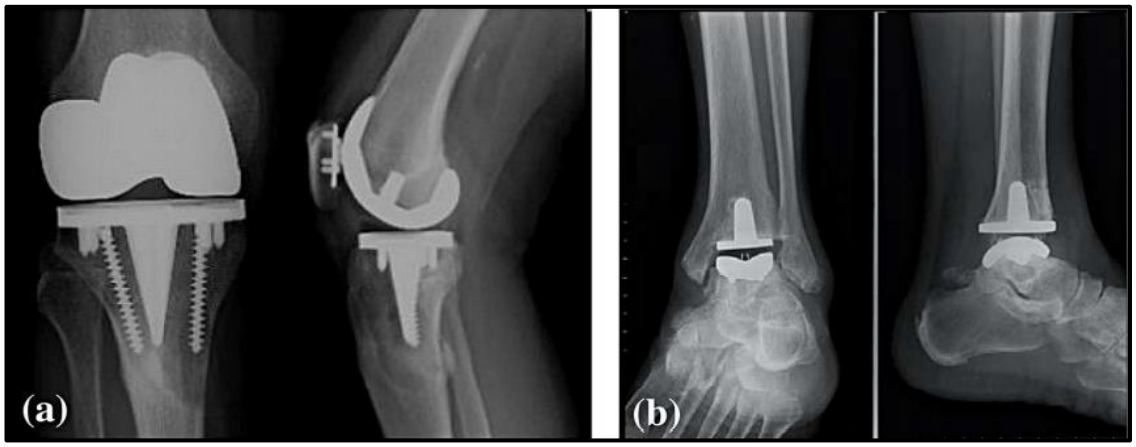

Figure 2.9. Two prosthetic joints that are incompatible with one another (a) knee joints and (b) ankle joints **[3].**

2.2.2.5.Osseointergration

Another important term to consider in the biomedical science domain is Osseo-combination. Osseo-combination is defined as “a word used to describe the process of bone recovery and new bone formation” and is a necessary orthopedic procedure **[68]**. The lack of a bone-implant interface and other tissue near the implant causes the prosthesis to loosen. As a result, the appropriate combination of an implant is important, that commonly necessitates it having an acceptable surface that will enhance combination with the tissues and bone in the vicinity. Chemistry surface, topography, and roughness, are all important factors to consider for great Osseo-combination **[69-72]**.

2.3 Titanium

Titanium alloys have become increasingly popular as biomaterials throughout the previous two decades. Some time ago, pure titanium α-phase Cp-Ti and the first generation titanium alloys α+βphase Ti-6Al-4V were introduced. However, Second generation titanium alloys, also known as β -phase titanium alloys, have received a lot of interest recently. This section will provide a summary of titanium's general properties, crystals structure of titanium, titanium Alloys, and alloying elements biocompatibility. **[73]**

2.3.1 Titanium's General Properties

After Al, Fe, and Mg, Ti is the fourth 18th most abundant metal and it is the ninth most plentiful element on earth. It has a metallic silver appearance. Titanium has a density of 0.6 that of iron and close to 0.5 that of cobalt. However, it is distinguished with a modulus of elasticity about 0.5 that of molybdenum-cobalt alloys and stainless steels **[74]**. Titanium outperforms cobalt-chromium and stainless steel alloys in terms of (specific strength), but falls short in terms of tribological properties**.** Because titanium's properties are intermediate between those of steel and aluminum **[75]**. Because of its low

density, exceptional corrosion resistance, and good biocompatibility, titanium is frequently utilized in medical applications. Titanium and its alloys, on the other hand, have several disadvantages, such as high cost, fabrication problems, embrittlement (at high temperatures, oxygen transport occurs in the surface oxide layer), high reactivity or strong sensitivity to temperatures over 480°C , and high energy content in production**[76].**

2.3.2. Crystals Structure of Titanium

At low point temperatures, pure titanium metal has a hexagonal close packed (hcp) structure (α-type phase), whereas heating the -transus temperature leads the alloy to β transition to the body centered cubic (BCC) β-type phase**[77]**. It is at 882°C and is determined by the titanium composition. Its microstructure can be manipulated through thermomechanical and thermal processes. Furthermore, crystallographic texture may be evolving; thus, the microstructure can be controlled **[74].**

2.3.3 Titanium Alloys

After processing, based on their microstructure, titanium alloys are classified into five categories. Among these are α-phase type alloys, near-α phase type alloys, α-β phase type alloys, metastableβ phase type alloys, and stable β -phase type alloys **[73]**. Near α-type and α-type alloy has high resistance to corrosion; α+β-type has greater strength; β-type (metastableβ and stableβ) has a lower elastic modulus and greater resistance to corrosion **[78]**. It has been demonstrated that theβ type phase has two phases that are stable, the first at lower temperature with α phase (having a crystal structure of HCP) and the second at high point temperature (with a BCC). These alloys also contain three metastable phases having a hexagonal structure (HCP): omega phase (ω), hexagonal martensite (α′), and an orthorhombic martensite (α″) **[79]**. It has been demonstrated that are produced by quenching from the phase **[80]**. There are three types of alloying elements that may be included in titanium (se figure

2.10) **[74]**. The first are α-stabilizers, which raise the β-transus temperature, such as Al, O, C, and N. The second type of stabilizer is an isomporphous element β-stabilizer (as in, Mo, Ta, V, and Nb) or a eutectoid element (for example, H, Mn, Fe, W, Cr, Ni, Si, and Co); the β-transus temperature is lowered by these elements. Elements of the third category, such as Sn and Zr, have a neutral influence; all of these elements have a negligible influence on the temperature of the β-transus **[81, 82]**.

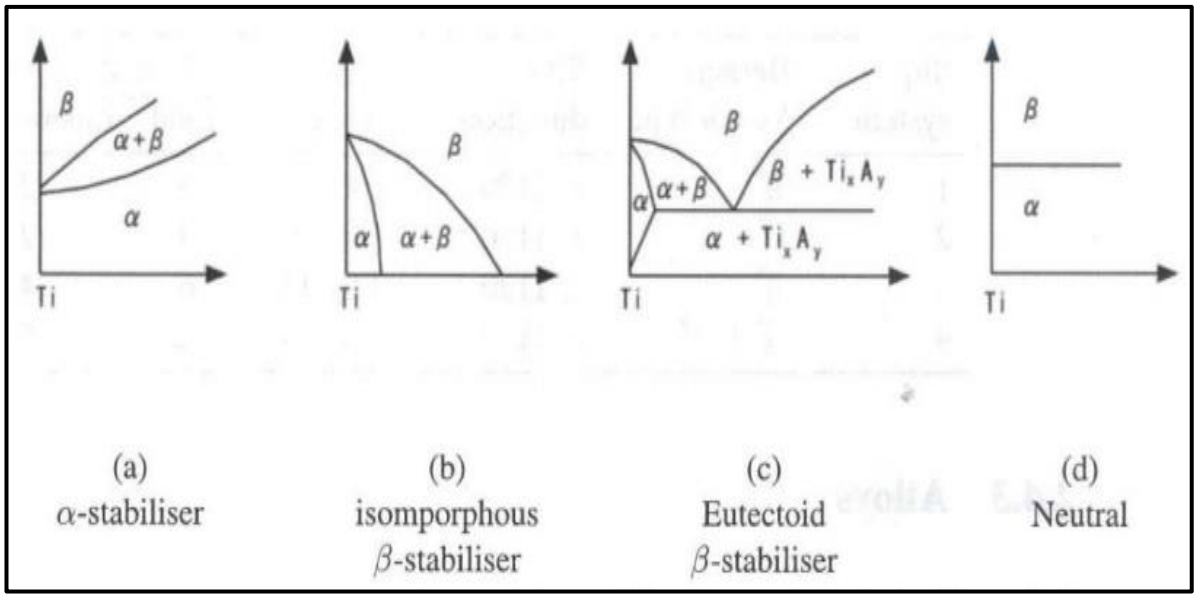

Figure.2.10. Patterns illustrating the influence of alloying elements on the β-transus temperature **[74].**

2.3.3.1 Near α and α- Titanium Alloys:

Near-alloys, Cp-Ti alloys, and super alloys are examples of these. Cp-Ti (98.-99.6% wt. Ti) with 100 percent α-phase has, high ductility, UTS in the range 240-550MPa, and yield strength in the range 170-480MPa (low strength), according to interstitial levels and impurity **[73]**. Even if they include some β-phase, alloys (designated as near-α or super-α alloys when modest quantities of βstabilizers are added) are more similar phase α phase Cp-Ti alloys than α-βalloys. Because of their lower strength at room temperature, near-α alloys and α alloys, as opposed to β or α-β alloys, have not been utilized in medical

implants in the same way. Therefore, Cp-Ti grades are chosen for their corrosion resistance and for non-load bearing applications **[3, 73]**.

2.3.3.2 α-β Phase Titanium Alloys

α - β - alloy ASTM standards, specifically first generation Ti-6Al-4V, Ti-5Al-2.5Fe, Ti-6Al-7Nb, and Ti-6Al-4V ELI, are found in medical equipment **[3]**. Ti6Al-4V alloy and Ti-6Al-4V ELI alloy are the used most often in medical devices. In comparison to Ti-6Al-4V, Ti-5Al-2.5Fe and Ti-6Al-7Nb are devoid of vanadium, which has a negative tissue influence and is known to be toxic; however, these alloys have the same metallurgy as Ti-6Al-4V **[73]**. The alloy composition, solution-treating temperature, cooling rate, and section size all have a delicate effect on the microstructure of α-βalloys. It was demonstrated that by using solution treatment and aging, the strength of these alloys could be increased by 0.3-0.5, while their modulus of elasticity stays unchanged. When contrast to -titanium alloys, these alloys' fatigue strength may be enhanced by aging and solution heat treatment, and it is equivalent to or greater than that of 316L s-steels and cobalt alloys **[83].**

2.3.3.3 Second-generation β-titanium

The modulus of elasticity of second-generation stable and metastable β-titanium alloys is closer to that of bone **[79-88]**. As a result, these alloys have piqued the interest of researchers because they able to alleviate stress shielding problems created by the implant's high Young's modulus **[3]**. In the 1990s, these alloys were developed for orthopedic implants. Titanium alloys of β-phase contain elements that are biocompatible and free of vanadium, such as iron, molybdenum, niobium, tantalum, and zirconium. When compared to α-βTi alloys such as (Ti-6Al-4V) first-generation titanium biomaterials, these alloys exhibit high corrosion resistance, fewer elastic moduli, and improved biocompatibility **[34, 58]**. β-phase titanium alloys have yield strengths comparable to cobalt alloys and 316L stainless steels**[3]**. While these alloys

have several disadvantages, for instance, they have inferior wear resistance and their fatigue strength is lower than that of cobalt alloys **[76]**.

2.3.4. Phase diagram of Titanium alloys used:

Below are the phase diagrams of the titanium alloys used in this study. Figure2.11 shows the phase diagram of the Ti-Al-V alloy. Figure 2.12 shows the phase diagram of Ti-Mo alloy. Figure 2.13 shows the phase diagram of Ti-Zr-Nb alloy.

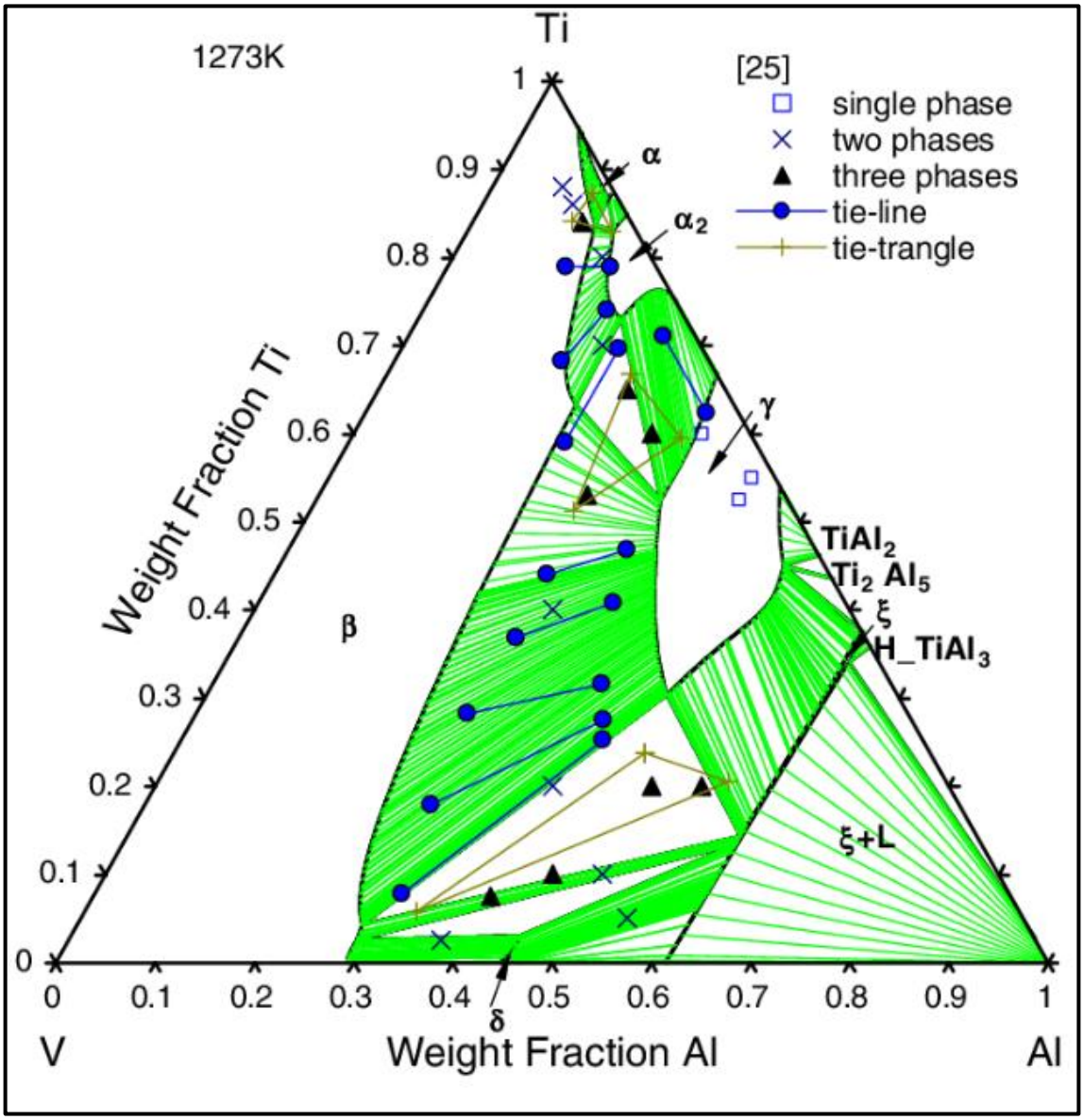

Figure.2.11. phase diagram of the Ti-Al-V alloy.**[89]**

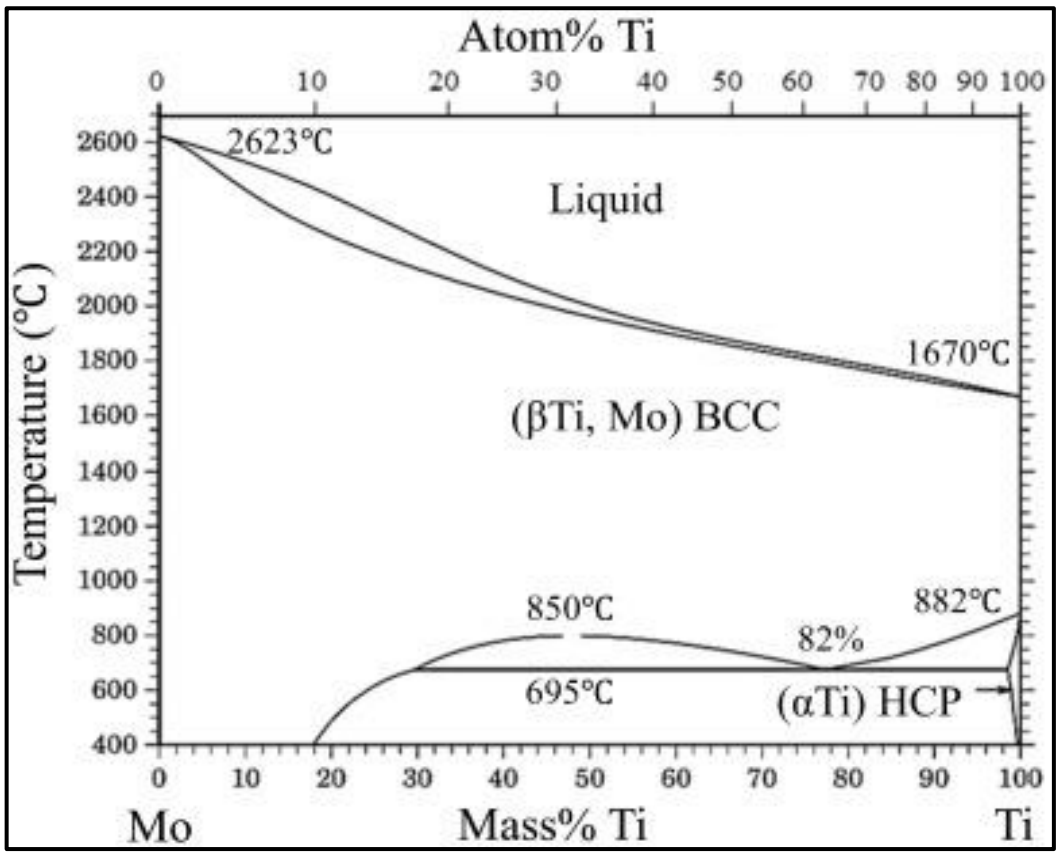

Figure.2.12. phase diagram of Ti-Mo alloy**[90]**

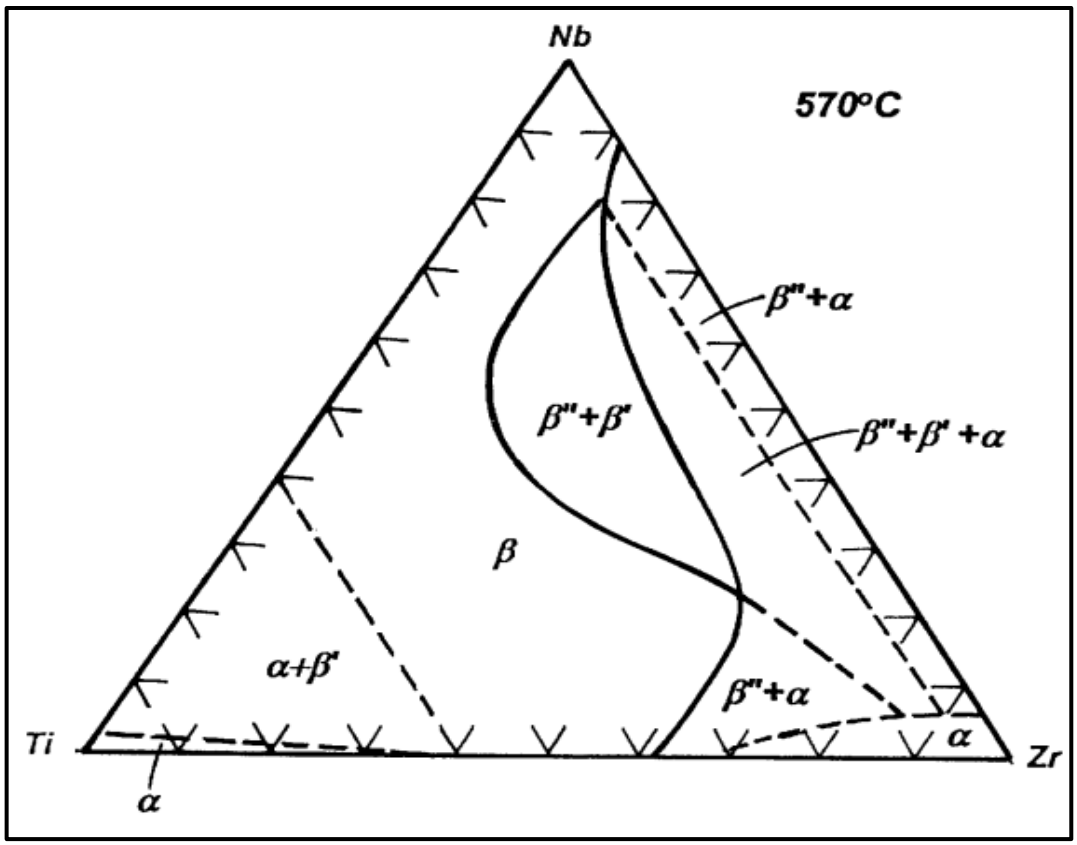

Figure.2.13. phase diagram of Ti-Zr-Nb alloy.**[91]**

2.3.5. Alloying Elements Biocompatibility

The most significant alloying elements typically added to titanium alloys for medical biomaterials are Al, V, Nb, Mo, Ta, and Zr, as shown in table 2.11**[92]**.

Table.2.11:Concentration of titanium in tissues surrounding titanium implants**[93]**.

Tissue	*Concentrations (ppm)*	*Ref.*
Bone	< 2100	Ducheyne, 1984
Soft tissue	2000	Meachim, 1973
Soft tissue	56–3700	Agins, 1988

Table.2.12: Concentration (jxg/1) of metals in tissues and blood retrieved during total arthroplasty of cementless stems**[93].**

	TiAlV stems			*CoCr stems*			
Sample	*Ti*	*Al*	*V*	*Co*	*Cr*	*Mo*	*Ni*
SF	556	654	62	588	385	58	32
SF (control)	13	109	5	5	3	21	5
CAP	1540	2053	288	821	3329	447	5789
CAP (control)	723	951	122	25	133	17	3996
FM	20813	10581	1027	2229	12554	1524	13234
Blood	67	218	23	20	110	10	29
Blood (control)	17	12.5	5.8	0.1–1.2	2–6	0.5–1.8	2.9–7.0

• **Titanium (Ti)**: Even at high concentrations, is a non-toxic element **[94, 95]**. The body or the host bone does not tolerate titanium osseointegration. In vitro experiments revealed that titanium could inhibits osteogenic differentiation of mesenchymal stem cells and cause genetic changes in connective tissue **[96, 97]**. Additionally, when titanium particles of a certain size are present in the body, they have a biological effect on the body's white blood cells **[98]**.

• **Vanadium (V):** Though, It has a lesser-known biological significance in the human body in terms of favorable cellular responses **[99,100]**. The disadvantage of vanadium is that its oxide looks to be toxic**[101]**, In animal

experiments, oral exposure or inhalation to V compounds and V resulted in carcinogenicity and might have a wide range of negative effects on liver , neurological system, blood parameters, respiratory system, and other organs**[101-103]**. It has recently been discovered that vanadium release and implant failure are related. When used in titanium alloys, the toxicity of V is readily obvious **[104]**.

• **Aluminum (Al):** Despite its little-understood biological significance in the body, Al may become toxic and hazardous in large amounts **[105]**. Aluminum toxicity is a serious issue in individuals with renal illness; moreover, aluminum causes the blood-brain barrier and altered function of brain neurotoxicity **[106-108]**. Similarly, high exposure to aluminum has been linked to an increased breast cancer and risk of Alzheimer's disease **[109,110]**. According to the most recent data, because of its action in estrogen receptors, Al can boost gene expression in human breast cancer cells **[111]**.

• **Niobium (Nb):** In the human body, it has a poorly understood biological role. This is related to the toxicity of certain niobium compounds, such as niobates and niobium chloride **[112,113]**. According to one study, niobium is one of most poisonous metal ions, causing immune cell death and encouraging DNA damage **[113]**. As a result, until further information is known, niobium should be handled with caution, particularly when combined with other alloying elements **[3]**.

• **Molybdenum (Mo):** an important trace element that is required by numerous enzymes such as aldehyde oxidase, xanthine oxidase, and sulphite oxidase **[114]**. Mo concentrations are lower in the vertebrae and greater in the kidneys and liver **[115, 116**. Because Mo is present in human tooth enamel, it aids in the prevention of tooth decay **[116]**. As a result, it is less corrosive and toxic than Ni, Cr, and Co **[114,117,118]**. According to latest studies, Mo toxicity has not been documented in the human body, and almost there is no evidence on Molybdenum's chronic toxicity in humans. But, it has been observed in animal

research that prolonged consumption of more over 10 mg/day can have effects on the liver, lungs, kidneys, as well as growth retardation, gout, infertility, low birth weight, and diarrhoea**[117,119]**. Furthermore, it has been observed that the concentration of Mo in blood in patients with hip resurfacing arthroplasty and metal-on-metal (M-OM) THR is typically lower than that of Ni and Cr **[120,121]**. So yet, no research on the Mo toxicity when utilized as a metallic implant in the body have been published **[3]**.

• **Zirconium (Zr):** Because it has a 1mg content in the human body, It has no inherent biological function in humans (toxicity of Zr compounds is low). Furthermore, if zirconium is powdered, it should be handled with care since it causes irritation and can induce lung and skin granulomas when breathed. Long-term Zr tetrachloride exposure was found to cause increased mortality rates in guinea pigs, as well as a reduction in blood haemoglobin and red blood cells in dogs **[122-124]**.

2.4 Corrosion behavior

Corrosion is described as a natural phenomenon. For metals, it is described as an electrochemical process or irreversible chemical reaction that occurs when the metal is exposed to its environment. In addition, the system is going into more stable state thermodynamically, according to the second rule of thermodynamics **[125,126]**. When metal is placed in a corrosive surrounding environment, it might react in three ways, depending on the environment and the metal. The first is a corrosion-free condition in which the metal is not oxidized. While the second way of reaction, occurs when the metal is in a state of activity, when it will result in metal loss and corrode, as well as the incorporation or dissolving of a corrosive elements into metal. The third way of reaction is in a state of passivity, in which the alloy or metal can form a passive protective oxide layer on its surface, which reducing the rate of corrosion **[127,**

128]. The typical electrochemical process of corroding a passive metal and an active metal is depicted in Figure 2.11**[33]**.

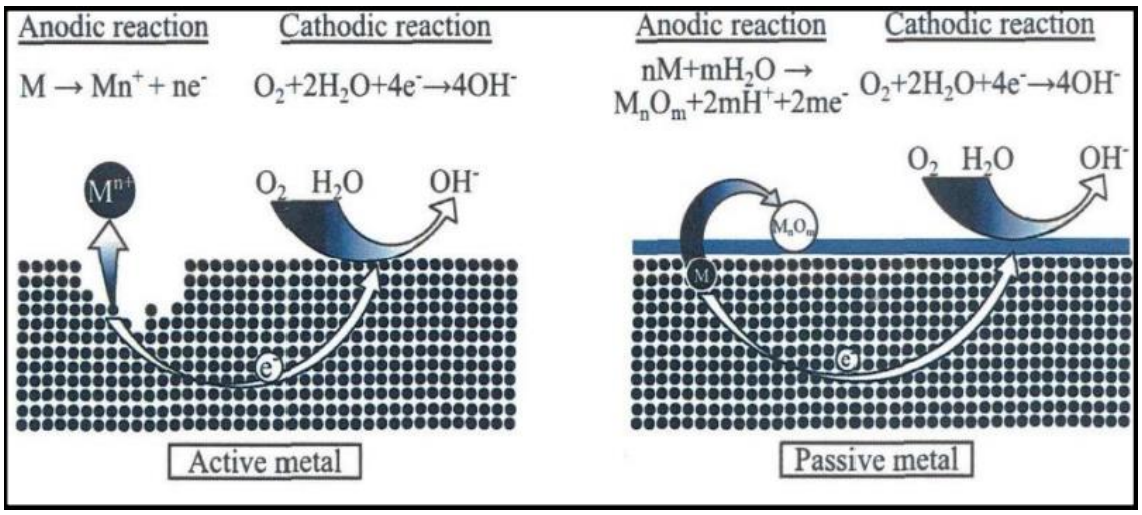

Figure 2.11. The diagram depicts the electrochemical processes that occur during the corrosion of a passive and an active metal **[33]**

In the case of metallic biomaterials, one of most popular kind of corrosion is aqueous corrosion. The anodic and cathodic reactions in an aqueous electrolyte occur on the metallic surface. The anodic process, which involves the loss of electrons from metal atoms (oxidation), and the cathodic process, It includes an oxidizing agent consuming electrons (reduction). The following equation can be used to illustrate the anodic half – cell reaction **[129]**:

$$M \rightarrow M^{+n} + n\ _{electrons} \qquad 2.1$$

The following equations can be used to depict the most frequent cathodic half – cell reactions:

$$2H + + 2e + \rightarrow H_2 \qquad 2.2$$

$$O_2 + 4H + + 4e \rightarrow H_2O \qquad 2.3$$

$$O_2 + 2H_2O + 4e \rightarrow 4OH^- \qquad 2.4$$

The cathodic half-cell process for hydrogen evolution was described by equation 2.2, whereas the cathodic half-cell reaction for oxygen reduction in acidic and alkaline solutions was represented by equations 2.3 and 2.4,

respectively **[129]**. Under equilibrium circumstances, in equation 2.1, the rate of reaction is utilized to determine the rate of corrosion for a metal (M). This is determined by the electrode potential and is known as the corrosion potential. However, during operating circumstances, a number of variables affect the corrosion potential. The kinetics of the reduction reaction, galvanic contacts with other metals, formation of passive surface film, temperature, and mass transport conditions, are variables that can affect the potential of corrosion for a metallic component. As a result, a metal's corrosion potential might vary based on the ambient conditions **[130, 131]**.

In biomedical applications, passive materials must be utilized. Titanium alloys are typically passive due to the spontaneous creation of a protecting oxides layer on the surface of titanium alloy as a result in the subsequent reaction:

$$Ti + 2H_2O \leftrightarrow TiO_2 + 4H^+ + 4e^- \qquad 2.5$$

Figure 2.12 depicts a possible polarization curve for protected passive material **[132]**. There are four possible domains identified: anodic, cathodic, trans-passive, and passive domains. The current is determined by the concentration of dissolved oxygen and water reduction, and this indicates the metal is located in the cathodic zone, when the potential is less than the Ecorr. The metal stays active (when the potential rises over the E_{corr}) in the anodic area until it reaches the region of passivation (E_{PP}). The current density falls at a moment called passive current density i_{pp}, and the potential approaches the value of passivation E_{PP}. The creation of a protective oxide layer of the metal's surface causes a decrease in current density. In the passivation area, the metal might still corrode, albeit at a slower pace. In the trans-passive zone, the potential will reach its breaking point, Eb, and the metal will begin to corrode fast. The metal has a more stable protective oxide layer if its Eb is value that is more positive. If the metal has a big differential between Ecorr and Eb, it will be more resistant to pitting and crevice corrosion. When the difference between

Eb and Er (re-passivation potential) is minimal, the metal is more resistant to localized corrosion **[133, 134]**.

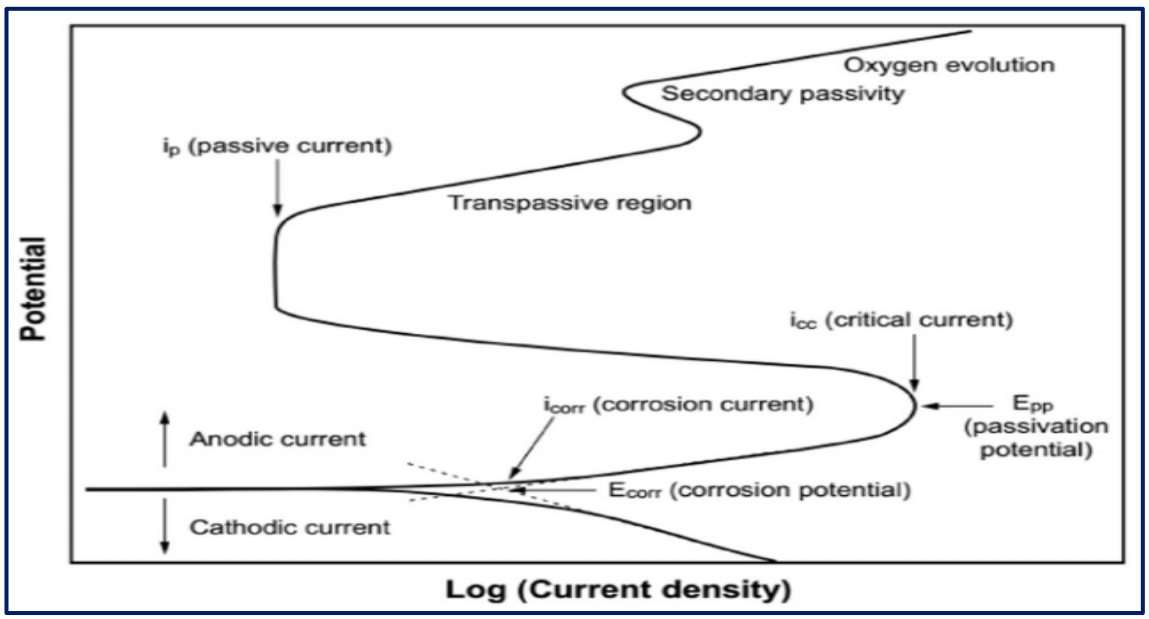

Figure 2.12. A passive material's typical polarization plot **[132]**

In a biosystem including metallic biomaterials, several corrosion processes can occur, including the localized corrosion, system being active, adsorption, passivation, passive dissolution, and transpassive. Figure 2.13 depicts a schematic of the processes that take place when a surface of metallic biomaterial coming into touch with an electrolyte. When the alloy or metal is free of the oxide layer, it becomes active. Passivation is the creation of a protective oxide film on a metal's surface. A metal will begin to corrode fast when it is in the transpassive case. When a strong attack happens in a restricted local area at a faster rate than the remainder of the surface, this is referred to as localized corrosion. In biosystems, adsorption is another prevalent phenomenon that happens when a specific species, such as proteins, biomolecules, or cells, is present in the bodily fluid. The rate of corrosion may be regulated by the mass transfer rate of anodic reaction products, the charge transfer reaction kinetics at the metal-electrolyte contact, and the characteristics of the passive oxide layers, according to adsorption phenomenon **[131]**.

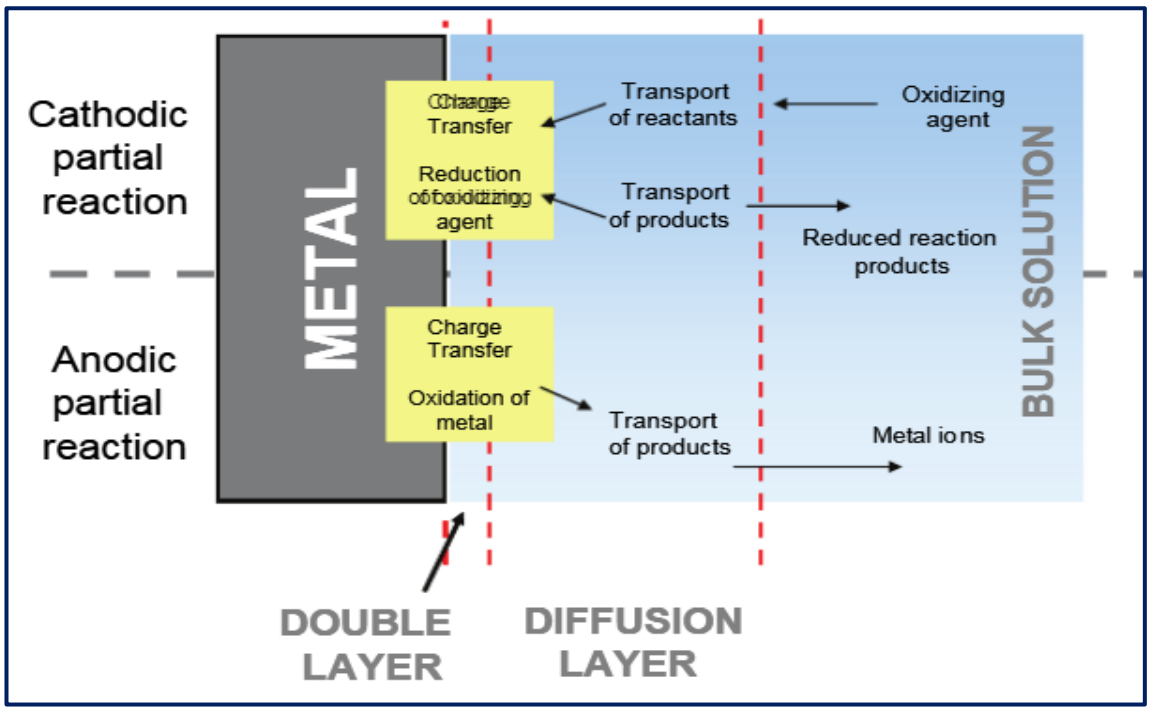

Figure 2.13 the reactions that occur when a surface of biomaterial metallic comes into touch with an electrolyte **[131].**

2.4.1 Electrochemical Techniques for Corrosion Study

There are several approaches available for measuring the corrosion rate of materials and understanding corrosion mechanisms. Simulated service and field approaches are utilized to examine the corrosion reaction of a certain portion of a substance over an extended time. Laboratory accelerated tests are performed in the event of a specific environment and to gain the corrosion rate and a more general understanding of the corrosion processes **[125]**. The laboratory practice of investigating the electrochemical characteristics of materials use a cell with three electrodes. To determine the working electrode's potential, a reference electrode (RE) is required in the three-electrode cell. The counter electrode (CE) is composed of platinum gold, or graphite, and is utilized to transport the current through the circuit. The examined sample is the working electrode (WE). An electro motive force (e.m.f.) source, a galvanometer and a voltmeter in electrolyte solution are joined to all electrodes **[125, 135]**. To examine the function of potential and the corrosion mechanisms on the electrochemical responses of the change in current at given potentials,

the materials, the potential, and current may be monitored **[125, 135]**. The techniques listed below are widely utilized to investigate material electrochemical reactions.

2.4.1.1 Open Circuit Potential (OCP)

The rates of anodic and cathodic reactions are identical in this sort of measurement. There is no external voltage or current provided in the course of the open circuit potential technique method (OCP), also known as free corrosion potential (E_{corr}), hence the net current flow is zero from or to the electrode. The value of E_{corr} is frequently estimated, and it provides preliminary description on whether the material is active or passive in the investigated environment, the material's surface state, and any changes that may occur in the material's surface condition.**[136]**

Moreover, OCP may be utilized to determine if the passive layer on the material's surface in the surrounding environment has been degraded over time or removed, as well as the point at which it has lost its integrity. The corrosion is more likely, and material is active if the OCP is low. When a material has an OCP that is high, it is in a passive condition. The importance of OCP in giving information on the state of the material over time cannot be overstated, and indicating any sudden changes in potential produced by a change in the surface of material during testing. When the open circuit potential changes from a high to a low value, cathodic shifting might occur in the material, indicating the presence of an active surface on the substance. In fact, When the OCP value shifts from a low to a high, passivation begins**[137]**.

Even though there are several benefits of employing OCP, it is necessary to discuss a few of the drawbacks. The OCP value obtained by this approach, for example, is an average value of the material's whole surface that does not exhibit discrete regions that may have anodic and/or cathodic potential. As a result, some of the material's surface may be corroded at a potential value lower

than the suggested OCP value. Additionally, the OCP only reflects the material's surface state in a corrosive medium at the time of the test, and provides no information regarding the quantity of corrosion or the rate of corrosion occurring over time. The data of OCP may be compared across different materials to get a sense of how these materials will corrode, as well as their corrosion resistance in relation to one another **[138]**.

2.4.1.2 Potentiodynamic polarization (PD)

For corrosion investigations, this is one of the most commonly used techniques of electrochemical behavior. Using this method, the passive current density as a function of the applied potential may be determined dynamically, it is referred to as a polarization curve. During a potential sweep, the substance is subjected to a potential that varies from cathodic potential to anodic potential. The rate of corrosion over time is shown by the change in current density during this operation **[136]**.

Figure 2.14 depicts a passive material's polarization curve **[139]**. If the material has a high corrosion potential, a low current density in the passive state, and a wide passive potential, it will be corrosion resistant. The material, on the other hand, is more active and is more susceptible to corrosion attack, when it has a higher current density **[140]**. In a certain corrosive environment the free corrosion potential of a material and corrosion current density (i_{corr}) estimated using Potentiodynamic polarization by using the Tafel plot, which is one of the easiest ways for measuring corrosion rate under free corroding circumstances**[139, 141]**. Figure 2.15 depicts a typical Tafel plot **[140]**.

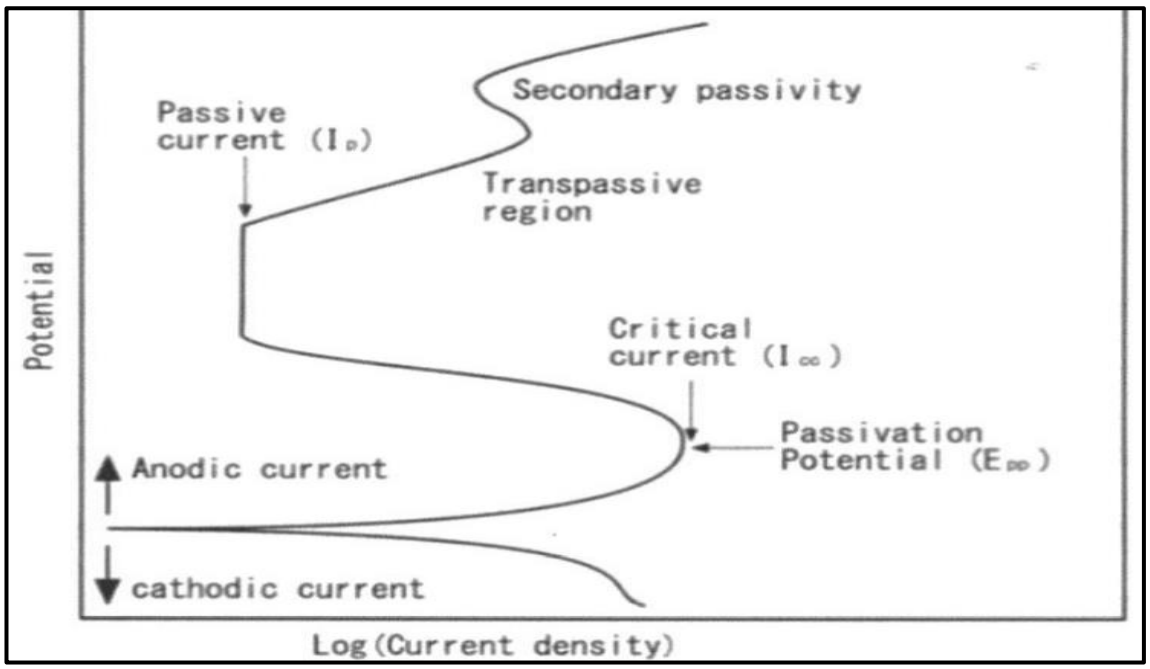

Figure 2.14. A fictitious polarization of a passive metal **[139]**

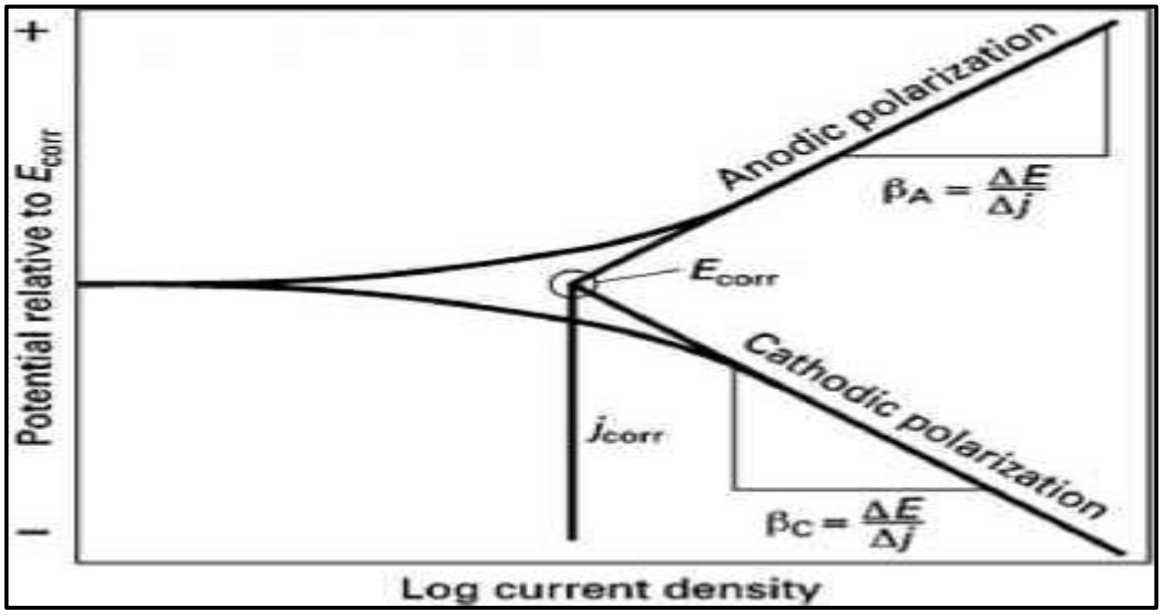

Figure 2.15. The Tafel plot for calculating corrosion parameters **[140]**

2.4.1.3 Potentiostatic Polarization (PS)

The substance is exposed to a stable potential in this method. The potential used either anodically or cathodically, and the current is computed over time. The time - current relationship between time and current can reveal information about the electrochemical kinetics of the test **[130]**.

This method may be used to determine the development or deterioration of inert oxide layers on the corrosive material surface. The Point Defect Model (PDM) and High Field Theory (HFT) are utilized to describe the change in ion flux at the protective and passive surface layer. As the thickness of the protective oxide surface layer rises over time, the ion flow decreases, causing conduction to decrease and, as a result, the current density to decrease **[142-144].**

To estimate the rate of current decay over the time, use the following equation **[143-145]**:

$$I = 10^{(-A+K\ logt)} \qquad 2.6$$

K denotes the slope of the log I against log t curve. The k value provide knowledge about the passive film's structure as well as the state of passive material's surface in an environment. For example, if K= -1, the oxide layer is likely to be robust and protective. If the K value is -0.5, the oxide layer does not serve as a barrier and may be that a passive layer is not present or damaged. If the K value is near or equal to -1, the passive oxide layer is more protective, robust, and stable in a certain corrosive surrounding environments **[143, 145]**.

2.4.2 Mechanisms of Corrosion

The mechanism of corrosion, the appearance of the damaged material, and the nature of the corrosion are defining variables that may be utilized to determine the kind of corrosion. The kind of corrosion can also be determined visually **[146]**. Corrosion is influenced by not only the metals type or alloys used, the surrounding environment also plays a major role. Environmental factors such as electrolyte concentration, temperature, and the presence of living organisms, pH, and electrolyte motioncan all affect the corrosion reaction of metals or alloys. Corrosion environments with alkaline or acidic electrolytes can be air, aquatic, subterranean, or soil; mixtures of these conditions are conceivable **[138, 146]**.

2.4.3 Corrosion of Titanium Alloys

Titanium alloys are naturally capable of producing and growing a protective oxide layer with a thickness ranging between 2 and 5nm. As a result, titanium alloys exhibit high corrosion resistance in a variety of corrosive environments. Titanium oxide films have strong adhesion to the substrate surface and the capacity to self-repair if broken. This enables titanium alloys to withstand the majority of oxidizing media, such as nitric acid solution, chlorides, sulfates, hydrochlorides, salt, and sulfides **[82,147]**. Titanium alloys, on the other hand, are unable to tolerate fluoride ion presence in strongly oxidizing and reducing environments **[82,147,148].** These corrosive environments have the potential to degrade and damage the passivating oxide layer **[148]**.

There are four of corrosion behavior responses, which are depicted in Fig. 2.16**.** An active reaction is the first state of response, where titanium oxidized rapidly, resulting in Ti (III) ions. The second state of response is a passive state (inactive state), wherein titanium is protected by passive oxide films, where it significantly reduces the rate of oxidation. Ti (IV) ions, on the other hand, produced by raising the immersion time. This ion can move through into oxide passive film on the substrate surface (base material surface) or enter solution. The 3rd state (known as a translational state) which combines active and passive state, in which the oxide layer only partly blankets the titanium's surface, keeping it from passivating. Hydrogen evolution state is the fourth state when exposed to a sufficiently negative voltage; titanium may be damaged by hydrogen evolution. Wherefore, There are several environmental factors influences the responses, these include pH, duration of exposure, and temperature **[149].**

When adding alloying elements such as Zr ,Nb, Mo, and Ta, it was found that they are oxide layer stabilizer on the surface in biological conditions and

create protective stable oxides, for instance ZrO_2, Nb_2O_5, Ta_2O_5, and MO_2**[150-154]**. With these elements titanium alloys show superior corrosion resistance to that of stainless steel (AISI 316L) and wrought (CoNiCr) alloys **[150]**. Effect of the Ti-alloy microstructures is noticeable on the corrosion property. The passive corrosion current density increased if rising the transition ratio for α to β phase in Ti6Al-4V. These rises are due to the formation of a galvanic cell between the different phases (α and β phases). The microstructure type when employed as biomedical metals, titanium alloys play an extremely essential function in corrosion resistance **[155]**. The kind of thermomechanical technique and thermal heat treatment used have a major influence on the corrosion reactions **[156].** For instance, the reaction of corrosion following heat treatment aging differs from the reactions following heat treatment solution. Moreover, the kind of forging, heat treatment, cooling medium, thermomechanical process, cold rolling, and hot rolling will all have an influence in titanium alloy corrosion reaction **[156-161]**.

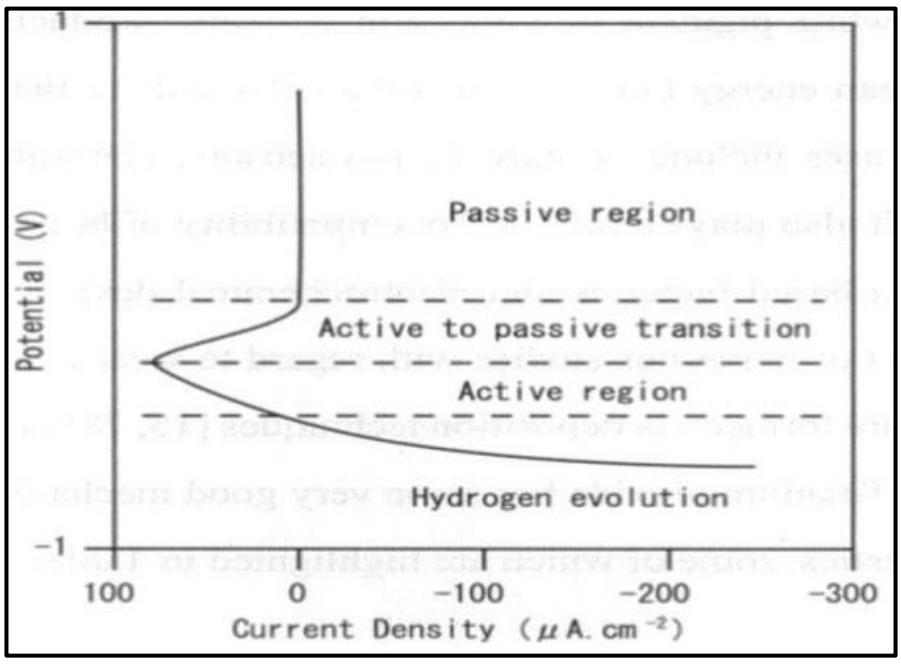

Figure 2.16. The relationship of current-potential for titanium in an acidic solution **[149].**

2.5 Tribology behavior:

2.5.1 Friction

A resistance force known as friction is created during the movement of two touching bodies. Any material's friction response is determined by its structure, surface condition, and whether the contact is corrosive, lubricated, or dry **[162]**. In different applications, friction has a negative and positive side. Whenever friction behavior is desired, clutches and brakes are instances of friction's positive side. In contrast, bearings and gears are examples when friction is unwanted **[163**, **164]**. Because friction is usually connected with mechanical wear, controlling the degree of friction between the two bodies' contact surfaces is critical **[127]**.

2.5.1.1 The Coefficient of Friction

The friction coefficient (COF) is the most popular method to measure friction. COF is affected by multiple factors, such as structural changes, chemical changes, and topological changes, this factor change throughout the, mechanical wear process **[162, 164]**. The friction coefficient between any two surfaces that come into contact is measured using **[162]**:

$$\mu = F_t / F_n \qquad 2.7$$

Where: Ft is the tangential force it is essential for two opposing bodies be moved if they are pushed relative to one another, and F_n denotes the intended moving body's normal load.

2.5.1.2 Frictional components

Friction has two components: adhesive friction force (F_a) and deformation friction force (F_d), and both of them will take place throughout slipping **[163,164,127]**:

$$F_t = F_d + F_a \quad 2.8$$

In which F_t denotes total frictional force, F_a is denotes adhesive friction force, and F_d denotes deformation friction force.

Roughness of the surfaces is an essential consideration for regulating friction processes (figure 2.17). Figure 2.17 shows that adhesive friction dominates at low roughness of the surface, whereas when the roughness of surfaces is significant, deformation friction predominate. Additionally, in an optimal roughness range, The friction is the lowest, grows below the optimal roughness range owing to improved adhesion of opposing smooth surfaces, and then rises beyond the optimal range of roughness because of an increasing in asperity deformation **[163-165]**.

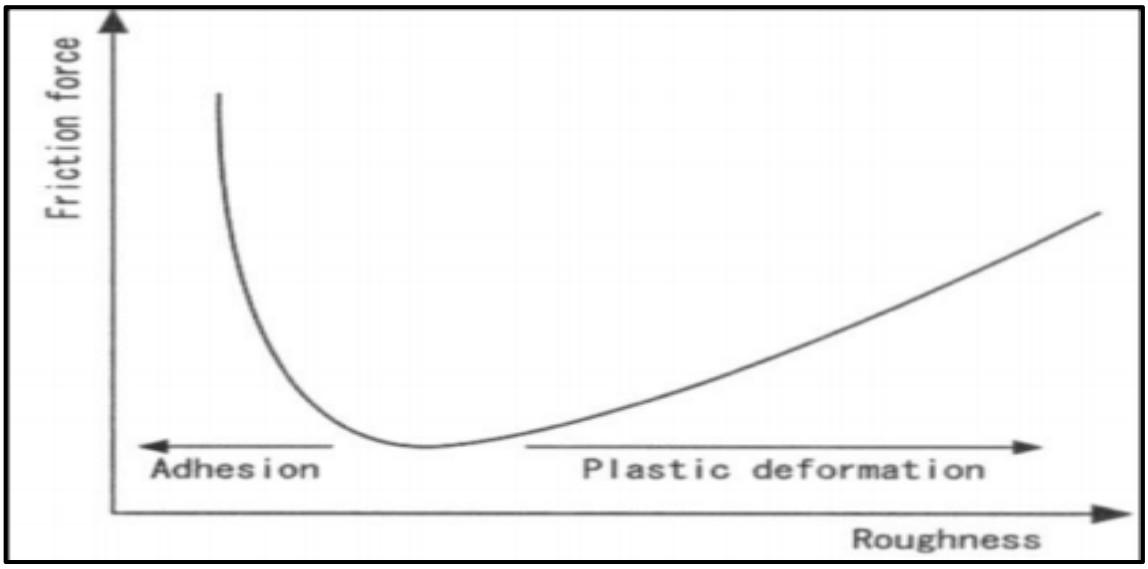

Figure 2.17. Roughness' effect on friction. **[165]**

2.5.2 Wear phenomenon

Wear is one of the most common types of material surface damage caused by the movement of two surfaces relative to one another. Wear causes material deterioration, which can result in the rate of material degradation, and failure. Is largely linked to environmental conditions and the surface of the two materials in touch **[162, 127,165-167]**. The following equation can be utilized

to estimate the amount of missing or lost material throughout the wearing process **[167]**:

$$V/L = K\ (F_n/\ H) \qquad 2.9$$

In which V denotes the volume loss throughout the wear test, K denotes the wear coefficient, L denotes the overall distance of sliding throughout the wear test, F_n denotes the normal applied load throughout the wear test, and H denotes the material's hardness.

The preceding equation may be adjusted to compute the substance volume loss throughout the wear test per unit force and per unit distance, as shown below **[167]**:

$$k' = K/H \qquad 2.10$$

$$k' = V/LF_n \qquad 2.11$$

The dimensional wear coefficient is denoted by k′. ($mm^3N^{-1}m^{-1}$)

2.5.2.1 Wear Mechanisms

Wear might be lubricated (wet wear) or non-lubricated (dry wear). To slow down the rate of wear lubricants are often utilized. On the other hand, wear, may be categorized depending on the material wear response mechanisms. The most common approaches, which include abrasive wear, corrosion wear, adhesive wear, and surface fatigue wear **[127]**. As shown in figure 2.18, welding (Micro-junctions) between two opposite surfaces during rubbing can cause adhesive wear. When a softer surface comes into contact and rubs with a hard surface, abrasive wear occurs. As a result, as seen in figure 2.18, two or three bodies of abrasive wear can develop. In the system of abrasive wear for two opposite body, two rubbing components are engaged, but in the system of abrasive wear for three contact bodies, a hard particle is caught between the rubbing surfaces. Cracking (brittle fracture),

Ploughing, and cutting, can all cause abrasive wear. Figure 2.18 shows how when there is a cyclic loading during wear fatigue wear can occur. Rubbing surface corroded (oxidation) can accelerate corrosion wear when rubbing occurs in a corrosive environment **[166]**.

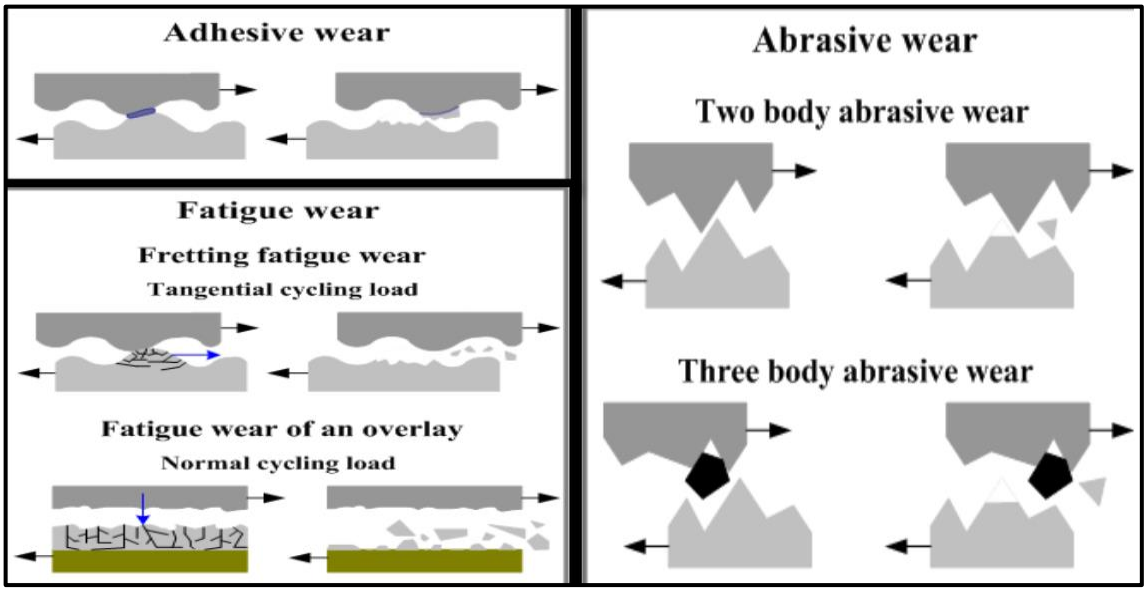

Figure 2.18. Wear mechanism diagram **[168]**

2.5.3 Lubrication

Lubrication is commonly utilised to minimize the friction along rubbing surfaces. The most often used kind of lubricant is oil or grease. Lubricants, on the other hand, can be solid or liquid **[127,166,167]**. According to one study, Lubricating liquid flow characteristics are closely connected to friction reduction during lubricated sliding. The following equation provides a measure of the likelihood and severity of lubricated sliding asperity contact λ **[169]**:

$$\lambda = t_{min} / \sigma * \qquad 2.12$$

Where minimal layer thickness denoted by t_{min} and $\sigma*$ is the rubbing surface's root mean square surface roughness, this may be calculated using the following formula:

$$\sigma*^{2} = R_{q1}^{2} + R_{q2}^{2} \qquad 2.13$$

Where Rq_1^2 is the initial surface's mean square surface roughness value, and Rq_2^2 denotes the second surface's mean square surface roughness.

The hydrodynamic lubrication regime is represented by a full separation of the rubbing surface by fluid, resulting in decreased wear and friction. The mixed elastrohydrodynamic lubrication regime is indicated by $1<\lambda<3$ when a There is a fluid layer between the rubbing surfaces, yet asperity contact occurs. When 1, generally coupled with slow sliding speeds or high loads, boundary lubrication occurs, that can cause significant surface damage **[127, 166, 167]**.

The friction coefficient (COF) is proportional to the relative speed of the two surfaces (ω), the contact pressure inverse (P), and the lubricant viscosity (η), and can be computed using the equation below **[169]**:

$$\mu = \eta\omega / P \qquad 2.14$$

Stribeck's diagram (figure 2.19) depicts this relationship, with the value on the right-hand side of the lubrication parameter equation. The figure depicts three lubrication regimes: hydrodynamic lubrication, boundary lubrication, and mixed elastrohydrodynamic lubrication. Because of the enormous quantities of contacting surfaces during rubbing, the coefficient of friction in boundary lubrication varies slightly in relation to the lubrication parameter. When the lubrication parameter is increased, a fluid layer forms between the rubbing surfaces; as a result, surface contact distance was minimized, It is known as the mixed lubrication regime. In this regime, increasing the lubrication parameter leads to lowest friction factor, shown in figure 2.19. Although, as the lubrication parameter is increased further, Because of shear and fluid drag inside the lubricant, the coefficient of friction rises **[167]**

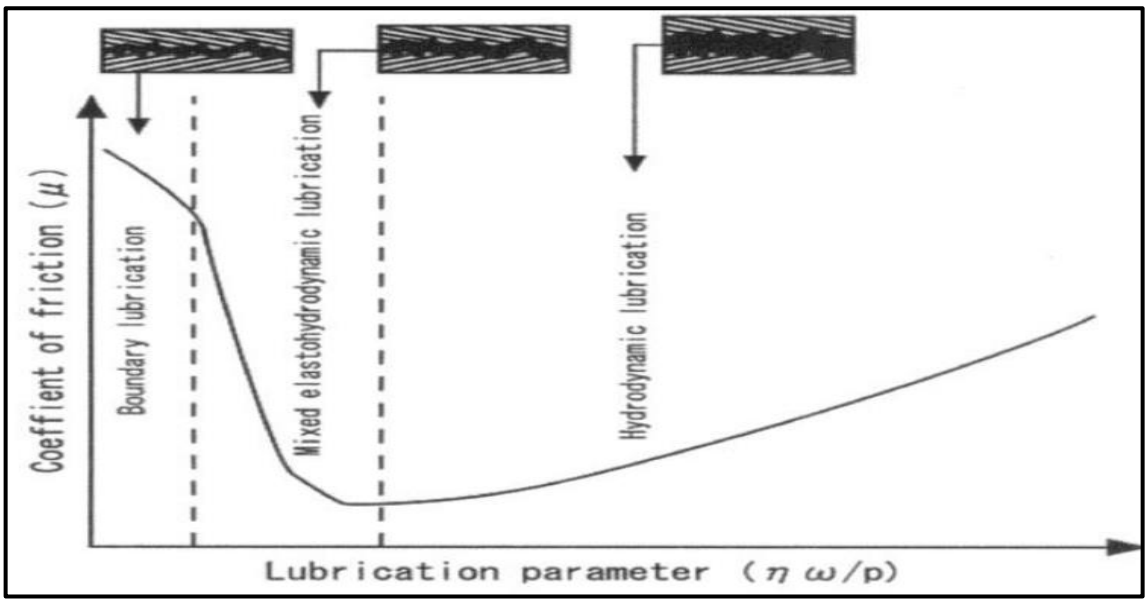

Figure 2.19. Stribeck's curve **[167]**

2.5.4 Techniques for Tribological Testing and Characterization

Generally, the tribometer can be used to monitor the test system's tribological response and the purpose of measuring the development of the friction coefficient is often to examine the tribological behavior of metallic biomaterials, varieties of methods are utilized, such as pin-on-disc, block on-disc, and ball-on-disc (figure 2.20). At 37±2 ° C, simulated bodily fluid is utilized as surroundings in the tribological testing system to simulate actual or ambient circumstances. However, dry sliding conditions are also used for tribological testing **[7, 170-177]**. Table 2-12 lists the benefits and drawbacks of numerous methods of wearing are employed in the system of tribological testing**[178]**.

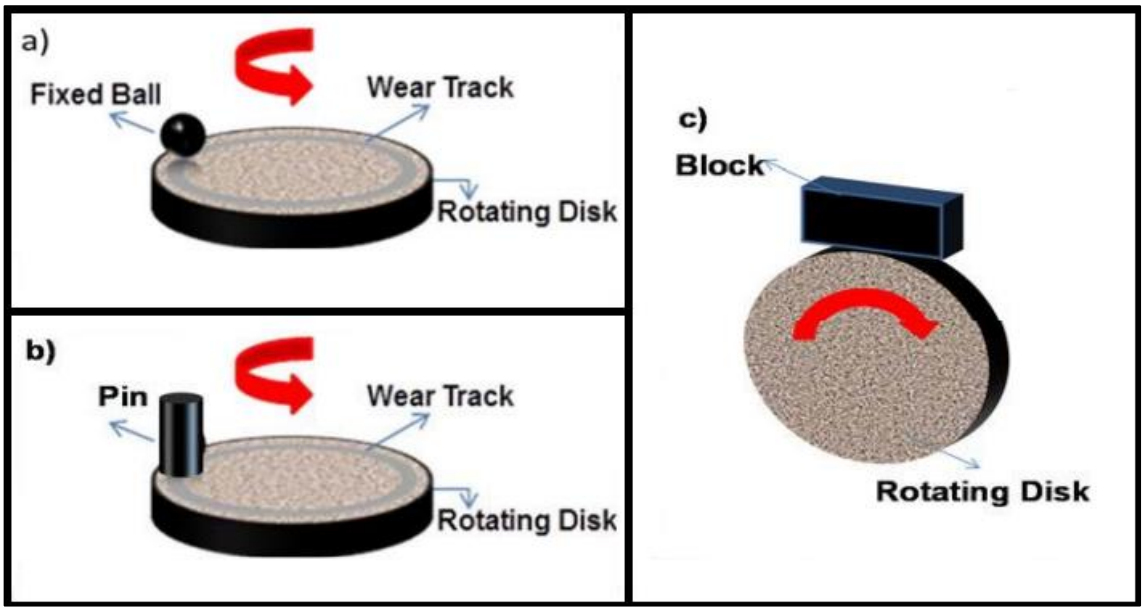

Figure 2.20. Methods of wear testing are depicted in a flowchart **[7]**.

Table 2-12 the benefits and drawbacks of different techniques of wear testing **[178]**.

Test	Advantages	Disadvantages
Pin-on-Disk	After run-in, surface pressure remains constant. Easy to determine wear volume and wear rate. The model closely simulates a linear friction bearing.	Difficult to align pin. If the pin does not stand perfectly vertical on the plate, edge contact results. A very long run-in time is therefore necessary. The front edge of the pin can skim off lubricant. This makes a defined lubrication state impossible.
Ball-on-Disk	High surface pressures are possible. The ball skims off lubricant less than a pin does. The model is similar to a linear friction bearing and a radial friction bearing.	Very small contact ratio: The contact surface of the ball is small compared to the sliding track on the disk. The contact area is enlarged by wear. Difficult to determine the wear volume of the ball.
Block-on-disc	The model is capable of simulating a variety of harsh field conditions, e.g., high temperature, high speed, and high loading pressure.	

2.5.5 Tribology of Titanium Alloys

Titanium alloys have been widely investigated in recent decades owing to titanium's unique mix of characteristics, which include high corrosion resistance, lightweight, biocompatibility, and good strength. However, published research on titanium's tribology reaction has found that the metal is unsuited for tribological uses **[179, 180]**. Throughout titanium's frictional response, more than one factor is at work. During tribology testing, the combined effect of lubrication ineffectiveness, electron configuration, and crystal structure are the primary contributing variables that cause in severe

adhesive wear and high wear rates (figure 2.21). In tribological applications, this combined effect leads in very unstable titanium friction **[179, 181]**.

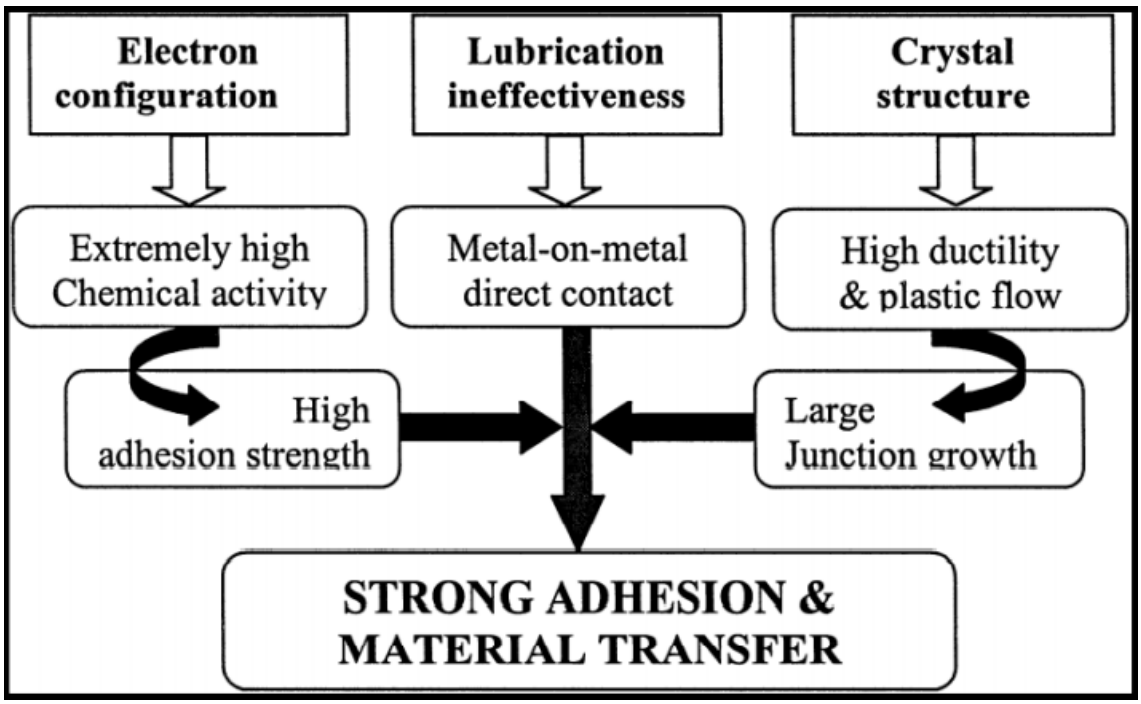

Figure 2.21 Materials factors influencing titanium's tribological performance**[179].**

Titanium alloys have increased their wear resistance under a variety of situations. In general, adding Nb to titanium alloys improves their wear resistance and raises their COF. The formation of Nb_2O_5 particles during the heat treatment of Nb-containing titanium alloys improves wear resistance. Coating and surface treatment are essential in improving titanium alloy wear and friction resistance. Abrasive wear was found to be the most common wear mechanism **[7, 182, 177, 183-186]**.

2.6 Literature Review:

2.6.1 Literature Review about Corrosion

The electrochemical behavior of Ti-alloys in various solutions has been widely studied. They discovered that the creation of a protective passive on the titanium alloys' surfaces significantly reduces the rate of

corrosion. They also discovered that the electrochemical behavior of titanium alloys that affected by the repassivation behavior after corroding.

Alves et al. [187] shown that the resistance to corrosion of titanium alloys from β-phase type depends on the stability of protective layers. Therefore, they discovered that Ti–10Mo alloy primarily after the heat treatment process (solution heat treatment at 1000 °C in argon atmosphere) has obviously low passive current densities.

Alves et al. **[188]** also studied the corrosion resistance of Ti–6Al–4V and CP–Ti alloy at 25°C (Room temperature) and 37°C (body temperature) in simulated body fluid. They discovered that at 25°C, the corrosion resistance of Ti–6Al–4V and CP–Ti alloys is higher. As a result, temperature has a significant effect on the corrosion behavior of Ti–6Al–4V and CP–Ti alloy.

Kumar et al. [189] found that, CP–Ti, Ti–6Al–4V and Ti–15Mo alloy, all in Ringer's solution have perfect corrosion resistance, however only the Ti–15Mo alloy exhibits an inert and stable oxide layer in fluoride solution. High fluoride solution can be found in the body, for example, during dental cleaning. They also studied the corrosion behavior in the Ringer's solution for CP–Ti, Ti–6Al–4V, and Ti–15Mo alloy, and they conclude that the passivation range for Ti–6Al–4V (155–1460 mV versus SCE), and CP–Ti (145–1522 mV versus SCE) is less than for Ti–15Mo alloy (166–2513 mV versus SCE). They compared Ti–15Mo alloy against Ti–6Al–4V alloy and CP–Ti alloy. Therefore, they concluded that Ti–15Mo alloy has better corrosion resistance than the other.

Bai et al. [190] study the corrosion performance in the simulated physiological environment between Ti–24Nb–4Zr–8Sn, CP–Ti, and Ti–6Al–4V. Their results presented the Ti–24Nb–4Zr–8Sn alloy exhibits during the corrosion low current density when compared to CP–Ti and Ti–6Al–4V alloys. Moreover, the Ti–24Nb–4Zr–8Sn has a wider passive area than CP–Ti and Ti–6Al–4V alloys. According to the formation of the stable

inactive, film mainly, because of the formation of niobium and titanium oxides on the surface.

Bolate et al. [191] , this research presents three Ti-Mo alloys exposed to electrochemical tests in neutral and acidified Ringer's solution (pH3.1). Both the oxide films effectively protect the surface of these alloys in potential range (up to +1.00V vs SCE). Two layers of oxide films are formed, the outer layer was porous and the inner layer was compact. The inner compact oxide film has smaller corrosion resistance in the acidic environment. However, with increasing Mo content corrosion resistance increase.

Simsek et al. [191], in this study, they used the Ti-6Al-4V and Ti-5Al-2.5Fe alloys, and the electrochemical corrosion behavior of them was studied in simulated body fluid environment. They found that the α phase is the dominant phase in both alloys. According to the literature, they found that the Ti–6Al–4V alloy showed longitudinal pits along the grain boundaries, it has been considered that the reason for this is the dissolution of V-rich zones. Eventually, they concluded that the Ti-5Al-2.5Fe alloy has the higher corrosion resistance(the I_{corr} value of the Ti5Al2.5Fe alloy was measured to be 18.24 mA/cm^2, and the I_{corr} value of the Ti6Al4V alloy was measured to be 43.58 mA/cm^2).

Wang et al. [193], they found that Ti–35Nb contains β phase dendrites and undissolved Nb particles. It can directly form an instant stable passive film oxide layer to protect its surface (chiefly consisting of TiO_2 and Nb_2O_5). A heterogeneous structure is always caused by SLM-produced Ti–35Nb utilizing mixed powder the use of the powder method, with Individual Nb grains. They found that the heat treatment in an Ar atmosphere at 1000 °C for 24 h seriously enhance the chemical homogeneity. Then, the treated SLM-Ti–35Nb has a greater corrosion potential than the SLM-produced Ti–35Nb)-0.46 V versus saturated Calomel electrode) and (-0.55 V versus SCE) respectively.

Chui et al. [194] used as-cast Ti–Zr–Nb– Mo alloys with varying Mo concentrations, to investigate the corrosion behavior. They found that when the ratio of molybdenum in the alloy increases, the grain size of the alloy will decrease, this is because the molybdenum content causes constitutional undercooling. In addition, the results showed that alloy containing Mo with 15% has lowest current density (2.31 ±0.03 μA cm^2).

Zareidoost et al. [195] used Ti–25Zr–10Nb–10Ta alloy and studied in the Ringer's solution its corrosion resistance when adding separately Ag, Fe, and Sn they found that the best corrosion resistance obtained with Ag addition. The Ag addition leading to increase the formation of stability passive Ti–25Zr–10Nb–10Ta alloy surface, This is due to its more positive standard electrode potential(0.799 V) compared to that of titanium (-0.98 V), for this reason, the Ti–25Zr–10Nb–10Ta–1.5Ag alloy is more corrosion resistant.

Jawed et al. [196] studied the addition of Mn and Zr to Ti–Nb alloys which gave different microstructures. Clearly, the microstructures of Ti–Nb–Zr–Mn alloys β-type vary when the Zr and Mn concentrations change. In all Ti–Nb–Zr–Mn alloys the equiaxed β grains has appeared. Mn element is a functional and effective growth-restriction factor with Ti alloys. They found that the addition of molybdenum to the Ti–Nb–Zr–Mn alloy leads to a reduction in the grain size. However, the addition of Mn during solidification process causes a fast buildup of constitutional undercooling. Thus, the grains are refined because nucleation occurs prior to an approaching solid–liquid interface. In comparison, also the average grain size of Ti–Nb–Zr–Mn alloys grows as the Zr concentration increases. This leads to fine-grain strengthening effect, in addition to being a beta-phase stabilizer, Zr element also serves as a β -stabilizer. The stability of the β -phase enhances, when the proportion of zirconium exceeds the required limit, remarkably. In addition, it will lower the (α + β)/ β phase transition temperature .

2.6.2 Literature Review about Wear

Several recent research focusing on tribological phenomenon of different types of titanium alloys. Have found that friction coefficient and wear resistance have progressed in many situations. Repassivation and passivity of titanium alloys due to the production of an oxide layer formed while rubbing can have a significant influence on their tribological behavior.

The production of Nb_2O_5 particles during heat treatment with Nb increases the wear resistance of titanium alloys. Furthermore, titanium alloys require surface treatment and coating to improve their friction and wear resistance. Abrasive wear was discovered to be the most common wear mechanism. In this light, one of the goals of the current research is to better understand the tribological behavior of various phases of titanium alloys in Ringers solution.

Alam et al. [182], the authors utilized Ti-24Al-11Nb alloy of α″+β microstructure and Ti-6Al4V alloy, were subjected to dry sliding wear against hardened-steel counter bodies. A pin-on-disc type apparatus was used with a normal load of 15-45N and sliding speed of 1.88 ms -1. While rubbing this Alloys have the capability to induce an adhesive oxide films, as a consequence of which wear resistance is increased. As a consequence, the rate of wear for α″+β Ti-24Al-11Nb alloy was around 48 times less than that of the α+β Ti-6Al4V alloy at standard load 45N.

Choubey et al. **[197]**, in this research, they used Ti-13Nb-13Zr, Co-28Cr-6Mo, Ti-5Al-2.5Fe, Ti-6Al-4V and Cp-Ti alloys, to study the tribological behavior. The fretting experiments were carried out on candidate biometallic alloys against bearing steel at 10 N normal load for 10,000 cycles with relative displacement stroke between the flat and ball set to 80 μm and the frequency at 10 Hz on a fretting (low amplitude

reciprocatory tangential sliding) wear tester. The tests were performed in Hank's balanced salt solution to assess the performance of the materials in simulated body fluid (physiological) solution. As a result, they found that the lowest friction coefficient for Ti-5Al-2.5Fe alloy (0.3), while for other Ti-based alloys COF was in the range of (0.46–0.50).

Chiba et al [198], in this research, they examined the effects of carbides and microstructures of biomedical Co-Cr-Mo alloy (hereafter designated the forged CoCr alloy) and a high carbon cast CoCr alloy (hereafter designated the cast CoCr alloy), in hank solution on wear behavior. They using a pin-on-disk wear test with high carbon cast CoCr alloy. They found that Carbide precipitation in the coarse-grained structure of the cast CoCr alloy would account for the higher abrasive wear loss. The forged CoCr alloy, with no carbide and a refined grain size, which is more prone to strain-induced martensitic transformation, would exhibit excellent like-on-like wear resistance, mostly against surface fatigue wear, compared to the carbide-hardened cast CoCr alloy.

Ramos Saenz et al. **[199]**, this research looked at the compare between non-oxidized and oxidized Cp-Ti, Ti-6Al4V and γ-phase (Ti-48Al-2Nb-2Cr) , using a custom made bone pin arrangement and by using a linear reciprocating wear testing machine under both dry and simulated biological conditions with Ringer's solution. As a result, the highest friction coefficient of the oxidized γ- phase TiAl alloy appeared(0.9). They also concluded that the oxidized γ-TiAl alloy having a smaller amount of wear volume than Cp-Ti and Ti-6Al-4V alloys(0.0071g with lubricant and 0.01222g without lubricant).

CvijovićAlagić et al. [171], they used α′+β Ti-13Nb-13Zr and α+β Ti-6Al-4V ELI alloys, and their study discovered tribological behavior under various heat treatments. The friction and wear tests were performed by using a block-on-disc tribometer in Ringer's solution at ambient temperature with a normal load of 20-60 N and sliding speed of 0.26-1.0

m/s. As a result, they discovered that under all heat treatment conditions, α+β Ti-6Al-4V alloy outperformed α′+β Ti-13Nb-13Zr alloy in terms of wear resistance.

S.J.Li et al. [200], used Ti-Nb-Ta-Zr β_phase alloy with variation in Nb content improved by oxidation treatment, and compare this alloy with Ti-6Al-4V and stainless steel alloy, using a reciprocal pin-on-disc wear device in a 0.9% NaCl solution. They noted that wear resistant increase with Nb content. Therefore, they found that the wear losses of both Ti–Nb–Ta–Zr and Ti–6Al–4V are much less compared with that sliding on stainless steel and there is almost no wear on the surface of oxided Ti–29Nb–13Ta–4.6Zr. The wear resistance of Ti–29Nb–13Ta–4.6Zr improved significantly after oxidation treatment, due to the presence of Nb_2O_5 oxide particles on the diffusion hardened surface of the alloy.

Fellah et al. [201], this paper presents the tribology behavior for total hip prosthesis of titanium alloys. In this study, the alloys utilized are Ti-6Al-4V and Ti-6Al-7Nb; both of them have α+β phase. These two alloys have been studied under different normal load (6 and 10N). Furthermore, the sliding speeds used are (1, 15 and 25m/s). As the result, both alloys displayed similar friction and wear performance. They found that there is no important variation in obtained with Ti-6Al-7Nb, but with Ti-6Al4V alloy coefficient of friction increased linearly when sliding speed increased. Generally, the addition of Nb to Ti alloys can increases the COF, and improve wear resistance for titanium alloys

Lee et al. [202], their research displayed tribological behavior in Hanks solution of hot and warm-rolled Ti-13Nb-13Zr (β+α alloy), at temperature 37 °C. They came to the conclusion that there was no noticeable variance in resistance of wear between of them. Similarly, they indicated that for both alloys the friction coefficient of around (0.42-0.45).

Hooyar Attar[203], this paper studies the wear for commercial titanium prepared by two methods by using casting and selective laser

melting (SLM). SEM test show that Cp-Ti products by SLM have a (α′) martensite structure, and cast Cp-Ti have a plate like (α) microstructure. At load of 15 N, wear surface of both alloy show in SEM test shallow ploughing grooves. It is observed that when the load is increased to 30N, very shallow ploughing grooves observed in SLM Cp-Ti compared with cast Cp-Ti, so SLM has better wear resistance because of the fine grain size, martensitic microstructure, and micro hardness.

2.6.3 Literature Review about Elastic Modulus

Hon et al. [204], this study trying to develop Ti-Nb alloys to approximate the value of its modulus of elasticity to the modulus of elasticity of human bone. The experimental results of a Ti-Nb alloy that contains 14 mass percentage Nb reveal that the microstructure consists of dominant α phase and β phases. As the Nb content increases, the proportion of the α phase decreases gradually, and when the Nb content exceeds 34 mass%, then the microstructure becomes totally the β phase. As a result Ti-Nb alloy with Nb content (above 36 mass %) is favored to use in medical implants, with reducing the stress shielding effect. They stated that the various phases like (ω, βand α) have varying elastic moduli. It was discovered that they were related by $E\omega = 2.0E\beta$ and $E\alpha = 1.5E\beta$.

Moreover, **Kim et al. [205]** Ternary Ti–Nb–Si alloys consisting of biocompatible alloying elements have been produced to investigate the effect of alloying on microstructure and elastic modulus. It was found that Si has an effective role in suppressing the occurrence of ω-phase and decreasing the elastic modulus in the meta-stable β-phase region. Have reported that the metastable β phase has lower elastic modulus than stable β phase.

Majumdar et al. [206] they used β titanium alloys and near β, and furthermore they measured the elastic modulus by ultrasonic and Nano-

indentation methods. The information gathered from ultrasonic and nano-indentation techniques were analyzed and then compared with each other. They found the modulus of elastic for Ti–35Nb–5.7Ta–7.2Zr β-phase was half of that for Ti–13Zr–13Nb near β-phase alloy hot worked and then treated at 800 ◦C followed by water quenching plus it displayed low value of modulus of elasticity. The reliability of these techniques of elastic moduli calculation is being investigated in terms of microstructures of alloy.

Wen-Fu Ho et al, [207] they studied the effect of molybdenum content (1-20 wt.%) on mechanical properties and microstructure of a Ti–10Zr-based system, focusing on improving the strength/modulus ratio. In order to obtain the mechanical properties of the samples, a three-point bending test was carried out. Cast Ti–10Zr has α′ phase (hexagonal), when adding 1 wt. % Mo the structure remained essentially unchanged. However, with adding 3 or 5 wt. % Mo, the martensitic α″ structure was found. And when the molybdenum content is increased to 7.5 wt.% or greater, stability of the metastable β phase started. However, ω phase was detected only in Ti–10Zr–7.5Mo alloy. Ti–10Zr–5Mo alloy with α″-phase had the lowest elastic modulus among all Ti–10Zr-xMo alloys. As result, both of Ti–10Zr–5Mo and Ti–10Zr–12.5Mo alloys showed greater bending strength/modulus ratios (20.1 and 20.4), respectively.

Xu et al. [208], they created a novel β-titanium alloy Ti–5Mo–Fe–3Sn with a high yield strength of 740 MPa and a low elastic modulus of 52 GPa. The inclusion of Fe and Sn together inhibits the creation of the ω-type phase. In addition to insertion solid solution strengthening, this is the reason for these special properties of this alloy. Therefore, the selecting of the appropriate elements added to Ti alloys with β -type is helpful to controlling the mechanical properties for them.

2.6.4. Conclusion of The Peppers:

- Corrosion resistance is affected by the temperature of the medium, at a temperature of 37°C the corrosion resistance is lower than at a temperature of 25°C.**[188]**.
- Titanium alloys containing a β phase exhibit the lowest current density and therefore the lowest corrosion rate. **[187,189,190,193]**.
- Mo has an effective role in corrosion resistance and stabilization of the β phase at (10-15% Mo), as well as for Nb and Zr **[189-191, 193-196]**.
- Heat treatment also has an effective effect in increasing the corrosion resistance (for example at a temperature of 1000°C for a period of 24 hours the corrosion resistance of Ti-35Nb alloy with β phase)**[193]**.
- The wear resistance of titanium alloys depends on the alloy components. Some β-phase titanium alloys exhibit low wear resistance**[197,171]**. While some titanium alloys with a β phase show high wear resistance**[200]**. Zirconium plays an important role in increasing the wear resistance of β-phase titanium alloys.**[200]**
- Each phase has a different Young's modulus. ω phase shows the highest value of the Young's modulus, while β phase shows the lowest Young's modulus.**[204]**

Chapter Three

Experimental Procedure

Experimental Procedure

3.1. General View:

This chapter deals with the main features of experimental procedures, which were required to achieve the aims of this investigation. This chapter presents the alloys compositions, methods, devices and tests used in this investigation. Thus including, alloys preparation, chemical composition using X-Ray fluoresce (XRF), microstructure investigation using optical microscopy OM, Field Emission Scanning Electron Microscopy FESEM, energy dispersive X-ray spectrometer (EDX), and X-ray diffraction (XRD). In addition, it presents the mechanical tests such as micro – Vickers hardness (Hv) and elastic modulus measurement. Finally, it presents in vitro tests conditions of electrochemical measurements and tribology test. Figure3.1 shows the summary of the overall experiments used in this investigation to give the reader an overview of everything that was used.

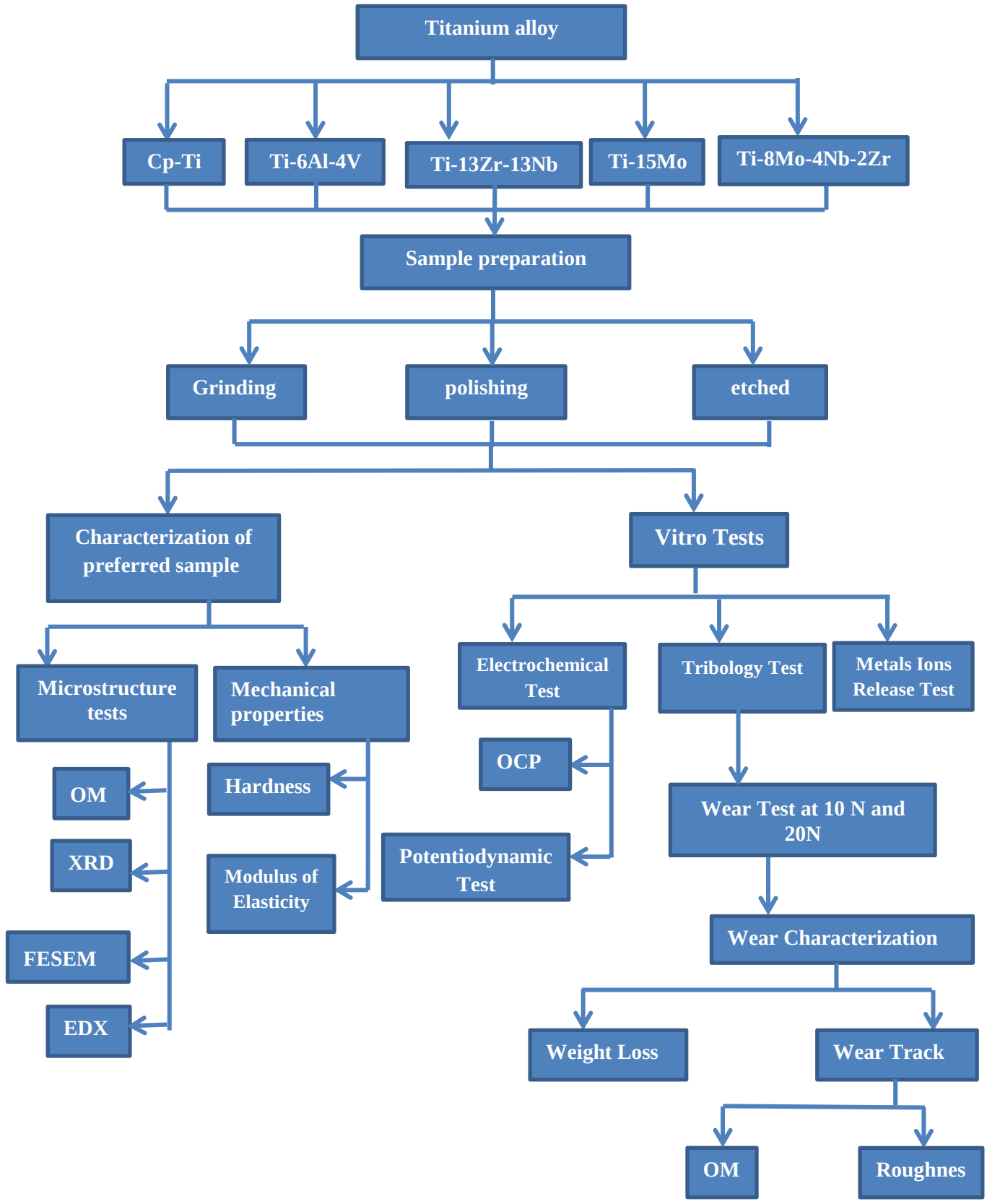

Figure 3.1: program of the present work

3.2. Used Alloys

In this investigation, five different titanium-based alloys Cp-Ti, Ti-6Al-4V, Ti-15Mo, Ti-13Zr-13Nb and Ti-8Mo-4Nb- 2Zr were used. Cp-Ti, Ti-6Al-4V, Ti-15Mo, Ti-13Zr-13Nb rods were purchased from Tianjin Xinija Albert Steel Trade Co., Ltd, China. Ti-8Mo-4Nb-2Zr was prepared in mercury center (UK) as a part of work of Zuheir Talib Khulief **[200]**. The chemical compositions of the alloys used in this investigation except Ti-8Mo-4Nb-2Zr was analyzed using (XRF PW2404) Calibrate with Philips Analytical X-Ray B.V. standards with certificate of the secondary for the SEMIQ, at Iran/ Tehran/ Tarbiat Modarres University/ T.MU. Analytical Lab. The chemical composition of Ti-8Mo-4Nb-2Zr was analysed using PANalytical Zetium X-Ray Fluoresce (XRF). The chemical compositions of alloys used in this investigation are listed in table 3.1.

Ti-15Mo, Ti-13Zr-13Nb, and Ti-8Mo-4Nb-2Zr alloys were selected on the basis that these alloys provide β- titanium alloys (second generation) with a range of stabilities varied from metastable through to highly stable β-phase. Also, based upon investigation data for these alloys, which reported that these alloys are believed to be acceptable for biomedical applications **[171, 189, 191, 197, 102, 906, 209]**. The traditionally used Cp – Ti and Ti-6Al-4V (first generation) were selected in order to comparison.

Table (3.1): Chemical compositions of titanium alloys used in this investigation.

Alloy	*Alloying Elements wt.%*						*ingot metallurgy parameters*
	Mo	*Nb*	*Zr*	*Al*	*V*	*Ti*	
Cp-Ti	-	-	-	-	-	99.667	Casting and hot rolling
Ti-6Al-4V4	-	-	-	6.133	2.973	Balance	Casting and hot rolling
Ti-15Mo	12.054			-	-	Balance	Casting and hot rolling
Ti- 13Zr-13Nb		12.561	11.266	-	-	Balance	Casting and hot rolling
Ti-8Mo-4Nb-2Zr	14.64	6.49	2.8	-	-	Balance	Cold rolling + solution treatment 900 C for 2h +water quenched

3.3 Titanium Alloys Characterization

The procedures used for microstructure investigation, mechanical properties, electrochemical and tribological investigation are described in the following section.

3.3.1 Microstructural Investigation

The microstructures of the titanium alloys used in this investigation were analyzed using optical microscopy (OM), X-Ray Diffraction (XRD), and Field Emission Scanning electron microscopy (FESEM). Before the microstructure investigation, alloys must be prepared in advance. The following is an explanation of how to prepare alloys for microstructure investigation.

3.3.1.1 Alloys Preparation

The ultimate goal of alloys preparation is to have a flat, mirror-like surface that is free from scratches, to obtain an ideal alloy ready for microstructure investigation. The alloy must meet certain conditions, such as having the least deformation after being cut, the alloys should be free from scratches caused by grinding and polishing, finally the sample should have a flatness sufficient to allow highest magnification. All alloys except Ti-8Mo-4Nb-2Zr were cut into the desired shapes 20mm in diameter and 3mm in thickness using wire cut machine. Ti-8Mo-4Nb-2Zr was cut into size of 20mm x 20mm x 3mm. Prior to OM, FESEM, XRD, micro-hardness, elastic modulus, electrochemical and tribological tests the alloys were prepared in consistent with the standard metallographic techniques using the following steps:

Grinding: At this stage, the cross-section of the alloys is grinded using fine grinding papers (SiC papers) and in the sequence from small numbers to the largest, from the coarsest to the softest (800, 1000, 1200, 1500, 2000, 2500, 3000, 5000, 7000, 10000). A series of parallel and one-way scratches run through the alloys, and light pressure is applied to obtain a surface with

the fewest possible scratches and a flat surface in addition to using water for cooling. Grinding was performed by using a grinding-polishing machine type Buehler, Metaserv-200, 200-240V AC, 50HZ, and Made in UK.

Polishing: The polishing stage is necessary in order to get rid of any scratches and be ready for the stage of etching and microscopy. The polishing cloth and diamond past type nature diamond with size 0.1 micron for 5 – 10 min. were used. After using the diamond paste, it is preferable to use water only with a cloth to obtain a shinier surface, using a grinding-polishing device and cooling with distilled water free of chlorine and continuous drying to avoid the formation of oxide layers. After finishing the polishing process, the alloys are stored in boxes containing moisture absorbent materials.

Etching: The alloys were etched according to ASTM (E407-07) standard using (10 ml HF + 5ml HNO_3+85 distilled water) for 15-20 sec. After the end of the immersion period, it must be stopped immediately by washing the sample with distilled water, after that it is sprayed with alcohol and finally dried with an air dryer to be ready for examination of the microstructure. Between each step, the alloys were washed with water, flushed with isopropanol and dried with an electric dryer.

3.3.1.2 X-Ray Diffraction Analysis (XRD)

The phase's constitutions of all titanium alloys used in this investigation were performed before electrochemical and tribological tests at room temperature. XRD instrument type a SHIMADZU Lab XRD-600, Japan, with Cu K_α, with wavelength (λ= 1.54060 Å). The test conditions were, radiation range of ($2\theta = 0°$ to $80°$), an accelerating voltage of 40 Kv, an electrical current of 30 mA, with 0.02 step size and 0.17s dwell time. The XRD was used in order to determine the phase constitution of alloys used at room temperature by compared it with standard charts. XRD tests

was done at laboratories of the Ceramic Department – College of Materials Engineering, University of Babylon.

3.3.1.3 Optical Microscopy Analysis (OM)

The microstructures of the Ti-alloys used in this investigation was tests using optical microscopy in order to identify the existing phase and see the shape and size of the grains after grinding, polishing and etched in a solution. This test was done at specimen's preparation laboratory, using an optical microscope type (BEL PHOTONICS), located in the laboratory of thermal transactions in the laboratories of the Metallurgical Department – College of Materials Engineering University of Babylon.

3.3.1.4 Field Emission Scanning Electron Microscopy (FESEM)

The FESEM and EDX analysis was undertaken using a (ΣIGMA, JSM-7610F, Carl Zeiss, mead in DE) equipped with an Energy Instruments Dispersive X-ray spectrometer (EDX). The FESEM and EDX were done at Iran/ Tehran/ Eria Electron Lap.

3.3.2 Mechanical Properties

3.3.2.1 Micro-Hardness Test

The micro-hardness measurements were implemented by three point measurements with a 100g load for 20s holding time according to ASTM (E92-17) standard. The test was done using the TH-717, Digital Micro Vickers Hardness Tester at the Metallurgical Department – College of Materials Engineering University of Babylon. The hardness was recorded as an average of three reading for each alloy.

3.3.2.2 Elastic Modulus by Ultrasound Technique

The elastic modulus of all titanium alloys samples used in this investigation was measured using ultrasound technique, and the sample

dimension was (3cm*2cm). A (cut-4) device, located in the Department of Polymer Engineering / College of Materials Engineering / University of Babylon, was used.

To calculate elastic modulus (E) of titanium alloys used in this investigation, the following equations were used **[209]**.

$$E = \frac{\rho V_S^2 \ (3V_L^2 - 4V_S^2)}{V_L^2 - V_S^2} \qquad 3-1$$

Where: E = Youngs modulus of alloy, ρ = density of alloys V_L = longitudinal ultrasonic wave velocity, V_S = shear ultrasonic wave velocity.

To calculate V_L and V_S, equations 3.2 and 3.3 were used **[209]**.

$$V_L = 2l/t_L \qquad 3-2$$

$$V_S = 2l/t_S \qquad 3-3$$

Where: t_L = longitudinal ultrasonic wave transit time, t_S = shear ultrasonic wave transit time, l= the thickness of the samples.

3.3.3 In Vitro Tests

3.3.3.1 Electrochemical Test

3.3.3.1.2 Electrochemical Media

In the present investigation, Ringers solution was selected as an electrochemical electrolyte for electrochemical test with pH 5.0 – 7.5. The chemical compositions of Ringer solution used in this investigation is listed in table 3.2 (The compositions were taken from the plastic containers of intravenous solutions).

Figer3.2: Chemical Compositions of Ringer Solution (Taken from the plastic containers of intravenous solutions)

3.3.3.1.3 Electrochemical Test

3.3.3.1.3.1 Open Circuit Potential (OCP) Measurement

During this test, free corrosion potential was measured. The electrolyte used for OCP was 100 ml of Ringer solution, with all the experiments conducted at 37±1°C and open to the air. The alloys used in this investigation were used as the working electrode. The test was carried out with the alloys immersed in ringer solution. Through the standard calomel electrode (SCE), the working electrode potential can be measured. A voltmeter is connected between the working electrode (the sample to be examined) and the reference electrode. Time spent for each alloy from (0

up to 300min) OCP measurements perform. The first voltage value was calculated immediately after immersion after it was established. Following voltage values were calculated for every five minutes. The test was stop when create a steady state condition with the Ringer solution (300 min). The tests of OCP was done at Metallurgical Department – College of Materials Engineering University of Babylon.

3.3.3.1.3.2 Potentiodynamic Measurements

Potentiodynamic polarization measurements was carried out using a potentiostat type WENKING M lap. The potential dynamic tests were measured in an electrochemical cell known as a three - electrodes cell. The cell consisting of a platinum electrode used as the counter electrode (CE), standard calomel electrode (SCE) as reference electrode (RE), and the alloys used in this investigation were used as the working electrode (WE) According to the American Society for Testing and Materials (ASTM). For all measurements the electrolyte used for potential dynamic measurements was 100 ml of Ringer solution, with all the experiments conducted at 37±1°C and open to the air. The test was done with ± 0.25V vs OCP at a sweep rate of 0.4 mV/s, and the exposed areas were 3.14 cm^2. All electrochemical parameters of titanium alloys used in this investigation including corrosion current (I_{corr}), corrosion potential (E_{corr}), cathodic slope, and anodic slope were estimated from potentiodynamic curves by Tafel plots methods.

The following equation can used to calculate the rate of corrosion **[210]**:

$$\text{Corrosion rate(mpy)} = \frac{0.13\ I_{corr}\ E.W}{A\rho} \qquad (3.\ 5)$$

Where, mpy = corrosion rate (mils per year). I_{corr}= corrosion current in across section area, get it from the potentiodynamic polarization test (μA/ m^2), E.W= equivalent weight for alloy elements (g/eq.), A= the

surface area exposed to the corrosion media (Cm^2), ρ= density of the alloy (g/cm^3) as for the number 0.13, it means metric and time conversion factor.

The tests of Potentiodynamic polarization was done at Metallurgical Department – College of Materials Engineering University of Babylon.

3.3.3.1.4 Metals Ions Release Test

The tests were carried out according to JIS T- 0304 standard for metals implant **[201]**. For all measurements, the electrolyte used for metals ions release was 100 ml of Ringer solution. All the experiments conducted at 37±1°C and open to the air. All alloys were immersed in a plastic containers with Ringer solution for one month in the incubator (Specimens are immersed in small containers, where these containers are immersed in controlled water temperatures 37˚C (±1). The tests was done by Analytika jena NOV 350 AA made in germany 2012, located at Ibn Sina Company (Baghdad/ Iraq).

3.3.3.1.5 Tribology Test

The wet wear tests of all titanium alloys under investigation at 37°C were performed on ball on disk MT 400 version 10, and the ball used is made of zirconia. The normal loads in the wet wear tests were 10 and 20 N for 1h **[88, 202-204]**. During the tests the friction coefficient (COF) and the sliding time were automatically recorded by the machine. Before starting the tests, all titanium alloys under investigation were weighed using a sensitive balance (0.0001). Then after 1h, the specimen test was weighed using the same balance. The test was done according to ASTM G99 **[214]**, and the volume loss was calculated using the following equation **[209]**.

$$\text{Volume loss} = \frac{Weight\ loss\ (g)}{\rho(\frac{g}{cm3})} \quad \ldots (3\text{-}6)$$

Where :

Weight loss (g) is the weight loss after 1h.

ρ (g/cm^3) is the density of titanium alloy under investigation.

The tests was carried out in the Department of Metallurgy Engineering / College of Materials Engineering / University of Babylon.

3.3.4.1 Wear Track Analysis

3.3.4.1.1 Worn Surface Characterization

In order to fully understand the wear behavior of the titanium alloys under investigation, the characterization of the worn track surface is very important. In this investigation, the worn surface of the wear track was investigated using various surface characterization technique, for examples, optical microscopy and roughness calculation .

3.3.4.1.1.1 Optical Microscopy Analysis

Surface morphology of the wear track of all titanium alloys under investigation was analyses using optical microscopy (OM) analysis. We used the same technique in 3.3.1.3.

3.3.4.1.1.2 Surface Roughness Calculation.

The surface roughness tester type HSR210 was used to evaluate the worn surface of the wear track of all samples of titanium alloys under investigation, located in the Laboratories of the Metallurgical Department, College of Materials - University of Babylon. The roughness measurement was implemented by three reading at diffrent points along specimen. The roughness was recorded as an average of three reading for each alloy.

CHapter Four

Result and Discussions

Result and Discussions

4.1. General View:

In this chapter, the results obtained in each parts of this investigation will be presented and followed by discussion of results. The results of alloys characterization including, optical microscopy, Filed Emission scanning electron microscopy, and X-ray diffraction, mechanical testing (elastic modulus and micro – hardness) results will be discussed. The results of electrochemical behavior of titanium alloys used in this investigation including open circuit potential, potentiodynamic and ion release will be discussed. The results of tribological behavior of titanium alloys used in this investigation including lubricated sliding friction, wear track characteristics (optical microscopy and roughness), and total removed wear volume will be discussed.

4.2. Microstructure and Phase Constitution of Titanium Alloys used in this Investigation

Optical images of typical microstructure of titanium alloys used in this investigation are shown in figure 4.1. The Filed Emission Scanning Electron Microscope FESEM of titanium alloys used in this investigation are shown in figure 4.2. The FESEM images and EDX results of titanium alloys are shown in figures 4.3 through to 4.6. The microstructures of Cp-Ti and Ti-6Al-4Vwere single α- phase and (α+β) respectively as expected. These results were confirmed by XRD results as can see in figures 4.7 and 4.8 respectively. The microstructure of Ti-13Nb-13Zr and Ti-15Mo consisted of two phases, α-phase and β-phase as you can see in figure 1.4. However, the microstructure of Ti-13Nb-13Zr were predominantly the β-phase with an equiaxed grain structure, with α- phase was observed in some region, these alloys known as (Rich β). While, the microstructure of

Ti-15Mo also was predominantly β-phase as fine grained with a small amount of α-phase in some region, these kind of alloys known as metastable β. The presence of α-phase in both alloys was confirmed by XRD results as can see in figures 4.9 and 4.10. The microstructure of Ti-8Mo-4Nb-2Zr consisted of single-phase β with equiaxed grains, with no evidence of second phases, confirmed by XRD results figure 4.11.

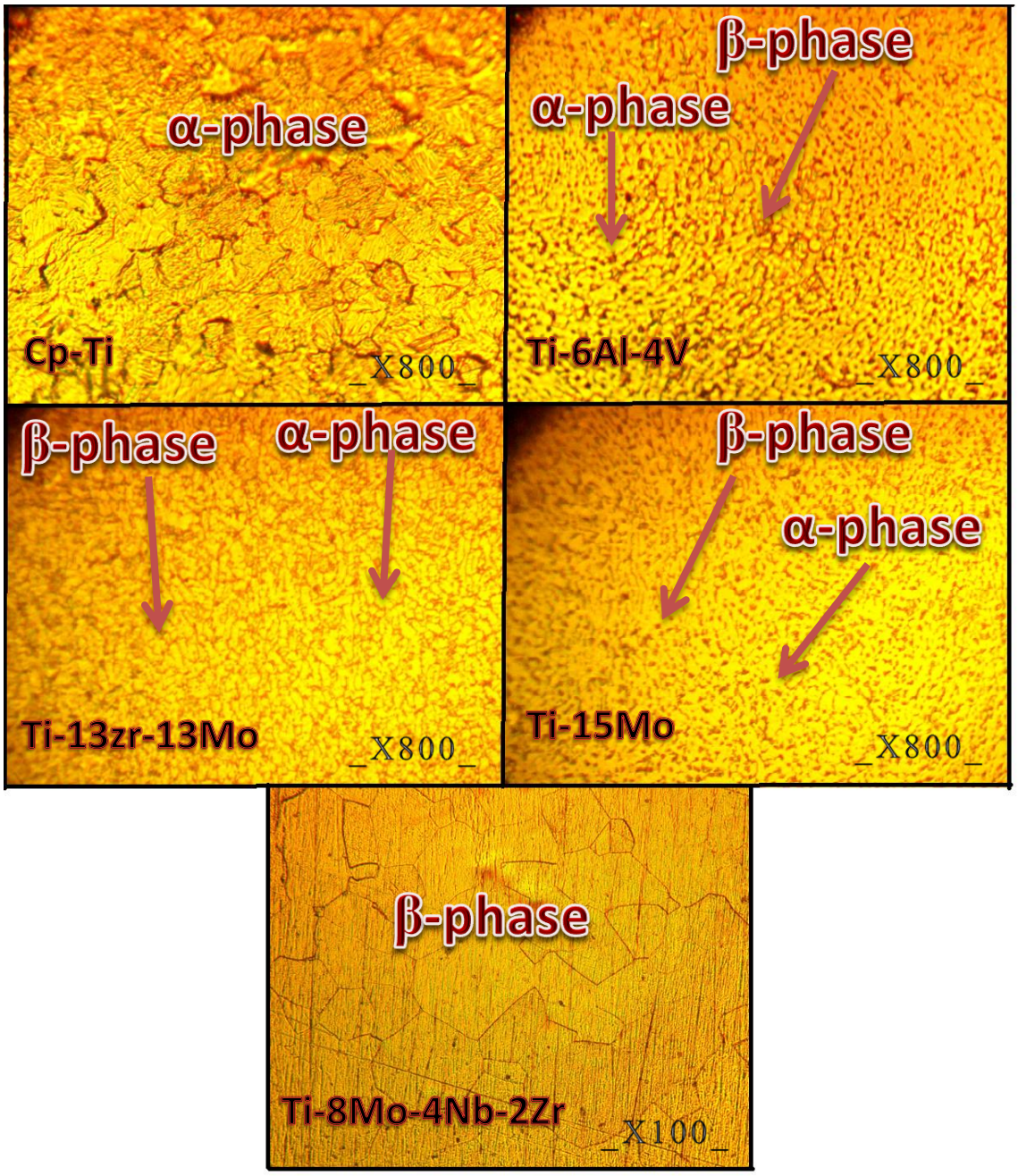

Figure (1.4): OM micrographs showing microstructure of titanium alloys samples utilized in this investigation

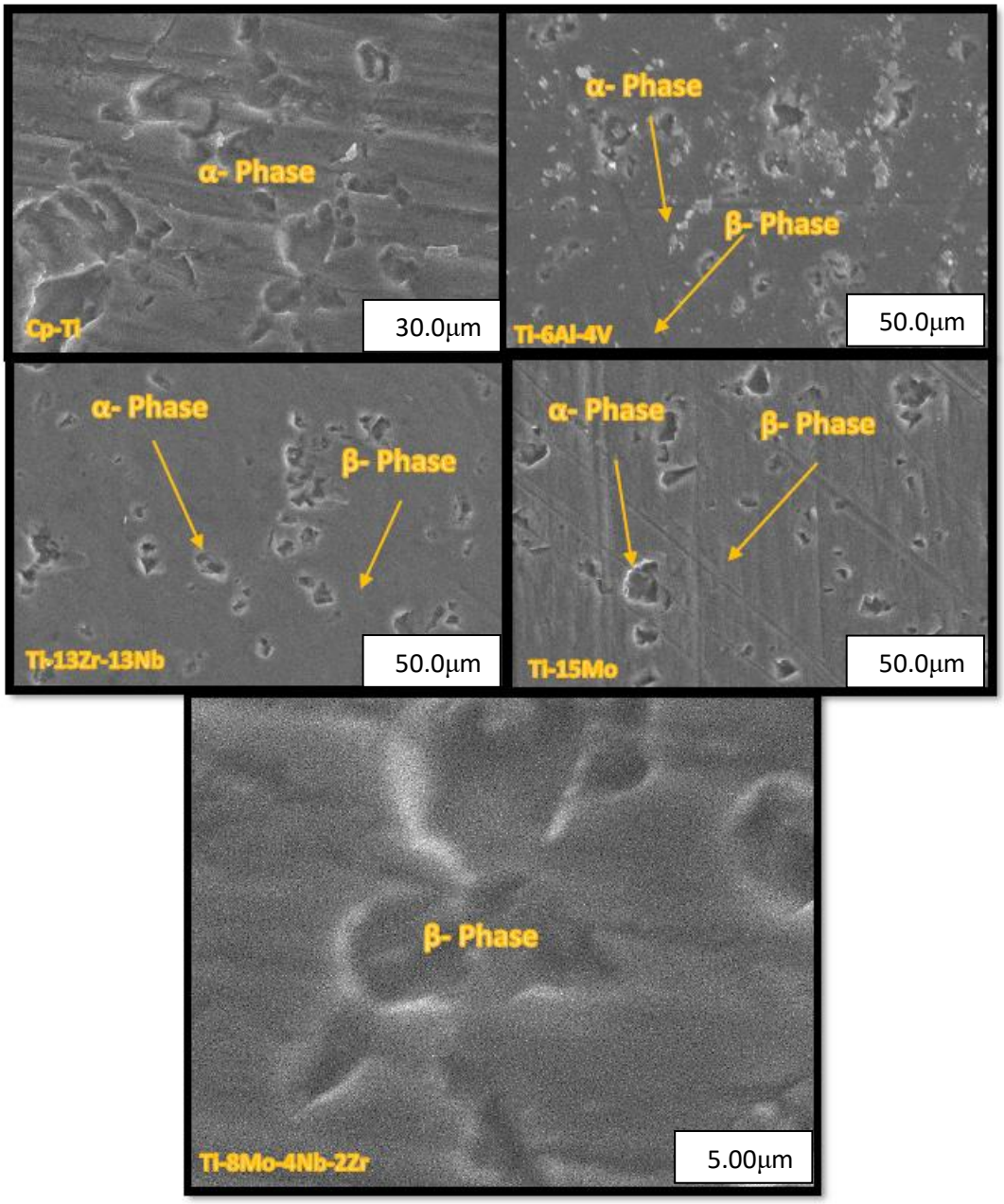

Figure 4.2 FESEM pictures of the titanium alloys samples utilised

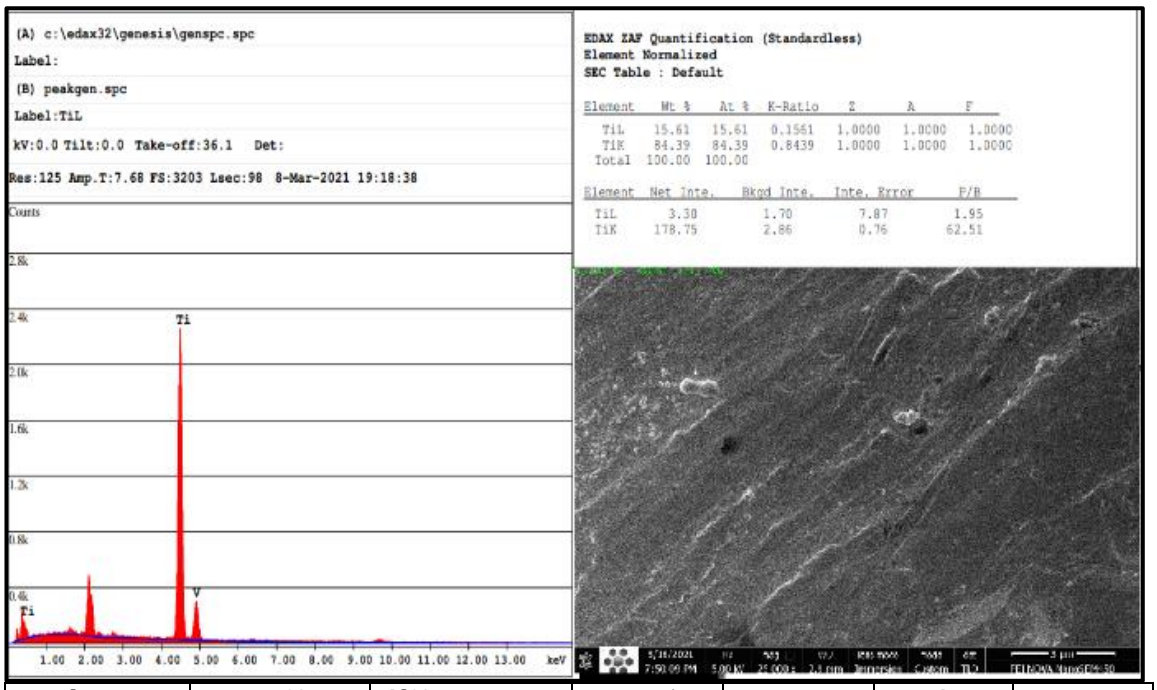

Element	Wt%	Al%	K-Ratio	Z	A	F
TiL	15.61	15.61	0.1551	1.0000	1.0000	1.0000
TiK	84.39	84.39	0.8439	1.0000	1.0000	1.0000
Total	100.00	100.00				

Element	Net Inte.	Bkgd Inte.	Inte. Error	P/D
TiL	3.30	1.70	7.87	1.95
TiK	178.75	2.86	0.76	62.52

Figure (4.3): FESEM+EDS for Cp-Ti

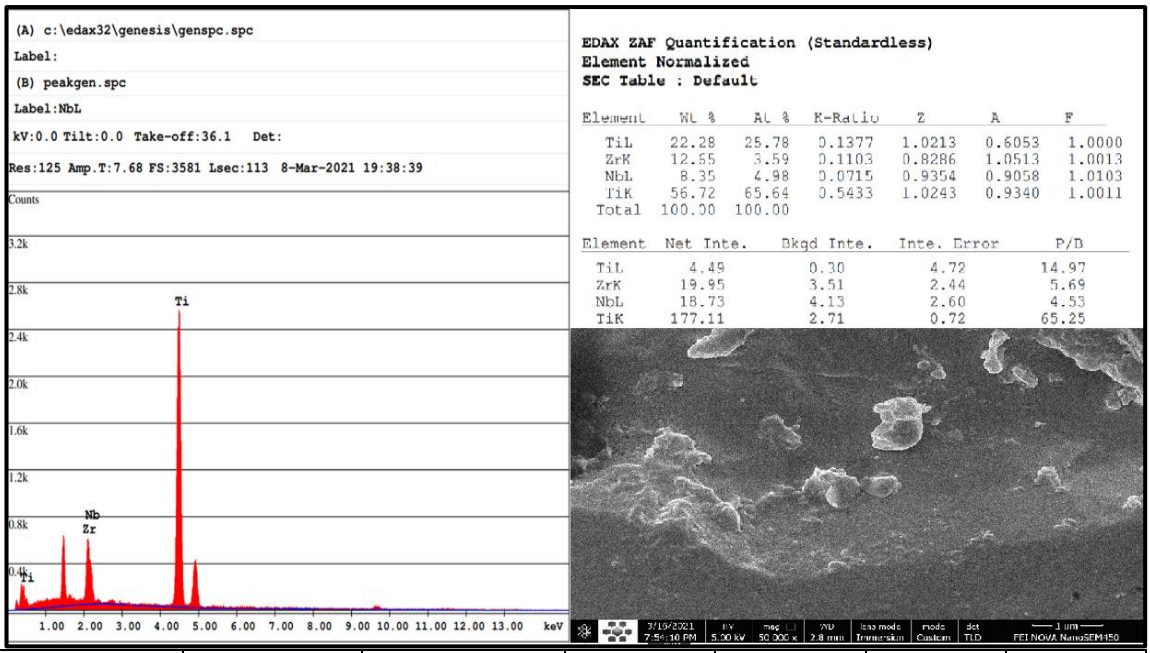

Element	Wt%	Al%	K-Ratio	Z	A	F
TiL	22.28	25.78	0.1377	1.0213	0.6053	1.0000
ZrK	12.55	3.59	0.1103	0.8286	1.0513	1.0013
NbL	8.35	4.98	0.0715	0.9354	0.9058	1.0103
TiK	56.72	65.64	0.5433	1.0243	0.9340	1.0011
Total	100.00	100.00				

Element	Net Inte.	Bkgd Inte.	Inte. Error	P/D
TiL	4.49	0.30	4.72	14.97
ZrK	19.98	3.51	2.44	5.69
NbL	18.73	4.13	2.60	4.53
TiK	177.11	2.71	0.72	65.25

Figure (4.4): FESEM+EDS for Ti-13Zr-13Nb.

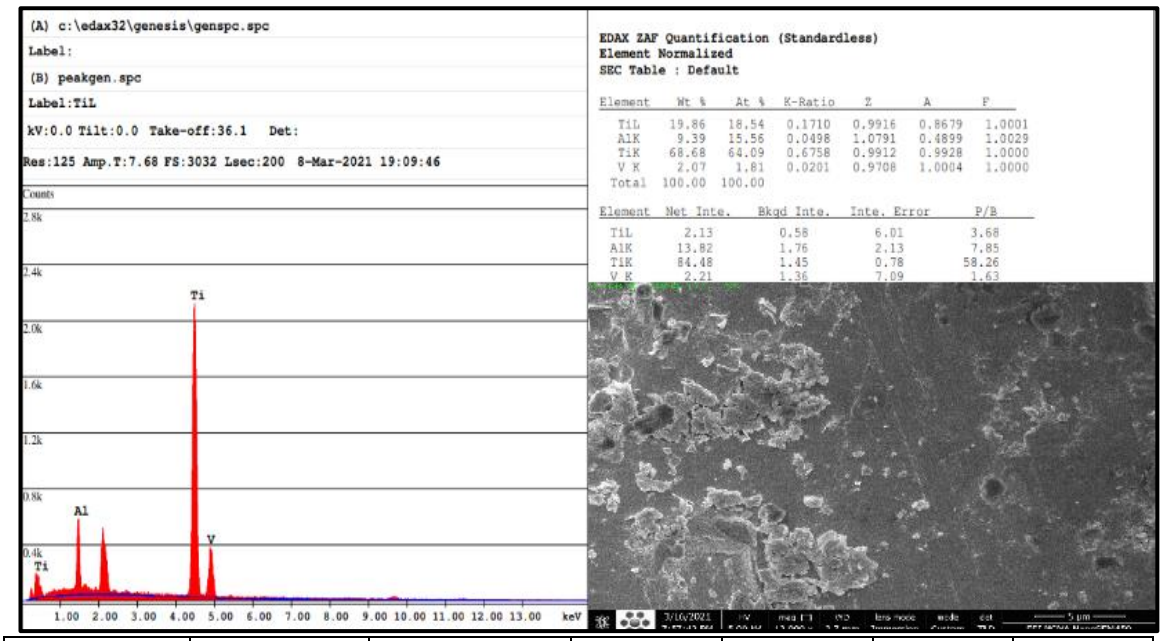

Element	Wt%	Al%	K-Ratio	Z	A	F
TiL	19.86	18.58	0.1710	0.9916	0.8679	1.0001
AlK	9.39	15.56	0.0498	1.0791	1.4899	1.0029
TiK	68.68	64.09	0.6758	0.9912	0.9928	1.0000
VK	2.07	1.81	0.0201	0.9708	1.0004	1.0000
Total	100.00	100.00				

Element	Net Inte.	Bkqd Inte.	Inte. Error	P/D
TiL	2.13	0.55	6.01	3.68
ZrK	13.82	1.76	2.13	7.85
NbL	84.48	1.45	0.78	58.26
TiK	2.21	1.36	7.09	1.63

Figure (4.5): FESEM+EDS for Ti-6Al-4V

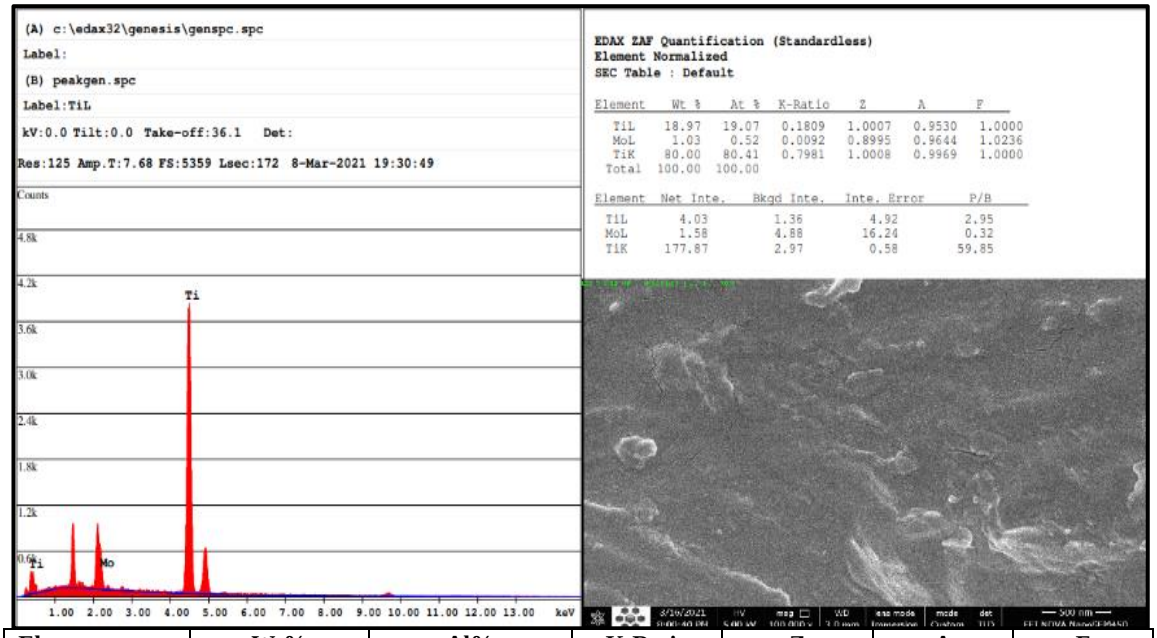

Element	Wt%	Al%	K-Ratio	Z	A	F
TiL	18.97	19.07	0.1809	1.0007	0.9530	1.0000
MoL	1.03	0.52	0.0092	0.8995	0.9644	1.0236
TiK	80.00	80.41	0.07981	1.0008	0.9969	1.0000
Total	100.00	100.00				

Element	Net Inte.	Bkqd Inte.	Inte. Error	P/D
TiL	4.03	1.36	4.92	2.95
MoL	1.58	4.88	16.24	0.32
TiK	177.87	2.97	0.58	59.85

Figures (4.6): FESEM+EDS for Ti-15Mo.

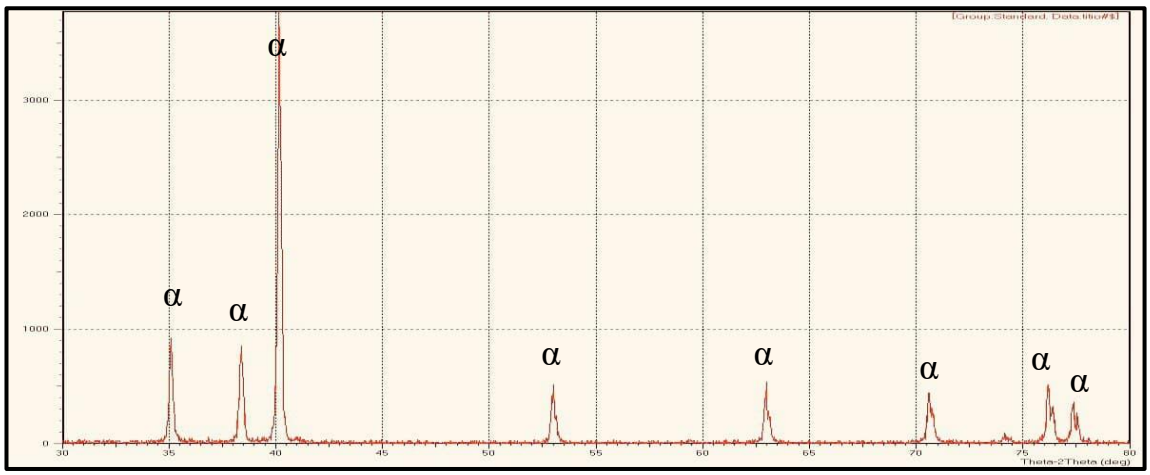

Figure (4.7): X-ray diffraction(XRD) peaks of Cp-Ti alloy

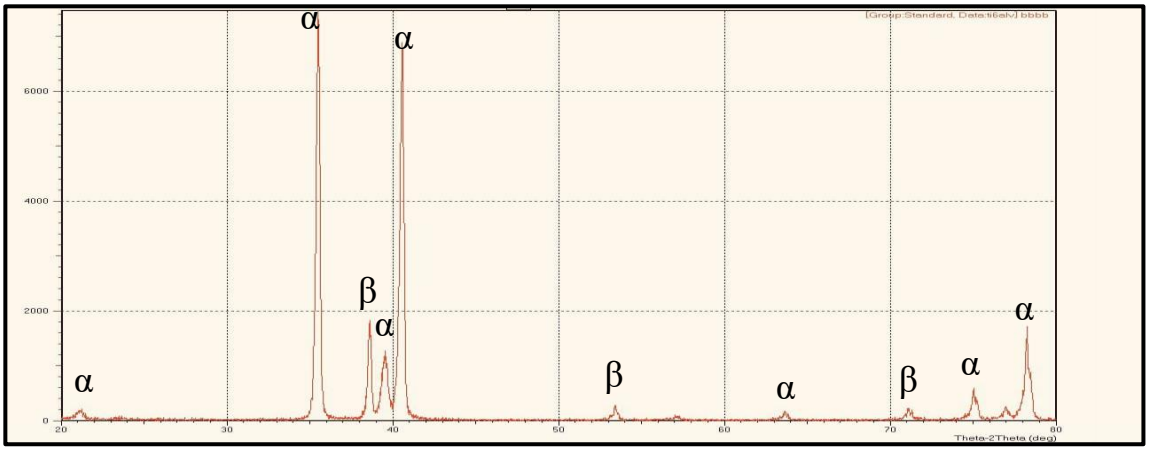

Figure (4.8). X-ray diffraction peaks of Ti-6Al-4V alloy.

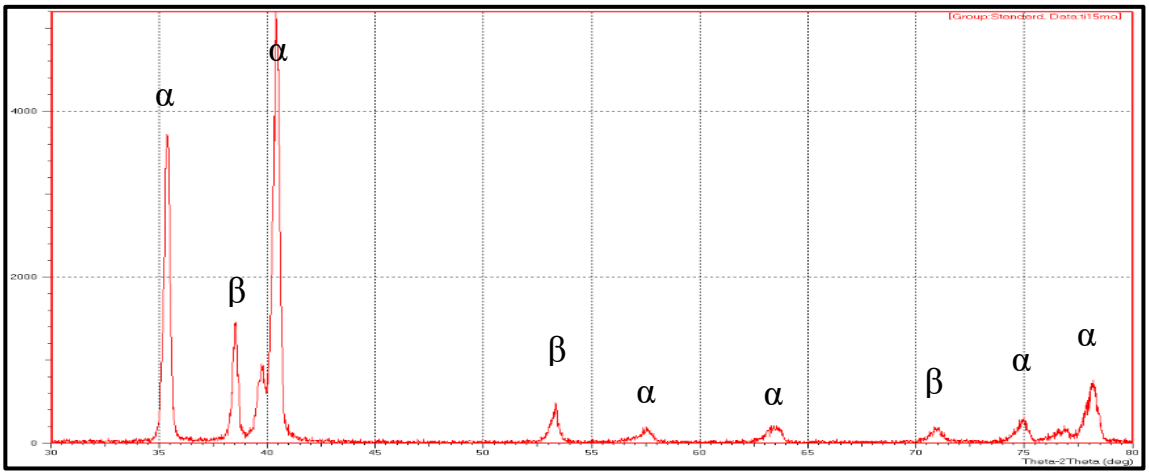

Figure (4.9): X-ray diffraction(XRD) peaks of Ti-13Zr-13Nb alloy

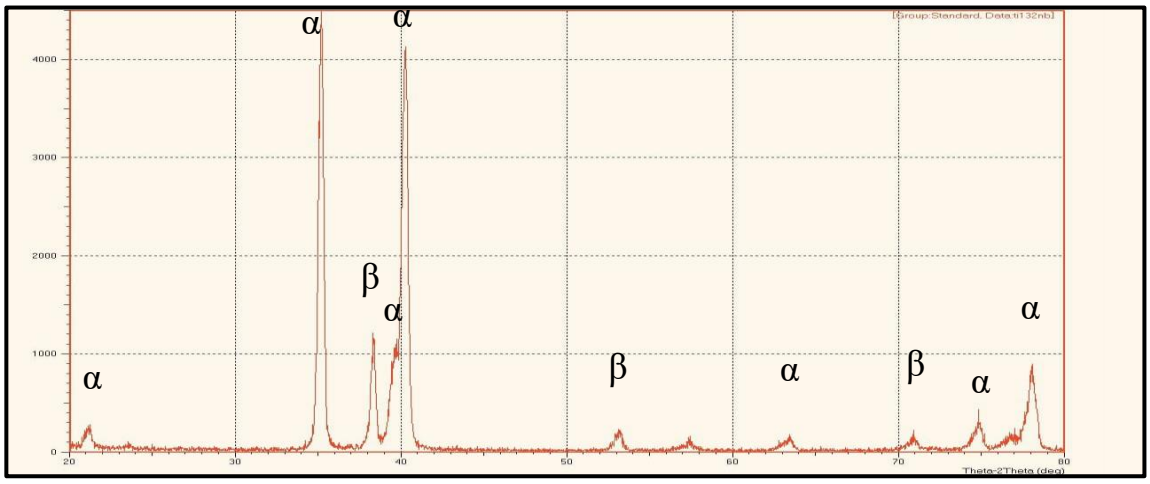

Figure 4.10): X-ray diffraction(XRD) peaks of Ti-15Mo alloy

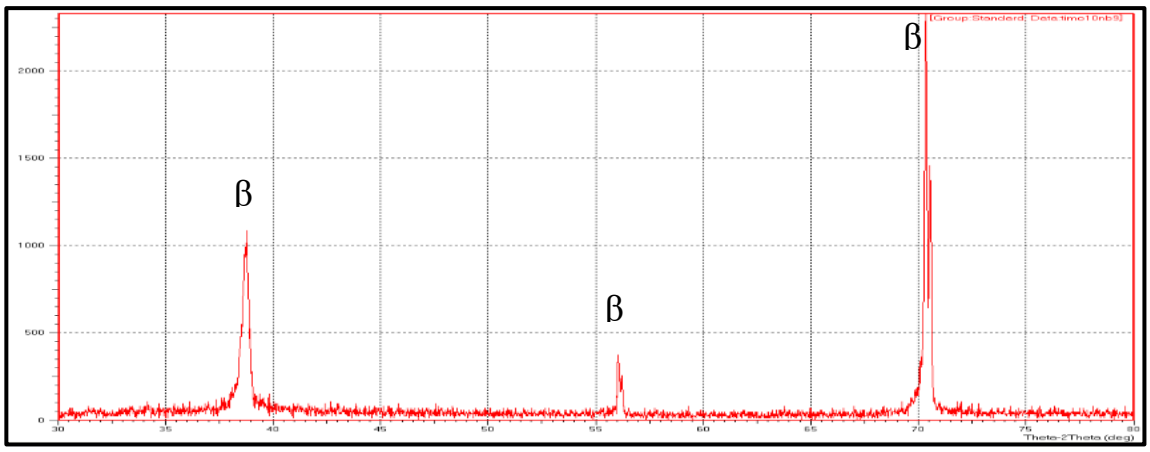

Figure (4.11): X-ray diffraction peaks of Ti-8Mo-4Nb-2Zr alloy.

4.3. Mechanical Characterization

4.3.1. Modulus of Elasticity

The elastic modulus of titanium alloys used in this investigation are listed in table 4.1. The secound generation β-microstracture Ti-8Mo-4Nb-2Zr alloy had the lowest elastic modulus of (102GPa). The first generation Ti-6Al-4V had the higher elastic modulus of (150GPa). All β-microstacture alloys used in this investigation rich – β Ti-13Zr-13Nb (112GPa) and metastable β Ti-15Mo (110GPa) showed an elastic modulus lower than that of α-microstracture Cp-Ti (136GPa) and the first generation Ti-6Al-4V alloy (150GPa). It was reported that the elastic modulus of α- phase is

higher than β- phase, $E_\alpha = 1.5E_\beta$ **[215]**. Also it was reported that the order of elastic modulus are ω>α>α″>β **[215-217]**. There fore we can explain our results depend on the fact each phase has a different elastic modulus, and β-phase has lower elastic modulus compared with other phases, α-phase in our investigation. Therfore, the first generation Ti-6Al-4V alloy and Cp-Ti alloy had the higher elastic modulus because of the α-phase structure, which is single phase in Cp-Ti and a higher volume fraction of α-phase compared with β-phase in the first generation Ti-6Al-4Valloy. All β-microstacture alloys used in this investigation had lower elastic modulus because of the β-phase structure, which is single β-phase in the secound generation Ti-8Mo-4Nb-2Zr and a higher volume fraction of the β-phase in the rich –β Ti-13Zr-13Nb and metastable β Ti-15Mo alloys.

Table (4.1): Estimation Ultrasonic Elastic Modulus

Alloy	**Phase Constituents**	**Elastic Modulus E (**GPa)
Cp-Ti	α	150
Ti6Al-4V	α+β	136
Ti-13Zr-13Nb	Rich β	112
Ti-15Mo	Metastable β	110
Ti-8Mo-4Nb-2Zr	β	102

4.3.2. Vickers Micro-Hardness

The average Vickers micro-hardness values of titanium alloys used in this study are listed in table 4.2. Ti-8Mo-4Nb-2Zr with single β-phase microstructure alloy had average Vickers micro-hardness values higher than Cp-Ti with α-phase microstructure, Ti-6Al-4V with α +β phase, Ti-13Zr-13Nb (Rich β-phase) and Ti-15MO (metastable β). Cp-Ti with α-phase microstructure had lower Vickers micro-hardness values compared with other titanium alloys used in this study. Ti-13Zr-13Nb (Rich β-phase)

and Ti-15MO (metastable β) had average Vickers micro-hardness values higher than Cp-Ti with α-phase microstructure and close to the Ti-6Al-4V with α +β phase. The increase in micro-hardness values of Ti -8Mo-4Nb-2Zr with single β-phase microstructure alloy compared to others could be related to the mechanism of solid solution strengthen of Ti with the addition of Mo, Nb, and Zr. It has been documented in the literature that Mo, Zr and Nb are stabilize the β-phase, which lead to solid solution strengthening, thus leading to increase the hardness. These results are in accordance with previous investigation by **[218-221]**.

Table (4.2): Average Vickers-hardness of titanium alloys samples utilized.

Alloy	Phase Constituents	Vickers Hardness
Cp-Ti	α	135 Hv
Ti-6Al-4V	α+β	258 Hv
Ti-13Zr-13Nb	Rich β	260 Hv
Ti-15Mo	Metastable β	257 Hv
Ti-8Mo-4Nb-2Zr	β	264 Hv

4.4 In Vitro Tests

4.4.1 Electrochemical Test

4.4.1.1 Open Circuit Potential (OCP) and Potentiodynamic Polarization

The time profile of the OCP of titanium alloys used in this investigation are presented in figure 4.12. Average values of OCP are listed in table 4.3. By comparing the OCP values of titanium alloys used in this investigation, it can be observed that the the secound generation β-microstracture Ti-8Mo-4Nb-2Zr alloy had the most positive value than the

other alloys. While, the Cp-Ti α-phase and the first generation Ti-6Al-4V (α+β) phase had the most negative value (-70 mV and -77 mV) respectively. The potentiodynamic curves of all titanium alloys used in this study are presented in figure 4.13. The corrosion rate of all titanium alloys used in this investigation are listed in table 4.3. All titanium alloys with different microstructure (α, α+β, β+α, and β) show the similar corrosion behavior. However, different corrosion rate obtain depended on the microstructure of titanium alloy (α, α+β, β+α, or β). It can be seen that the secound generation β-microstracture Ti-8Mo-4Nb-2Zr alloy had lower corrosion rate compared to other titanium alloys used in this investigation. While, Cp-Ti α-phase had the higher corrosion rate than other titanium alloys. These results indicated the positive contribution of Nb, Mo, and Zr alloying elements in the corrosion behavior of β- phase titanium alloys. The presence of oxides of the alloying elements (Nb, Zr) in the the secound generation β-microstracture Ti-8Mo-4Nb-2Zr alloy, may play a key role for improving the corrosion resistance. It was reported that the therrmodynamic stability of the TiO_2 can be improved by Nb_2O_5 **[155]**. Also, improve the resistance of titanium oxide to chemical dissolution by ZrO_2 **[155]**. Furthermore, it was reported that the alloys with single phase for example β-phase have more corrosion resistance of alloys with two phases for example (α +β) phases. The same results was reported by **[222]**.

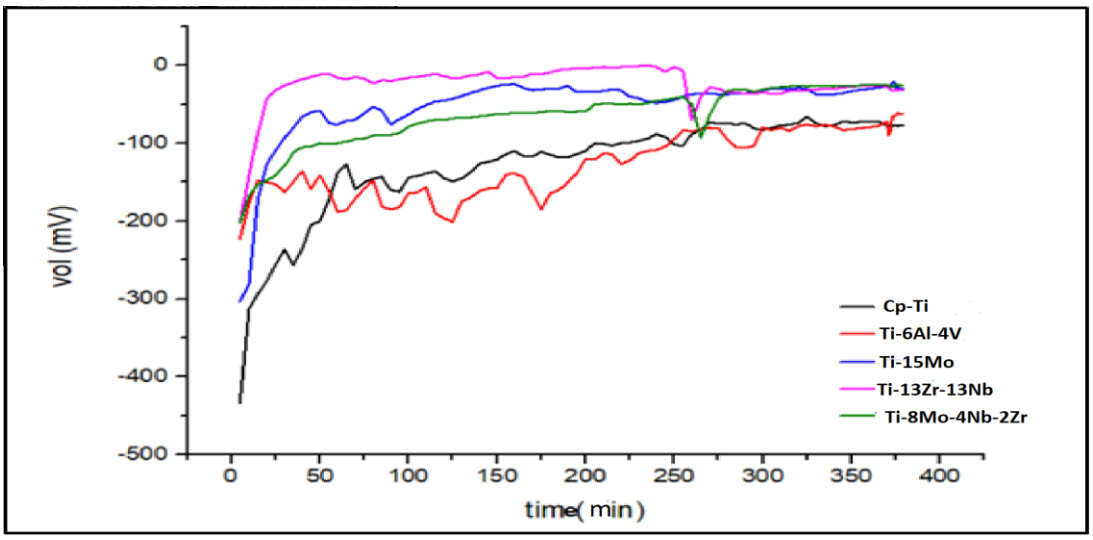

Figure 4.12: O.C.P for Titanium Alloys used in this investigation

Table (4.3): The average OCP values of titanium alloys used in this investigation

Alloy	Phase Constituents	OCP (mV)
Cp-Ti	α	-77 mV
Ti-6Al-4V	α+β	-70 mV
Ti-13Zr-13Nb	Rich β	-30 mV
Ti-15Mo	Metastable β	-30 mV
Ti-8Mo-4Nb-2Zr	β	-29 mV

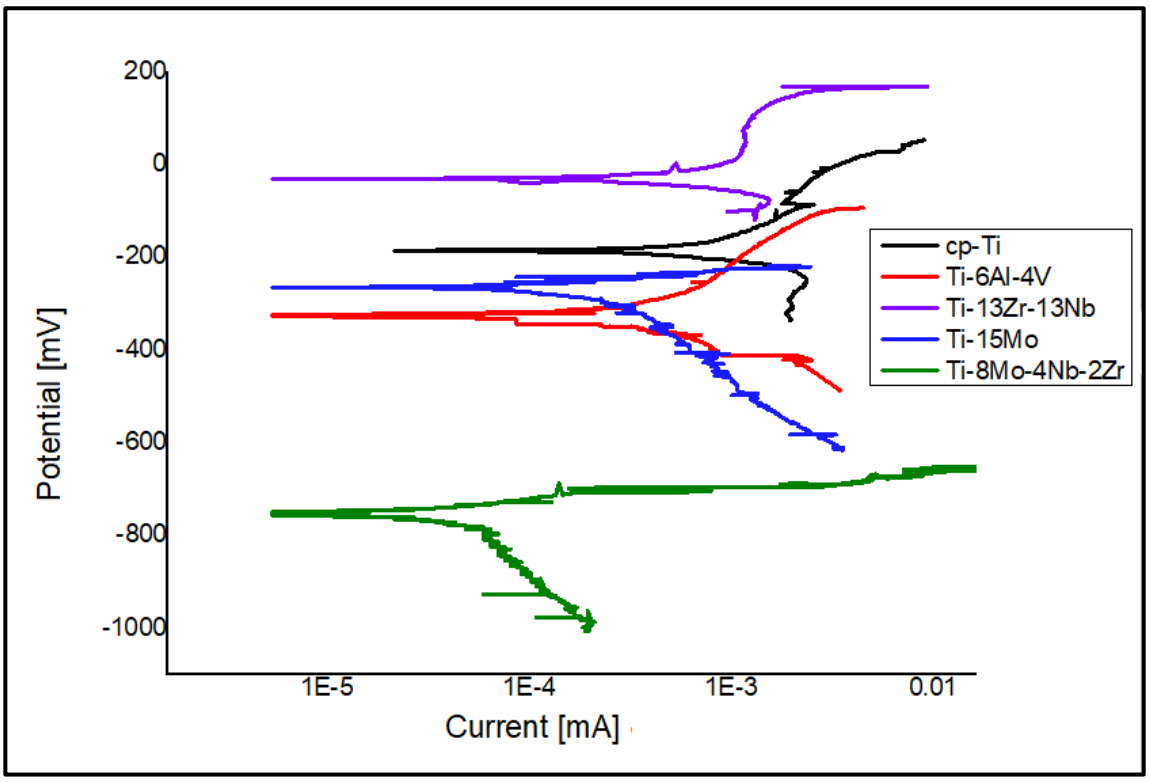

Figure4.13 Potentiodynamic Polarization for Titanium Alloys samples utilized in this investigation

Table 4.4: The rate of corrosion of titanium alloys samples utilized in this investigation

Alloy	Phase Constituents	I_{corr} (nA)	Equivalent weight E.W (g/mol)	Density (g/cm^3)	Corrosion Rate (mpy)
Cp-Ti	α	265.13	23.9335	4.515	$57.96*10^{-9}$
Ti-6Al-4V	α+β	99.61	23.0986	4.419	$21.55*10^{-9}$
Ti-13Zr-13Nb	Rich β	91.20	29.67926	4.520	$25.35*10^{-9}$
Ti-15Mo	Metastable β	57.39	27.54047	4.4171	$14.81*10^{-9}$
Ti-8Mo-4Nb-2Zr	β	22.71	27.19157	5.12	$6.124*10^{-9}$

4.4.1.2 Ion Release

The ion release was carried out for the elements Ti, Al, V, Zr, Nb, and Mo in Cp-Ti, Ti-6Al-4V, Ti-13Zr-13Nb, Ti-15Mo alloys using static immersion methods in Ringers solution for 30 days. Where the percentage of titanium ions released in Ringer's solution of was calculated from

commercial titanium alloy. The ions released of aluminum and vanadium elements were calculated from Ti-6Al– 4V alloy. In addition, ions released of zirconium and niobium were calculated from Ti-13Zr-13Nb alloy, and released molybdenum ions calculated from Ti-15Mo alloy. This alloy was taken for this examination because they are rich in these elements unlike the Ti-Mo-Nb-Zr alloy. The results of metals ion release in Ringers solution for 30 days are listed in table 4.5. We can observed from the table 4.5, molybdenum ions are release fewer than other elements ion (Ti, Al, V, Nb, and Zr) used in this investigation. In addition, it is possible to observe from the table 4.5, the titanium and zirconium ions more released in the Ringer solution as compared with the release of other elements ion used in this investigation (Mo, V and Nb). These results indicated that the second generation titanium alloy with Mo has a good corrosion resistance, with a good agrrement with the results of electrochemical tests OCP and potentiodynamic polarization.

Table (4.5): Ion Release of Titanium Alloys samples utilized in this investigation

Alloy	Phase Constituents	Element (ppm)					
		Ti	Al	V	Zr	Nb	Mo
Cp-Ti	α	109.397	-	-	-	-	-
Ti-6Al-4V	α+β	-	86.698	75.565	-	-	-
Ti-13Zr-13Nb	Rich β	-	-	-	140.397	89.78	-
Ti-15Mo	Metastable β	-	-	-	-	-	25.979

4.5. Tribological Behaviors

4.5.1. Lubricated sliding friction

The variation in the coefficient of friction (COF)of titanium alloys samples used in this investigation as a function of test time in Ringer

solution at a normal loads of 10 and 20 N under lubricated rubbing condition are shown in figures 4.14 through to 4.18 and 4.19 through to 4.23 respectively. The avarage COF values of titanium alloys samples used in this investigation at a normal loads of 10 and 20 N in lubricated conditions are listed in table 4.6. Under both normal loads 10 and 20 N, and for all titanium alloys used in this investigation, the COF as a function of time could be divided into more than one zone. There are three main friction zone, the first zone run – in period zone, depasivation zone, and repasivation zone. However, the number of friction zone depended on the titanium alloys composition and structure (α, α+β, rich β, metastable β, or β). Before start rubbing, the titanium alloys were in contact with the Ringer solution, it would be expected that the titanium oxide film would generate on the surface of all samples used in this investigation, and the compostion of oxide film depended on the compostion of titanium alloys samples. During the first zone I run-in period, rubbing was started and the oxide film breack up due to the mechanical contact between the counter face and the surface of samples used in this investigation. During the first zone, the COF has the maximmum value and then decreases before reaching the steady state. Howeve, the time requied to reach the stadey state of COF is depended on the titanium alloys composition and stracture (α, α+β, rich β, metastable β, or β). In the second zone II, during rubbing the COF increase, thus, could be related to the depassivation mechanism, which leading to remove the the oxide film in the contact zone during rubbing and exposing the fresh surface of titanium alloys used in this investigation to the Ringer solution. As rubbing continued, zone III, the COF reach the steady state indicating occurrence of repassavation and the passive state regained. The behaviour between zone II and zone III could related to the dynamic equilibrium betwwen recoverable the oxide and removal of oxide film (depasavation and repassivation). The three main zones can clearlly seen in figures(4.14 - 4.19).

For both normal loads, the curves of friction for the Cp-Ti α-microstructure alloy and the secound generation β-microstracture Ti-8Mo-4Nb-2Zr alloy were smother than those of the first generation Ti-6Al-4V α+β microstracture, rich β Ti-13Nb-13Zr, and metastable β Ti-15Mo alloys. At normal load of 10 N, the COF of the first generation Ti-6Al-4V α+β microstracture had higher fluctuation than the Cp-Ti α-microstructure alloy, rich β Ti-13Nb-13Zr, metastable β Ti-15Mo alloys and the secound generation β-microstracture Ti-8Mo-4Nb-2Zr alloy. While, at normal load of 20 N, rich β Ti-13Nb-13Zr had higher fluctuation than others used in this investigation. The higher COF was obtained from the secound generation β-microstracture Ti-8Mo-4Nb-2Zr alloy of 0.5 and 0.59 at normal loads of 10 and 20 N respectively as you can seen in table 4.7. The higher COF of the secound generation β-microstracture Ti-8Mo-4Nb-2Zr alloy may be related to the wear debris result from the remove of the passive oxide film and metal during rubbing, leading to interaction between the wear debris, thus the friction force will increase as a result of an increase in the ploughing action. The microstacture of the secound generation β-microstracture Ti-8Mo-4Nb-2Zr alloy also has influnce in the friction behaviour, it was reported that the BCC stracture shows COF higher than that of a hexagonal crystal structure **[179]**. The chemical constituents of the passive oxide film also has influnce in the friction behaviour of the titanium alloy samples used in this investigation**[223]**. In the secound generation β-microstracture Ti-8Mo-4Nb-2Zr alloy, the formation of the oxide including TiO_2, MoO_3, Nb_2O_2, and ZrO_2 is expected**[155]**, therefore, the higher COF may be related to remove the oxide during rubbing leading to the interaction of wear debris durring the wear test **[224]**.

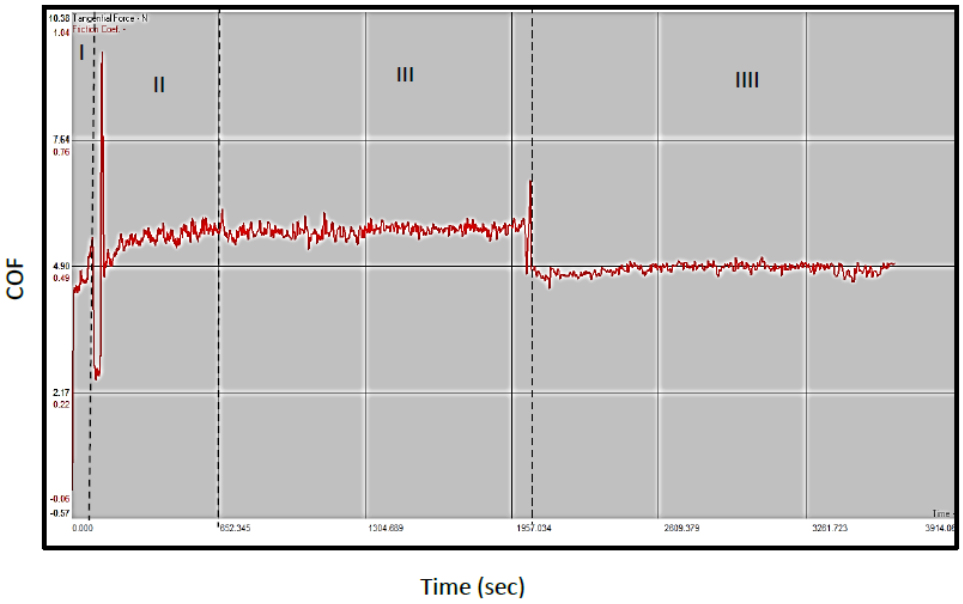

Figure (4.14): Lubricated sliding friction for CP-Ti alloy at 10N.

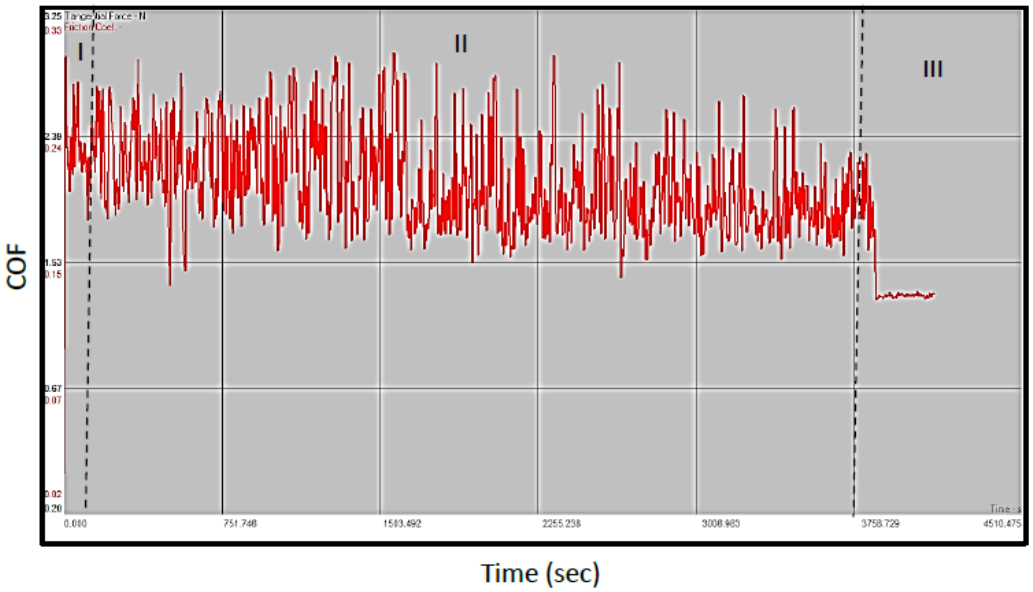

Figure (4.15): Lubricated sliding friction for Ti-Al6-V4Alloy at 10N.

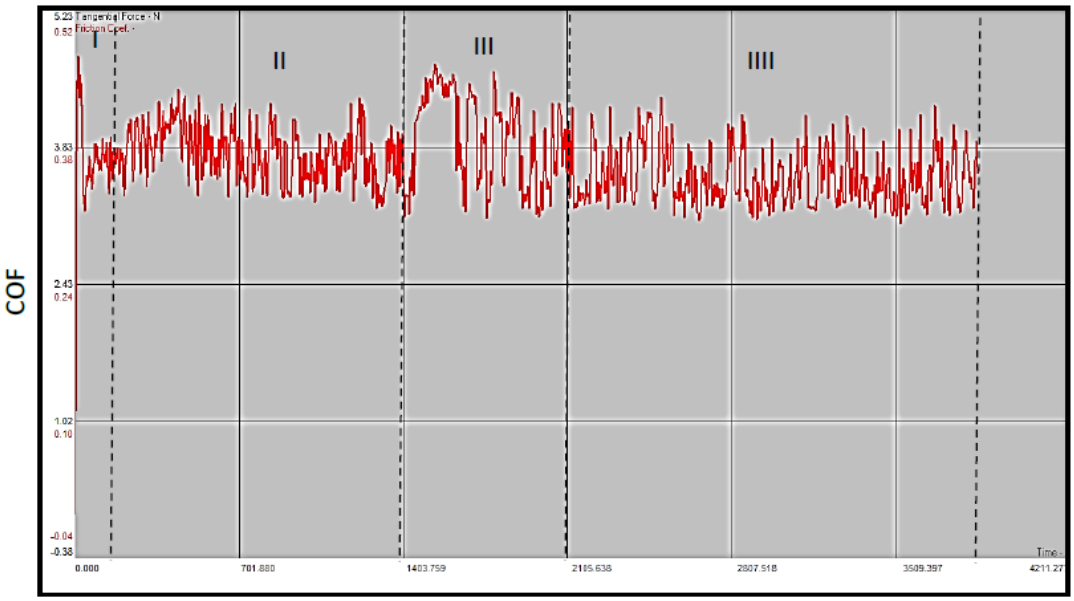

Figure (4.16): Lubricated sliding friction for Ti-13Zr-13Nb Alloy at 10N.

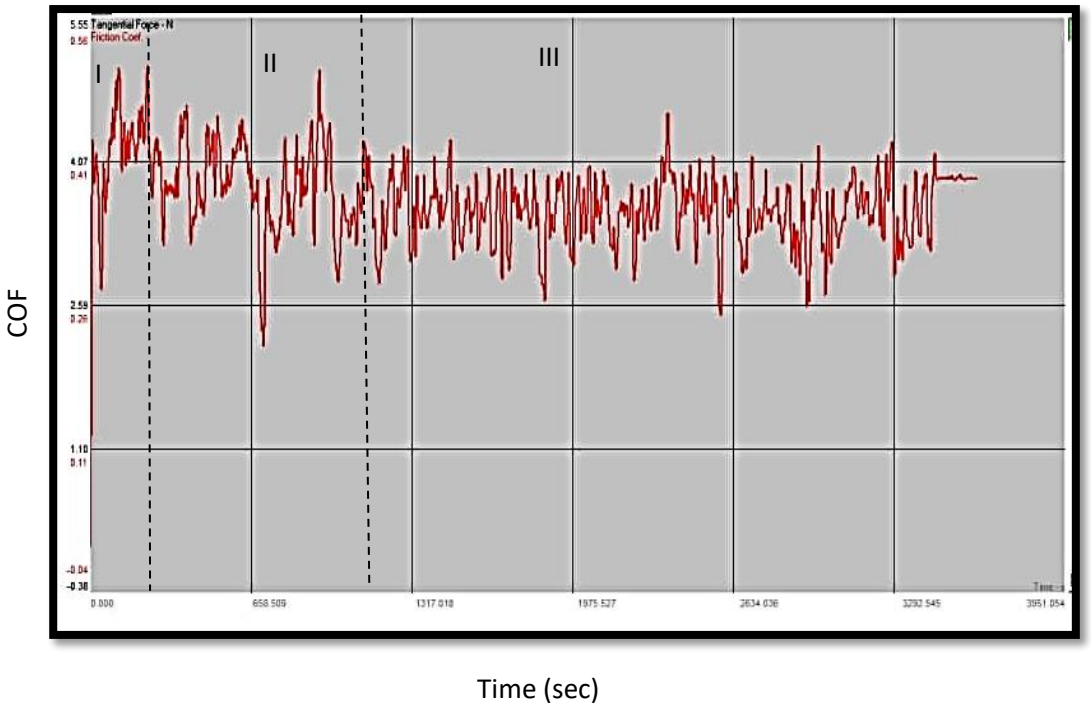

Figure (4.17): Lubricated sliding friction for Ti-15Mo Alloy at 10N.

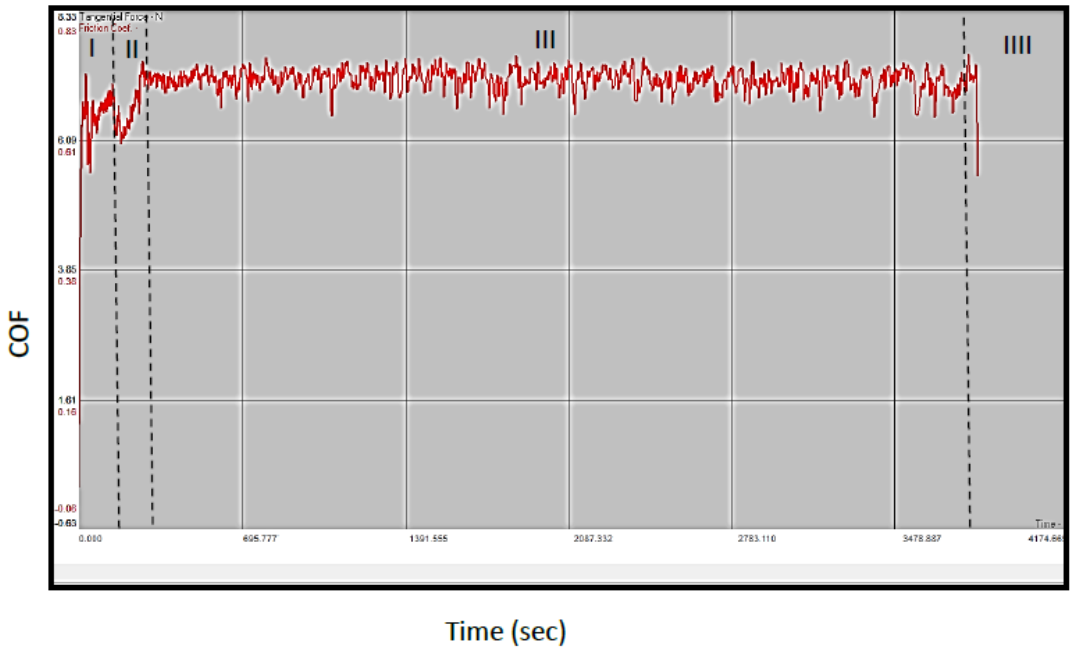

Figure (4.18): Lubricated sliding friction for Ti-8Mo-4Nb-2Zr Alloys at 10N.

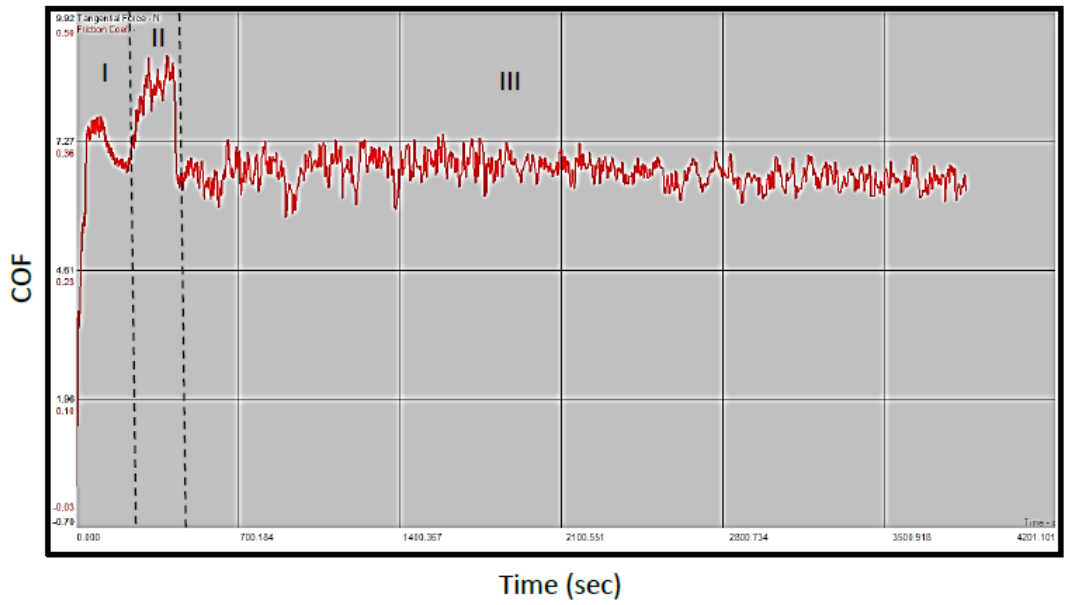

Figure (4.19): Lubricated sliding friction for Cp-Ti alloy at 20N**.**

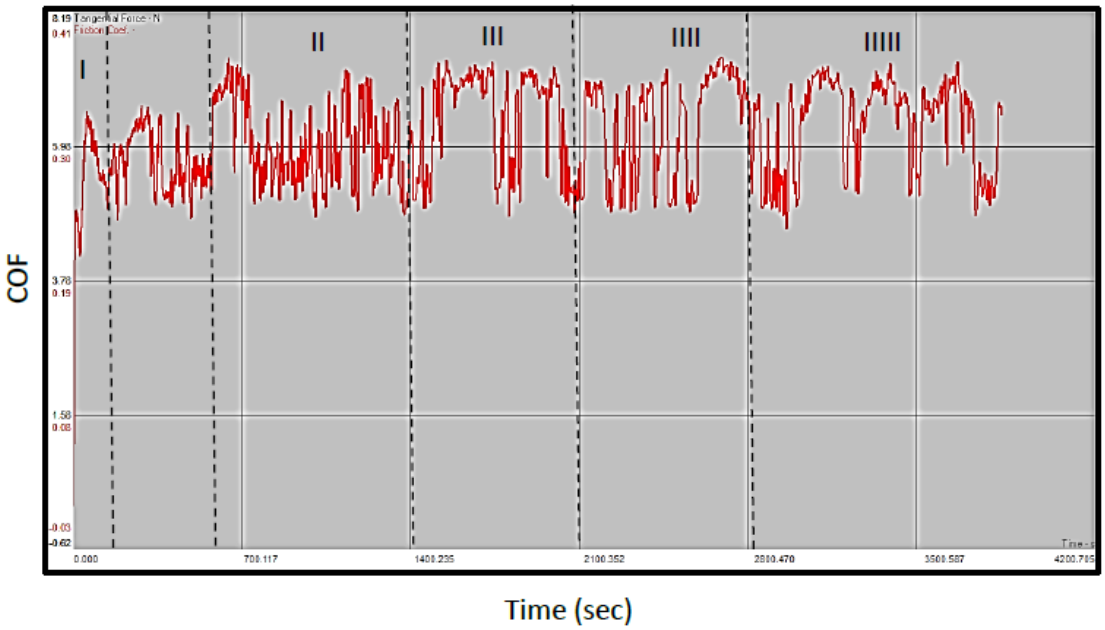

Figure (4.20): Lubricated sliding friction for Ti64 Alloy at 20N.

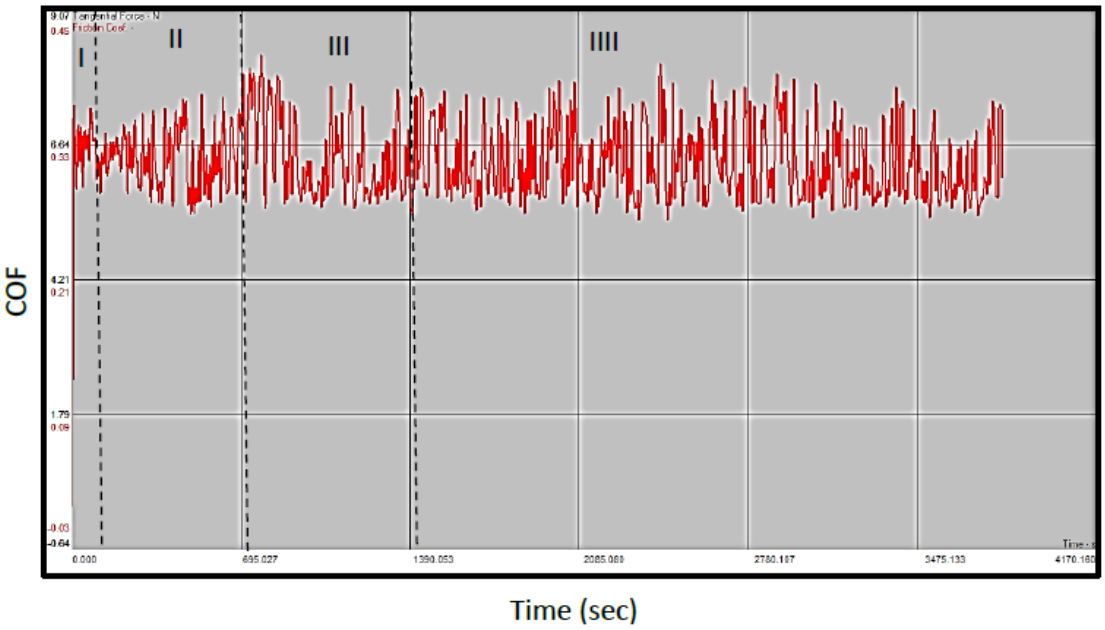

Figure (4.21): Lubricated sliding friction for Ti-13Zr-13Nb at 20N.

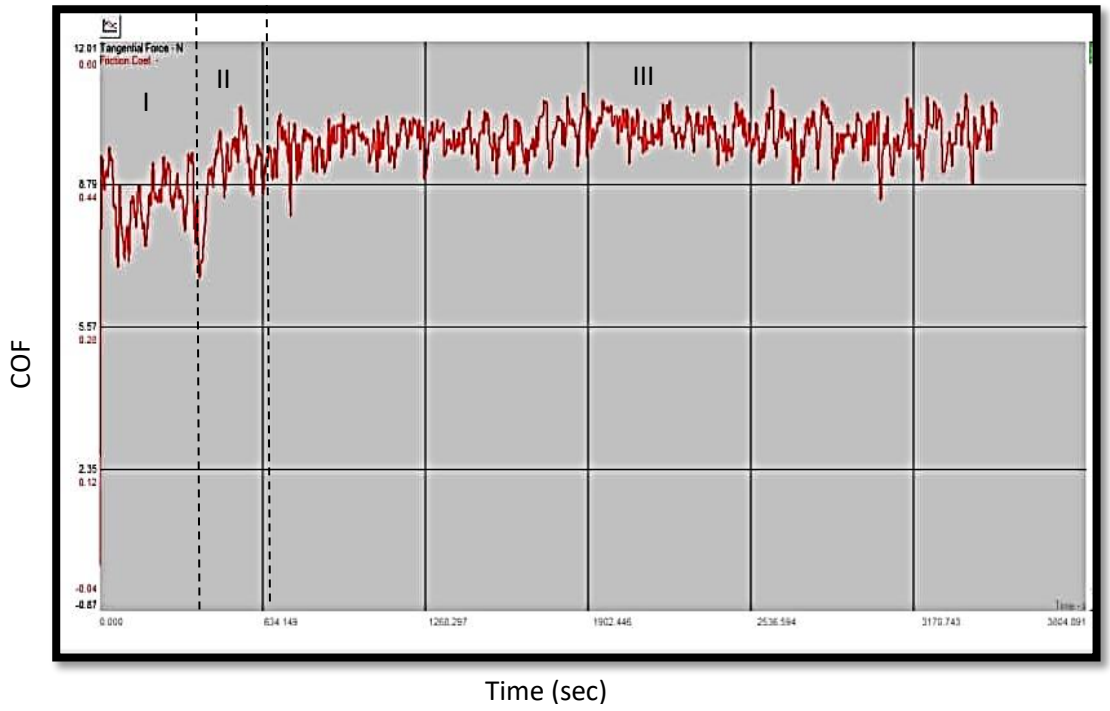

Figure (4.22): Lubricated sliding friction for Ti-15Mo Alloy at 20N.

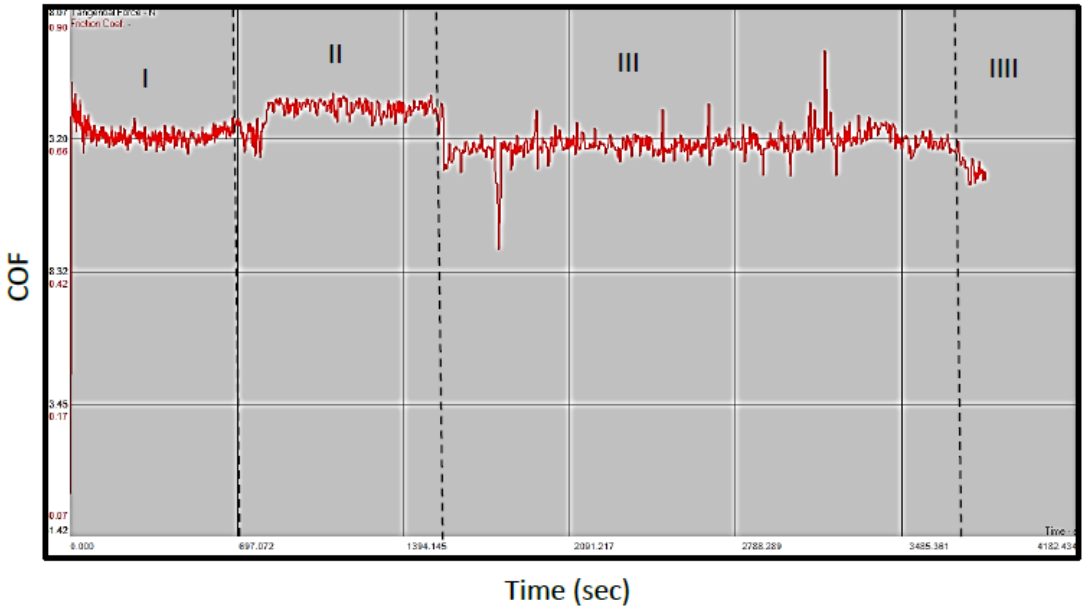

Figure (4.23): Lubricated sliding friction for Ti-8Mo-4Nb-2Zr Alloy at 20N.

Table (4.6): Average coefficient of friction of titanium alloys samples utilized in this investigation.

Alloy	Phase Constituents	COF at 10N	COF at 20N
CP-Ti	α	0.50	0.27
Ti-6Al-4V	α +β	0.10	0.33
Ti-13Zr-13Nb	Rich β	0.32	0.28
Ti-15Mo	Metastable β	0.37	0.94
Ti-8Mo-4Nb-2Zr	β	0.50	0.59

4.5.2. Wear Track Morphology and Roughness

Figures 4.24 and 4.25 display optical images of wear tracks and lines on titanium alloys used in this investigation and on the zirconia ball at 10 and 20N normal loads, respectively. The average surface roughness of titanium alloys samples used in this investigation at normal loads of 10 and 20N are listed in table 4.7. There are evidence of isolated debris particles, scratching and grooves developed on the worn track's surface. It is interesting to note that, on the surface of the β-microstracture Ti-8Mo-4Nb-2Zr, a light grey layer and tiny black spots appeared (see figure 4.24 highlighted with red arrow), these need more investigation. No evidence of crack was observed on the wear track of the all samples used in this investigation. With increase the load from 10N to 20N, the wear track shows deep scratching, increase the number of debris particles and extensive deformation with grooves were observed inside the wear track. These results are in a good agreement with what reported by **[225,184]**. Equally, no evidence of transfer from all titanium alloys used in this investigation to the zirconia ball surface, and transfer to the zirconia ball surface from all titanium alloys samples surface used in this investigation during rubbing at normal loads of 10 and 20N (see figures 4.24 and 4.25). The mechanisms of wear for all titanium alloys samples under rubbing at

normal loads of 10 and 20N were primarily related to abrasive ploughing wear.

It can see from the table 4.7, the the secound generation β-microstracture Ti-8Mo-4Nb-2Zr alloy had higher average roughnees at normal loads of 10 and 20N. Thus, might related to that the β-microstracture Ti-8Mo-4Nb-2Zr alloy had higher COF at normal loads of 10 and 20N of 0.5 (see table 4.7). No surprising that, the average roughness of the Cp-Ti and the first generation Ti-6Al-4V alloy increased with increase the load from 10 to 20N. The increase in roughness with load indicates that the Cp-Ti and the first generation Ti-6Al-4V alloy suffering from more extensive surface plastic deformation, as well as deep scratches and grooves on a large scale with increase the load from 10 to 20N. It is interesting to note that the average roughness of the β-microstracture Ti-8Mo-4Nb-2Zr, rich β Ti-13Zr-13Nb and metastable β Ti-15Mo decrease with load. According to these results, the β-microstracture alloys can recover there passivity and decrease the roughness with increase load 20N in this investigation. However, the secound generation β-microstracture are more suffring from wear at 10 N.

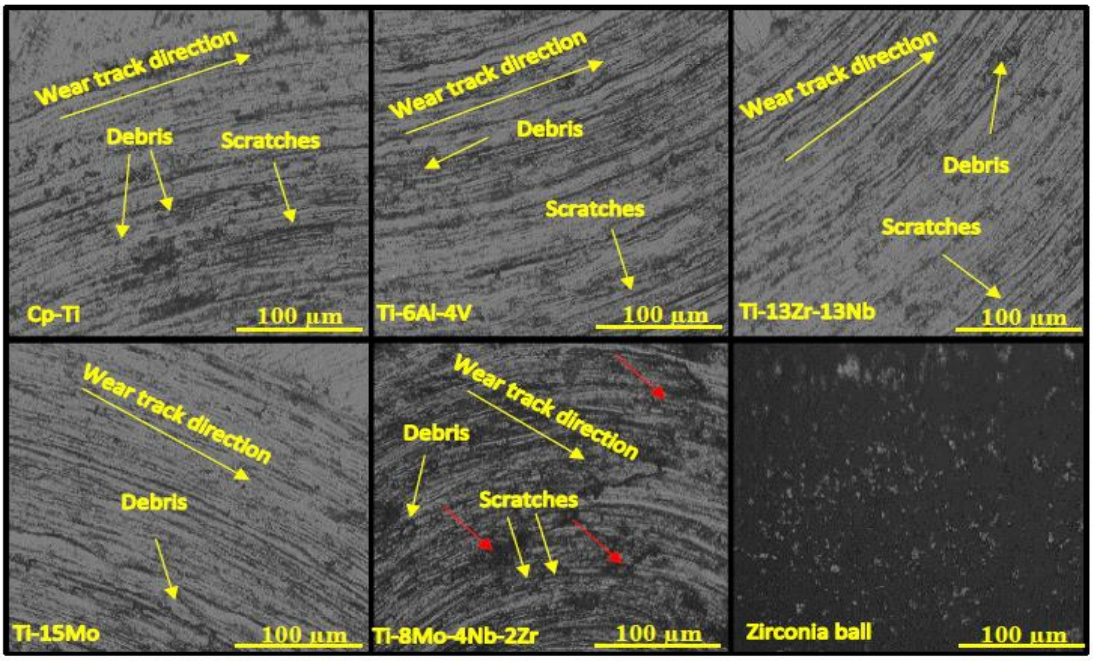

Figure (4.24): Wear Track for Titanium Alloys and the ball used in this investigation at 10N.

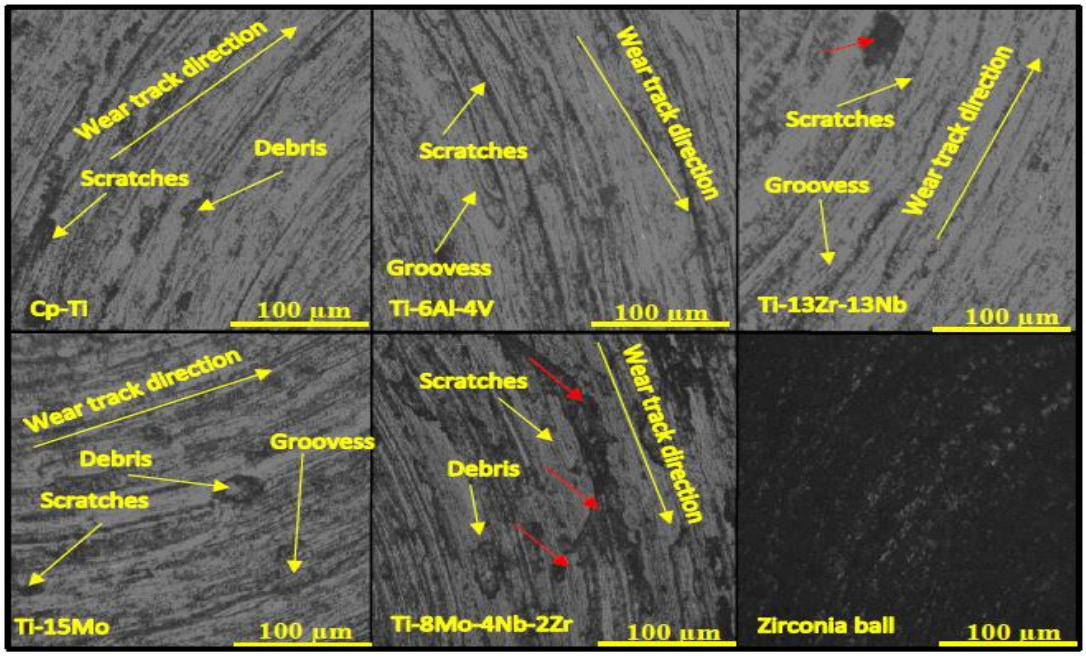

Figure (4.25): Wear Track for Titanium Alloys and the ball used in this investigation at 20N.

Table (4.7): Average roughness of the wear track of titanium alloys used in this investigation

Alloy	Phase Constituents	Average Roughness at 10N (μm)	Average Roughness at 20N (μm)
CP-Ti	α	0.505	1.083
Ti-6Al-4V	α +β	0.119	0.763
Ti-13Zr-13Nb	Rich - β	0.975	0.194
Ti-15Mo	Metastable - β	1.585	0.669
Ti-8Mo-4Nb-2Zr	β	2.030	1.715

4.5.3. Total Removed wear volume

The total volume removed due to wear of the titanium alloys samples used in this investigation after the wear tests are shown in the table 4.8. As you can see from the table 4.8, the total removed wear volume was relatively insensitive to the normal applied loads during the wear tests. All titanium alloys Cp-Ti, the first generation titanium alloy Ti-6Al-4V, rich – β Ti-13Zr-13Nb, and metastable – β Ti-15Mo exhibit an increase in the total removed wear volume with load. In contrast, the secound generation β-microstracture Ti-8Mo-4Nb-2Zr alloy exhibte decrease in total removed volume with load. The smallest removed wear volume was obtained with the first generating titanium alloy Ti-6Al-4V (see table 4.8) at normal load of 10N, while, the second generation β-microstracture Ti-8Mo-4Nb-2Zr showed the smallest total removed wear volume at normal load of 20N. The secound generation β-microstracture Ti-8Mo-4Nb-2Zr showed the highest total removed wear volume at normal load of 10N, while, the Cp-Ti α – microstracture alloy had the highest total removed wear volume at normal load of 20N.

At higher loads, 20 N in this investigation, the wear behaviour (total removed wear volume) could be explanied by the influnce of the

mechanical characteristics, such as hardness (H) and elastic modulus (E). It was reported that the wear ressistance may be better investigated using the ration between hardness and elastic modules H/E or H^3/E^2 instead of relying only on hardness **[226]**. The alloy has a good wear resistance with higher values of H/E or H^3/E^2. In this investigation, the maximam value of H/E ratio was about 2.5 for the secound generation β-microstracture Ti-8Mo-4Nb-2Zr, follwed by metastable – β Ti-15Mo and rich – β Ti-13Zr-13Nb with ratio of 2.3. Cp-Ti α – microstructure and first generation Ti-6Al-4V α+β microstructure had 0.99 and 1.7 ratio values of H/E respectively. However, at 10 N our results show that there is no direct link between the hardness and elastic modules for titanium alloys used in this investigation and the total removed wear volume. The same behavior for α +β and β phase titanium alloys was reported by **[223,227, 228]**.

It is interesting to note that the total removed wear volume of the secound generation β-microstracture Ti-8Mo-4Nb-2Zr decrease with load. This meant that the worn wear track on the secound generation β-microstracture Ti-8Mo-4Nb-2Zr has capacity to regain passivity under rubbing. However, the capacity of an alloy to revert to its passive state after rubbing is a crucial characteristic that is dependent on several factors. The main factors influnce the phenomenon of passiviting under rubbing are the critical pressure required to depassivation mechanism, the thickness of the passive oxide developed on the alloy's surface, and the chemical compostion of the oxide **[229]**. This phenomenon is very benficial to biomdeical applicatipons since the phenomenon of passivity will play a key role to decrease the material loss and reduce the amount of debris during wear, also decrease the release of metal inos. The same phenomenon was also reported in other β-microstracture titanium alloys by **[10,227,229]**.

Table (4.8): Total removed wear volume of titanium alloys used in this investigation

Alloy	Phase Constituents	Total removed wear volume at 10N (mm^3)	Total removed wear volume at 20N (mm^3)
CP-Ti	α	1.882234	2.258681
Ti-6Al-4V	α+β	0.678852	1.762752
Ti-13Zr-13Nb	Rich - β	0.769218	1.199076
Ti-15Mo	Metastable β	0.85341	1.335718
Ti-8Mo-4Nb-2Zr	β	2.095703	1.035156

Chapter Five

Conclusions and Suggestions

Conclusions and Suggestions

5.1. Conclusions

In this investigation, the microstructure, the electrochemical and tribological behavior that correlates microstructure of the traditionally used Cp-Ti α-microstructure, the first generation Ti-6Al-4V α+β microstructure, and the second-generation titanium-based alloys β, rich β, and metastable β were investigated in Ringer solution. From the results obtained in this investigation, the main conclusions can be drawn:

1- The average Vickers microhardness values of the second-generation Ti -8Mo-4Nb-2Zr β- microstructure alloy were greater than those of other alloys used in this investigating. While, Ti-13Zr-13Nb (Richβ) and Ti-15Mo (metastable β) alloys showed Vickers microhardness values that were greater than Cp-Ti (α-phase) and near to first generation values. (α +β) Ti-6Al-4V

2- The second-generation Ti -8Mo-4Nb-2Zr β- microstructure alloy had a lower elastic modulus as compare to the other alloys used in this investigation.

3- The alloy microstructure (α, α+β, rich β, metastable β and β) hardly influenced the electrochemical behavior of alloys used in this investigation.

4- The second generation Ti -8Mo-4Nb-2Zr β- microstructure, Ti-13Zr-13Nb (Rich β) and Ti-15Mo (metastable β) alloys with the highest positive OCP values outperformed Cp-Ti (α -phase) and the first generation of Ti-6Al-4V α +β.

5- The second-generation Ti -8Mo-4Nb-2Zr β- microstructure alloy had lower corrosion rate compared to other titanium alloys used in this investigation.

6- The tribological mechanism is predominantly abrasive mechanism.

7- No evidence of material transfer from all alloys to the zirconia ball or from the zirconia ball counterbody to all titanium alloys used in this investigation after the wear tests.

8- At high load used in this investigation, the wear behavior has direct relationship with mechanical properties. However, the ratio of depassivation / repassivation influenced the wear behavior of the second-generation titanium alloys.

9- The second-generation Ti -8Mo-4Nb-2Zr - microstructure alloy was found to be the greatest option for biomedical application due to its elevated hardness and low modulus of elastic, low corrosion rate, comparable tribological behavior and with nontoxic alloying elements limit compared with other alloys used in this investigation.

5.2. Suggestions

During this investigation, the microstructure, electrochemical and tribological behavior that correlates microstructure of the second generation of titanium alloys, traditionally used α-microstructure phase Cp-Ti alloy, and the first generation alloy (Ti-6Al-4V) were documented in this dissertation. It may be necessary to accomplish the following in order to have a better knowledge of all phenomena:

1- Investigation the electrochemical and tribological behavior that correlates microstructure of the second generation of titanium alloys that not used in this investigation, for example, near β, α′ + β, α″ + β, and ω+β.

2. To gain additional information about the electrochemical behavior of alloys, the electrochemical study should be completed utilizing electrochemical impedance spectroscopy EIS.

3- The subsurface structure after the wear need more investigation applying focused ion beam test (FIB) and transmission electron microscopy test (TEM).

4- Light grey layer and small black spots formed on the surface of the secound generation β-microstracture Ti-8Mo-4Nb-2Zr after the wear need more investigation using Raman spectroscopy.

5- Antibacterial test for oxide film forming on the surface.

6- Coating modification of alloys surfaces.

Reference

References:

[1] Y. Li, C. Yang, H. Zhao, S. Qu, X. Li, and Y. Li, "New developments of Ti-based alloys for biomedical applications," Materials, vol. 7, pp. 1709-1800, 2014.

[2] A. T. Sidambe, "Biocompatibility of advanced manufactured titanium implants—A review," Materials, vol. 7, pp. 8168-8188, 2014.

[3] Q. Chen and G. A. Thouas, "Metallic implant biomaterials," Materials Science and Engineering: R: Reports, vol. 87, pp. 1-57, 2015.

[4] M. Long and H. J. Rack, "Titanium alloys in total joint replacement—a materials science perspective," Biomaterials, vol. 19, pp. 1621-1639, 1998.

[5] G. Lütjering and J. C. Williams, Titanium vol. 2: Springer, 2003.

[6] T. Hanawa, "Recent development of new alloys for biomedical use," in Materials science forum, 2006, pp. 243-248.

[7] M. A. Hussein, A. S. Mohammed, and N. Al-Aqeeli, "Wear characteristics of metallic biomaterials: a review," Materials, vol. 8, pp. 2749-2768, 2015.

[8] V. Oliveira, R. Chaves, R. Bertazzoli, and R. Caram, "Preparation and characterization of Ti-Al-Nb alloys for orthopedic implants," Brazilian Journal of Chemical Engineering, vol. 15, pp. 326-333, 1998.

[9] Y. T. Zhu, T. C. Lowe, R. Z. Valiev, V. V. Stolyarov, V. V. Latysh, and G. J. Raab, "Ultrafine-grained titanium for medical implants," ed: Google Patents, 2002.

[10] N. More, N. Diomidis, S. Paul, M. Roy, and S. Mischler, "Tribocorrosion behavior of β titanium alloys in physiological solutions containing synovial components," Materials Science and Engineering: C, vol. 31, pp. 400-408, 2011.

[11] D. Kuroda, M. Niinomi, M. Morinaga, Y. Kato, and T. Yashiro, "Design and mechanical properties of new β type titanium alloys for implant materials," Materials Science and Engineering: A, vol. 243, pp. 244-249, 1998.

[12] Y. Okazaki and E. Gotoh, "Comparison of metal release from various metallic biomaterials in vitro," Biomaterials, vol. 26, pp. 11-21, 2005.

[13] R. Banerjee, S. Das, K. Mukhopadhyay, S. Nag, A. Chakrabortty, and K. Chaudhuri, "Involvement of in vivo induced cheY-4 gene of Vibrio cholerae in motility, early adherence to intestinal epithelial cells and regulation of virulence factors," FEBS letters, vol. 532, pp. 221-226, 2002.

[14] Y. Song, D. Xu, R. Yang, D. Li, and Z. Hu, "Theoretical investigation of ductilizing effects of alloying elements on TiAl," Intermetallics, vol. 6, pp. 157-165, 1998.

[15] M. G. Joshi, S. G. Advani, F. Miller, and M. H. Santare, "Analysis of a femoral hip prosthesis designed to reduce stress shielding," Journal of biomechanics, vol. 33, pp. 1655-1662, 2000.

[16] S. Gross and E. Abel, "A finite element analysis of hollow stemmed hip prostheses as a means of reducing stress shielding of the femur," Journal of Biomechanics, vol. 34, pp. 995-1003, 2001.

[17] S. Sahu, M. Palaniappa, S. Paul, and M. Roy, "Potentiodynamic behaviour of Ti alloys in physiological solution containing lubricant," Materials Letters, vol. 64, pp. 12-14, 2010.

[18] B. Obadele, A. Andrews, P. Olubambi, M. Mathew, and S. Pityana, "Tribocorrosion behaviour of laser cladded biomedical grade titanium alloy," Materials and Corrosion, vol. 66, pp. 1133-1139, 2015.

[19] M. Geetha, A. Singh, R. Asokamani, and A. Gogia, "Ti based biomaterials, the ultimate choice for orthopaedic implants–a review," Progress in Materials science, vol. 54, pp. 397-425, 2009.

[20] M. Niinomi, M. Nakai, and J. Hieda, "Development of new metallic alloys for biomedical applications," Acta Biomaterialia, vol. 8, pp. 3888-3903, 2012

[21] D. Banerjee and J. Williams, "Perspectives on titanium science and technology," Acta Materialia, vol. 61, pp. 844-879, 2013.

[22] G. Colombo, "The Effect of Equal Channel Angular Extrusion (ECAE) and Boron Additions on the Mechanical Properties of a Biomedical Ti-Nb-Zr-Ta (TNZT) Alloy," 2010.

[23] S. Kumar and T. S. Narayanan, "Corrosion behaviour of Ti–15Mo alloy for dental implant applications," Journal of Dentistry, vol. 36, pp. 500-507, 2008.

[24] R.Prakash kolli and Arun Davaraj, "A Review of Metastable Beta Titanium Alloys," MDPI, 2018.

[25] Carsten Siemers and Christian Stocker , " Develpments in Titanium Research and Applicatin in Germany," MATEC Web of Cnferences, 2020

[26] Australian Government Publishing Service Melbourne, “NEW AND ADVANCED MATERIALS”, REPORT NO. 42, 8 MARCH 1995.

[27] Joyce Y. Wong and Joseph D.Bronzino, BIOMATERIALS, Group, LLC, 2007

[28] Swee Hin TEOH, Mauli AGRAWAL, Joost D. de Bruijn, and Yasuhiko TABATA, EN G IN E E RING MATERIALS FOR BIOMEDICAL APPLICATI0N, Copyright 0 2004 by World Scientific Publishing Co. Pte. Ltd.

[29] Myer Kutz, BIOMEDICAL ENGINEERING AND DESIGN HANDBOOK Volume 1: Fundamentals, , Copyright © 2009, 2003 by The McGraw-Hill Companies, Inc.

[30] ROLANDO BARBUCCI, Integrated Biomaterials Science, ©2002 Kluwer Academic Publishers New York, Boston, Dordrecht, London, Moscow.

[31] A. F. von Recum, Handbook of biomaterials evaluation: scientific, technical and clinical testing of implant materials: CRC Press, 1998.

[32] J. Park and R. S. Lakes, Biomaterials: an introduction: Springer Science & Business Media, 2007.

[33] J. R. Sin, "Investigation of the corrosion and tribocorrosion behaviour of metallic biomaterials," Luleå tekniska universitet, 2015.

[34] M. Niinomi, "Recent metallic materials for biomedical applications," Metallurgical and materials transactions A, vol. 33, pp. 477-486, 2002.

[35] M. Niinomi, "Metallic biomaterials," Journal of Artificial Organs, vol. 11, pp. 105- 110, 2008.

[36] C. Elias, J. Lima, R. Valiev, and M. Meyers, "Biomedical applications of titanium and its alloys," Jom, vol. 60, pp. 46-49, 2008.

[37] R. Adell, U. Lekholm, B. Rockler, and P.-I. Brånemark, "A 15-year study of osseointegrated implants in the treatment of the edentulous jaw," International journal of oral surgery, vol. 10, pp. 387-416, 1981.

[38] D. BomBač, M. Brojan, P. Fajfar, F. Kosel, and R. Turk, "Review of materials in medical applications Pregled materialov v medicinskih aplikacijah," RMZ–Materials and Geoenvironment, vol. 54, pp. 471-499, 2007.

[39] J.-E. Bidaux, C. Closuit, M. Rodriguez-Arbaizar, D. Zufferey, and E. CarreñoMorelli, "Metal injection moulding of low modulus Ti–Nb alloys for biomedical applications," Powder Metallurgy, vol. 56, pp. 263-266, 2013.

[40] G. Shibo, Q. Xuanhui, H. Xinbo, Z. Ting, and D. Bohua, "Powder injection molding of Ti–6Al–4V alloy," Journal of Materials Processing Technology, vol. 173, pp. 310- 314, 2006.

[41] A. Sidambe, W. Choong, H. Hamilton, and I. Todd, "Correlation of metal injection moulded Ti6Al4V yield strength with resonance frequency (PCRT) measurements," Materials Science and Engineering: A, vol. 568, pp. 220-227, 2013.

[42] X. Zhao, J. Chen, X. Lin, and W. Huang, "Study on microstructure and mechanical properties of laser rapid forming Inconel 718," Materials Science and Engineering: A, vol. 478, pp. 119-124, 2008.

[43] S. Ponader, C. Von Wilmowsky, M. Widenmayer, R. Lutz, P. Heinl, C. Körner, et al., "In vivo performance of selective electron beam-melted Ti-6Al-4V structures," Journal of biomedical materials research Part A, vol. 92, pp. 56-62, 2010.

[44] J. Parthasarathy, B. Starly, S. Raman, and A. Christensen, "Mechanical evaluation of porous titanium (Ti6Al4V) structures with electron beam melting (EBM)," Journal of the mechanical behavior of biomedical materials, vol. 3, pp. 249-259, 2010.

[45] L. Murr, K. Amato, S. Li, Y. Tian, X. Cheng, S. Gaytan, et al., "Microstructure and mechanical properties of open-cellular biomaterials prototypes for total knee replacement implants fabricated by electron beam melting," Journal of the mechanical behavior of biomedical materials, vol. 4, pp. 1396-1411, 2011.

[46] A. Sidambe, I. Figueroa, H. Hamilton, and I. Todd, "Metal injection moulding of CPTi components for biomedical applications," Journal of Materials Processing Technology, vol. 212, pp. 1591-1597, 2012.

[47] W. E. Frazier, "Metal additive manufacturing: a review," Journal of Materials Engineering and Performance, vol. 23, pp. 1917-1928, 2014.

[48] A. T. Sidambe, I. A. Figueroa, H. G. Hamilton, and I. Todd, "Taguchi optimization of MIM titanium sintering," International journal of powder metallurgy, vol. 47, pp. 21- 28, 2011.

[49] R. Van Noort, "The future of dental devices is digital," Dental materials, vol. 28, pp. 3-12, 2012.

[50] O. Ferri, T. Ebel, and R. Bormann, "High cycle fatigue behaviour of Ti–6Al–4V fabricated by metal injection moulding technology," Materials Science and Engineering: A, vol. 504, pp. 107-113, 2009.

[51] T. Ebel, C. Blawert, R. Willumeit, B. J. Luthringer, O. M. Ferri, and F. Feyerabend, "Ti–6Al–4V–0.5 B—A Modified Alloy for Implants Produced by Metal Injection Molding," Advanced Engineering Materials, vol. 13, 2011.

[52] V. Biehl, T. Wack, S. Winter, U. Seyfert, and J. Breme, "Evaluation of the haemocompatibility of titanium based biomaterials," Biomolecular engineering, vol. 19, pp. 97-101, 2002.

[53] B. Zberg, P. J. Uggowitzer, and J. F. Löffler, "MgZnCa glasses without clinically observable hydrogen evolution for biodegradable implants," Nature materials, vol. 8, p. 887, 2009.

[54] D. Blackwood, "Biomaterials: past successes and future problems," Corrosion reviews, vol. 21, pp. 97-124, 2003.

[55] Y. Okazaki and E. Gotoh, "Metal release from stainless steel, Co–Cr–Mo–Ni–Fe and Ni–Ti alloys in vascular implants," Corrosion Science, vol. 50, pp. 3429-3438, 2008.

[56] E. Whitney and S. R. Rolfes, Understanding nutrition: Cengage Learning, 2007.

[57] J. Cruickshank, J. Thorp, and F. J. Zacharias, "Benefits and potential harm of lowering high blood pressure," The Lancet, vol. 329, pp. 581-584, 1987.

[58] M. Niinomi, "Recent titanium R&D for biomedical applications in Japan," Jom, vol. 51, p. 32, 1999.

[59] S. K. Misra, D. Mohn, T. J. Brunner, W. J. Stark, S. E. Philip, I. Roy, et al., "Comparison of nanoscale and microscale bioactive glass on the properties of P (3HB)/Bioglass® composites," Biomaterials, vol. 29, pp. 1750-1761, 2008.

[60] M. Sumita, T. Hanawa, I. Ohnishi, and T. Yoneyama, "Failure Processes in biometallic materials," Compr Struct Integr, vol. 9, pp. 131-67, 2003.

[61] S. Suresh, "Fatigue of Materials, Cambridge University Press," Cambridge, England, 1998

[62] R. A. Antunes and M. C. L. de Oliveira, "Corrosion fatigue of biomedical metallic alloys: mechanisms and mitigation," Acta biomaterialia, vol. 8, pp. 937-962, 2012.

[63] A. Yamamoto, T. Kobayashi, N. Maruyama, K. Nakazawa, and M. Sumita, "Fretting fatigue properties of Ti-6 Al-4 V alloy in pseudo-body fluid and evaluation of biocompatibility by cell culture method," J. Jpn. Inst. Met.(Japan), vol. 59, pp. 463- 470, 1995.

[64] M. Niinomi, "Fatigue characteristics of metallic biomaterials," International Journal of Fatigue, vol. 29, pp. 992-1000, 2007.

[65] D. W. Lennox, B. H. Schofield, D. F. Mcdonald, and L. H. Riley Jr, "A histologic comparison of aseptic loosening of cemented, press-fit, and biologic ingrowth prostheses," Clinical orthopaedics and related research, vol. 225, pp. 171-191, 1987.

[66] A. Schweizer, U. Riede, T. Maurer, and P. Ochsner, "Ten-year follow-up of primary straight-stem prosthesis (MEM) made of titanium or cobalt chromium alloy," Archives of orthopaedic and trauma surgery, vol. 123, pp. 353-356, 2003.

[67] I. Papageorgiou, V. Shadrick, S. Davis, L. Hails, R. Schins, R. Newson, et al., "Macrophages detoxify the genotoxic and cytotoxic effects of surgical cobalt chrome alloy particles but not quartz particles on human cells in vitro," Mutation Research/Fundamental and Molecular Mechanisms of Mutagenesis, vol. 643, pp. 11- 19, 2008.

[68] M. B. Nasab, M. R. Hassan, and B. B. Sahari, "Metallic biomaterials of knee and hipA review," Trends Biomater. Artif. Organs, vol. 24, pp. 69-82, 2010.

[69] B. Subramanian, R. Ananthakumar, A. Kobayashi, and M. Jayachandran, "Surface modification of 316L stainless steel with magnetron sputtered TiN/VN nanoscale multilayers for bio implant applications," Journal of Materials Science: Materials in Medicine, vol. 23, pp. 329-338, 2012.

[70] A. Parsapour, S. N. Khorasani, and M. H. Fathi, "Effect of surface treatment and metallic coating on corrosion behavior and biocompatibility of surgical 316L stainless steel implant," Journal of Materials Science & Technology, vol. 28, pp. 125-131, 2012.

[71] R. S. ONS, "Modifying biomaterial surfaces to optimise interactions with bone," Surface Modification of Biomaterials: Methods Analysis and Applications, p. 365, 2010.

[72] G. Mani, M. D. Feldman, S. Oh, and C. M. Agrawal, "Surface modification of cobalt– chromium–tungsten–nickel alloy using octadecyltrichlorosilanes," Applied Surface Science, vol. 255, pp. 5961-5970, 2009.

[73] A. Verstrynge, J. Van Humbeeck, and G. Willems, "In-vitro evaluation of the material characteristics of stainless steel and beta-titanium orthodontic wires," American journal of orthodontics and dentofacial orthopedics, vol. 130, pp. 460-470, 2006.

[74] C. Leyens and M. Peters, Titanium and titanium alloys: fundamentals and applications: John Wiley & Sons, 2003.

[75] G. Bedinger, "Mineral Commodity Summaries: Titanium and Titanium Dioxide," US Geological Survey, Washington DC, USA, pp. 170-171, 2014.

[76] A. International, Handbook of materials for medical devices: ASM international, 2003.

[77] P. B. Vila, "Phase transformation kinetics during continuous heating of α+ β and metastable β titanium alloys."

[78] M. T. Mohammed, Z. A. Khan, and A. N. Siddiquee, "Beta Titanium Alloys: The Lowest Elastic Modulus for Biomedical Applications: A Review."

[79] S. Miyazaki, H. Kim, and H. Hosoda, "Development and characterization of Ni-free Ti-base shape memory and superelastic alloys," Materials Science and Engineering: A, vol. 438, pp. 18-24, 2006.

[80] J. Kim, H. Kim, T. Inamura, H. Hosoda, and S. Miyazaki, "Shape memory characteristics of Ti–22Nb–(2–8) Zr (at.%) biomedical alloys," Materials Science and Engineering: A, vol. 403, pp. 334-339, 2005.

[81] I. Weiss and S. Semiatin, "Thermomechanical processing of beta titanium alloys—an overview," Materials Science and Engineering: A, vol. 243, pp. 46-65, 1998.

[82] M. J. Donachie, Titanium: a technical guide: ASM international, 2000.

[83] G. Lütjering and J. C. Williams, "Alpha+ beta alloys," Titanium, pp. 203-258, 2007.

[84] V. D. Cojocaru, D. Raducanu, T. Gloriant, E. Bertrand, and I. Cinca, "Structural observation of twinning deformation mechanism in a Ti-Ta-Nb alloy," in Solid State Phenomena, 2012, pp. 46-51.

[85] D. Raducanu, E. Vasilescu, V. Cojocaru, I. Cinca, P. Drob, C. Vasilescu, et al., "Mechanical and corrosion resistance of a new nanostructured Ti–Zr–Ta–Nb alloy," Journal of the mechanical behavior of biomedical materials, vol. 4, pp. 1421-1430, 2011.

[86] Y. Tong, B. Guo, Y. Zheng, C. Y. Chung, and L. W. Ma, "Effects of Sn and Zr on the microstructure and mechanical properties of Ti-Ta-based shape memory alloys," Journal of materials engineering and performance, vol. 20, pp. 762-766, 2011.

[87] M. Niinomi, "Mechanical properties of biomedical titanium alloys," Materials Science and Engineering: A, vol. 243, pp. 231-236, 1998.

[88] M. Niinomi, "Mechanical biocompatibilities of titanium alloys for biomedical applications," Journal of the mechanical behavior of biomedical materials, vol. 1, pp. 30-42, 2008.

[89] Xionggang Lu, Na Gui, Aitao Qiu, Chong He Li, Thermodynamic Modeling of the Al-Ti-V Ternary System, Aug 2014.

[90] S. Barzilai, C. Toher, and O. Levy , “The molybdenum-titanium phase diagram evaluated from ab-initio calculations”, and Published 6 October 2016, Materials Science, Physics

[91] E.W. Collings; The Physical Metallurgy of Titanium Alloys; American Society for Metals, 1984.

[92] A. Muñoz and M. Costa, "Elucidating the mechanisms of nickel compound uptake: a review of particulate and nano-nickel endocytosis and toxicity," Toxicology and applied pharmacology, vol. 260, pp. 1-16, 2012.

[93] Jonathan Black, and Garth Hastings, Handbook of Biomaterial Properties, © 1998 Chapman & Hall, p:430.

[94] I. Pais, M. Feher, E. Farkas, Z. Szabo, and I. Cornides, "Titanium as a new trace element," Communications in Soil Science & Plant Analysis, vol. 8, pp. 407-410, 1977.

[95] S. Yaghoubi, C. W. Schwietert, and J. P. McCue, "Biological roles of titanium," Biological trace element research, vol. 78, p. 205, 2000.

[96] M. L. Wang, R. Tuli, P. A. Manner, P. F. Sharkey, D. J. Hall, and R. S. Tuan, "Direct and indirect induction of apoptosis in human mesenchymal stem cells in response to titanium particles," Journal of Orthopaedic Research, vol. 21, pp. 697-707, 2003.

[97] N. Coen, M. Kadhim, E. Wright, C. Case, and C. Mothersill, "Particulate debris from a titanium metal prosthesis induces genomic instability in primary human fibroblast cells," British Journal of Cancer, vol. 88, p. 548, 2003.

[98] R. Kumazawa, F. Watari, N. Takashi, Y. Tanimura, M. Uo, and Y. Totsuka, "Effects of Ti ions and particles on neutrophil function and morphology," Biomaterials, vol. 23, pp. 3757-3764, 2002.

[99] V. Koval'skiĭ and L. Rezaeva, "The biological role of vanadium in ascidia," Uspekhi sovremennoi biologii, vol. 60, pp. 45-61, 1964.

[100] E. P. Daniel and E. M. Hewston, "VANADIUM-A CONSIDERATION OF ITS POSSIBLE BIOLOGICAL RÔLE," American Journal of Physiology--Legacy Content, vol. 136, pp. 772-775, 1942.

[101] J. J. Rodríguez-Mercado, R. A. Mateos-Nava, and M. A. Altamirano-Lozano, "DNA damage induction in human cells exposed to vanadium oxides in vitro," Toxicology in Vitro, vol. 25, pp. 1996-2002, 2011.

[102] L. S. Rhoads, W. T. Silkworth, M. L. Roppolo, and M. S. Whittingham, "Cytotoxicity of nanostructured vanadium oxide on human cells in vitro," Toxicology in Vitro, vol. 24, pp. 292-296, 2010.

[103] N. Ress, B. Chou, R. Renne, J. Dill, R. Miller, J. Roycroft, et al., "Carcinogenicity of inhaled vanadium pentoxide in F344/N rats and B6C3F1 mice," Toxicological Sciences, vol. 74, pp. 287-296, 2003.

[104] B. Moretti, V. Pesce, G. Maccagnano, G. Vicenti, P. Lovreglio, L. Soleo, et al., "Peripheral neuropathy after hip replacement failure: is vanadium the culprit?," The Lancet, vol. 379, p. 1676, 2012.

[105] S. V. Verstraeten, L. Aimo, and P. I. Oteiza, "Aluminium and lead: molecular mechanisms of brain toxicity," Archives of toxicology, vol. 82, pp. 789-802, 2008.

[106] W. A. Banks and A. J. Kastin, "Aluminum-induced neurotoxicity: alterations in membrane function at the blood-brain barrier," Neuroscience & Biobehavioral Reviews, vol. 13, pp. 47-53, 1989.

[107] R. A. Yokel, "The toxicology of aluminum," Neurotoxicology, vol. 21, pp. 813-828, 2000.

[108] D. N. Kerr, M. K. Ward, H. A. Ellis, W. Simpson, and I. Parkinson, "Aluminium intoxication in renal disease," Aluminium in biology and medicine, pp. 123-141, 1992.

[109] P. Darbre, "Environmental oestrogens, cosmetics and breast cancer," Best practice & research clinical endocrinology & metabolism, vol. 20, pp. 121-143, 2006.

[110] P. C. Ferreira, K. d. A. Piai, A. M. M. Takayanagui, and S. I. Segura-Muñoz, "Aluminum as a risk factor for Alzheimer's disease," Revista latino-americana de enfermagem, vol. 16, pp. 151-157, 2008.

[111] P. Darbre, "Metalloestrogens: an emerging class of inorganic xenoestrogens with potential to add to the oestrogenic burden of the human breast," Journal of Applied Toxicology, vol. 26, pp. 191-197, 2006.

[112] W. L. Downs, J. K. Scott, C. L. Yuile, F. S. Caruso, and L. C. Wong, "The toxicity of niobium salts," American Industrial Hygiene Association Journal, vol. 26, pp. 337- 346, 1965.

[113] M. Caicedo, J. J. Jacobs, A. Reddy, and N. J. Hallab, "Analysis of metal ion-induced DNA damage, apoptosis, and necrosis in human (Jurkat) T-cells demonstrates Ni2+ and V3+ are more toxic than other metals: Al3+, Be2+, Co2+, Cr3+, Cu2+, Fe3+, Mo5+, Nb5+, Zr2+," Journal of Biomedical Materials Research Part A, vol. 86, pp. 905-913, 2008.

[114] M. Nordberg and G. F. Nordberg, "Toxicology and biological monitoring of metals," General, Applied and Systems Toxicology, 2009.

[115] U. Pazzaglia, P. Apostoli, T. Congiu, S. Catalani, M. Marchese, and G. Zarattini, "Cobalt, chromium and molybdenum ions kinetics in the human body: data gained from a total hip replacement with massive third body wear of the head and neuropathy by cobalt intoxication," Archives of orthopaedic and trauma surgery, vol. 131, pp. 1299-1308, 2011.

[116] M. Curzon, J. Kubota, and B. Bibby, "Environmental effects of molybdenum on caries," Journal of Dental Research, vol. 50, pp. 74-77, 1971.

[117] D. G. Barceloux and D. Barceloux, "Molybdenum," Journal of Toxicology: Clinical Toxicology, vol. 37, pp. 231-237, 1999.

[118] M. Coughlan, "The role of molybdenum in human biology," Journal of inherited metabolic disease, vol. 6, pp. 70-77, 1983.

[119] M. Anke, M. Seifert, W. Arnhold, S. Anke, and U. Schäfer, "The biological and toxicological importance of molybdenum in the environment and in the nutrition of plants, animals and man: Part V: Essentiality and toxicity of molybdenum," Acta alimentaria, vol. 39, pp. 12-26, 2010.

[120] W.-C. Witzleb, J. Ziegler, F. Krummenauer, V. Neumeister, and K.-P. Guenther, "Exposure to chromium, cobalt and molybdenum from metal-on-metal total hip replacement and hip resurfacing arthroplasty," Acta orthopaedica, vol. 77, pp. 697- 705, 2006.

[121] J. Antoniou, D. J. Zukor, F. Mwale, W. Minarik, A. Petit, and O. L. Huk, "Metal ion levels in the blood of patients after hip resurfacing: a comparison between twentyeight and thirty-six-millimeter-head metal-on-metal prostheses," JBJS, vol. 90, pp. 142-148, 2008.

[122] A. S. Martins, P. M. Fresco, and M. J. Pereira, "Toxicity of Zirconium on Growth of Two Green Algae," Fresenius Environmental Bulletin, vol. 16, pp. 869-874, 2007.

[123] J. Delongeas, D. Burnel, P. Netter, M. Grignon, J. Mur, R. Royer, et al., "Toxicity and pharmacokinetics of zirconium oxychloride in mice and rats," Journal de pharmacologie, vol. 14, pp. 437-447, 1983.

[124] L. McClinton and J. Schubert, "The toxicity of some zirconium and thorium salts in rats," Journal of Pharmacology and Experimental Therapeutics, vol. 94, pp. 1-6, 1948.

[125] J. Chamberlain and K. R. Trethewey, Corrosion for Science and Engineering: Longman Scientific & Technical, 1995.

[126] V. CORROSION, "Y 2, LL Shreir, RA Jarman, GT Burnstein," ed: Butterworth Heinemann, Oxford, 1994.

[127] J. R. Davis, Surface engineering for corrosion and wear resistance: ASM international, 2001.

[128] C. Kajdas, E. Wilusz, and S. Harvey, Encyclopedia of tribology vol. 15: Elsevier, 1990.

[129] N. G. M.Fontanna, "Corrosion Engineering," New York: Mc Graw Hill, 1978.

[130] S. Mischler, "Triboelectrochemical techniques and interpretation methods in tribocorrosion: a comparative evaluation," Tribology International, vol. 41, pp. 573- 583, 2008.

[131] D. Landolt, Corrosion and surface chemistry of metals: EPFL press, 2007.

[132] R. Revie and H. H. Uhlig, "Thermodynamics: corrosion tendancy and electrode potentials," Corrosion and corrosion control, vol. 1, pp. 22-66, 2000.

[133] P. Süry and M. Semlitsch, "Corrosion behavior of cast and forged cobalt-based alloys for double-alloy joint endoprostheses," Journal of biomedical materials research, vol. 12, pp. 723-741, 1978.

[134] D. C. Silverman, "Tutorial on cyclic potentiodynamic polarization technique," in CORROSION 98, 1998.

[135] M. Mathew, P. Srinivasa Pai, R. Pourzal, A. Fischer, and M. Wimmer, "Significance of tribocorrosion in biomedical applications: overview and current status," Advances in tribology, vol. 2009, 2010.

[136] P. Ponthiaux, F. Wenger, D. Drees, and J.-P. Celis, "Electrochemical techniques for studying tribocorrosion processes," Wear, vol. 256, pp. 459-468, 2004.

[137] C. Valero Vidal, "Study of the degradation mechanisms of the CoCrMo biomedical alloy in physiological media by electrochemical techniques and surface analysis," 2012.

[138] J. R. Davis, Corrosion: understanding the basics: ASM International, 2000.

[139] P. R. Roberge, "Handbook of corrosion engineering," McGraw-Hill,, 2000.

[140] D. Landolt, S. Mischler, and M. Stemp, "Electrochemical methods in tribocorrosion: a critical appraisal," Electrochimica Acta, vol. 46, pp. 3913-3929, 2001.

[141] K. R. T. a. J. Chamberlain, "Corrosion for science and engineering," Longman,, vol. ISBN 9780582238695., 1995.

[142] Y. Zhang, D. D. Macdonald, M. Urquidi-Macdonald, G. R. Engelhardt, and R. B. Dooley, "Passivity breakdown on AISI Type 403 stainless steel in chloride-containing borate buffer solution," Corrosion science, vol. 48, pp. 3812-3823, 2006.

[143] K. Raja and D. Jones, "Effects of dissolved oxygen on passive behavior of stainless alloys," Corrosion science, vol. 48, pp. 1623-1638, 2006.

[144] Y. Sun, "Depth-profiling electrochemical measurements of low temperature plasma carburised 316L stainless steel in 1M H 2 SO 4 solution," Surface and Coatings Technology, vol. 204, pp. 2789-2796, 2010.

[145] Y. Qiao, Y. Zheng, W. Ke, and P. Okafor, "Electrochemical behaviour of high nitrogen stainless steel in acidic solutions," Corrosion Science, vol. 51, pp. 979-986, 2009.

[146] R. A. J. L. L. Shreir, and G. T. Burstein, "Corrosion (3rd Edition) Volumes 1-2. Elsevier,," 1994.

[147] M. J. Donachie, "Titanium," A Technical Guide, ASM International, Materials Park, OH, 2000.

[148] A. Revathi, A. D. Borrás, A. I. Muñoz, C. Richard, and G. Manivasagam, "Degradation mechanisms and future challenges of titanium and its alloys for dental implant applications in oral environment," Materials Science and Engineering: C, 2017.

[149] R. G. Kelly, J. R. Scully, D. Shoesmith, and R. G. Buchheit, Electrochemical techniques in corrosion science and engineering: CRC Press, 2002.

[150] I. Polmear, Light alloys: from traditional alloys to nanocrystals: ButterworthHeinemann, 2005.

[151] W.-F. Ho, "A comparison of tensile properties and corrosion behavior of cast Ti–7.5 Mo with cp Ti, Ti–15Mo and Ti–6Al–4V alloys," Journal of Alloys and Compounds, vol. 464, pp. 580-583, 2008.

[152] Y. Wang and Y. Zheng, "Corrosion behaviour and biocompatibility evaluation of low modulus Ti–16Nb shape memory alloy as potential biomaterial," Materials Letters, vol. 63, pp. 1293-1295, 2009.

[153] Y. L. Zhou, M. Niinomi, T. Akahori, H. Fukui, and H. Toda, "Corrosion resistance and biocompatibility of Ti–Ta alloys for biomedical applications," Materials Science and Engineering: A, vol. 398, pp. 28-36, 2005.

[154] D. Mareci, R. Chelariu, G. Bolat, A. Cailean, V. Grancea, and D. Sutiman, "Electrochemical behaviour of Ti alloys containing Mo and Ta as β-stabilizer elements for dental application," Transactions of Nonferrous Metals Society of China, vol. 23, pp. 3829-3836, 2013.

[155] M. Atapour, A. Pilchak, G. Frankel, and J. Williams, "Corrosion behavior of β titanium alloys for biomedical applications," Materials Science and Engineering: C, vol. 31, pp. 885-891, 2011.

[156] M. T. Mohammed and M. GEETHA, "Effect of thermo-mechanical processing on microstructure and electrochemical behavior of Ti–Nb–Zr–V

new metastable β titanium biomedical alloy," Transactions of Nonferrous Metals Society of China, vol. 25, pp. 759-769, 2015.

[157] E. Vasilescu, P. Drob, D. Raducanu, V. Cojocaru, I. Cinca, D. Iordachescu, et al., "In vitro biocompatibility and corrosion resistance of a new implant titanium base alloy," Journal of Materials Science: Materials in Medicine, vol. 21, pp. 1959-1968, 2010.

[158] I. Cvijović-Alagić, Z. Cvijović, S. Mitrović, V. Panić, and M. Rakin, "Wear and corrosion behaviour of Ti–13Nb–13Zr and Ti–6Al–4V alloys in simulated physiological solution," Corrosion Science, vol. 53, pp. 796-808, 2011.

[159] A. Alves, F. Santana, L. Rosa, S. Cursino, and E. Codaro, "A study on corrosion resistance of the Ti–10Mo experimental alloy after different processing methods," Materials Science and Engineering: C, vol. 24, pp. 693-696, 2004.

[160] M. T. Mohammed, Z. A. Khan, G. Manivasagam, and A. N. Siddiquee, "Influence of thermomechanical processing on biomechanical compatibility and electrochemical behavior of new near beta alloy, Ti-20.6 Nb-13.6 Zr-0.5 V," International journal of nanomedicine, vol. 10, p. 223, 2015.

[161] M. T. Mohammed, Z. A. Khan, M. Geetha, and A. N. Siddiquee, "Microstructure, mechanical properties and electrochemical behavior of a novel biomedical titanium alloy subjected to thermo-mechanical processing including aging," Journal of Alloys and Compounds, vol. 634, pp. 272-280, 2015.

[162] J. Williams, Engineering tribology: Cambridge University Press, 2005.

[163] J. Takadoum, "Materials for Tribology," Materials and Surface Engineering in Tribology, pp. 109-204, 2008.

[164] P. D. Jakobsen, A. Bruland, and F. Dahl, "Review and assessment of the NTNU/SINTEF Soil Abrasion Test (SAT™) for determination of abrasiveness of soil and soft ground," Tunnelling and underground space technology, vol. 37, pp. 107- 114, 2013.

[165] R. Bailey, "Surface Engineered Titanium for Improved Tribological, Electrochemical and Tribo-electrochmical Performance," 2015.

[166] J. F. Shackelford and M. K. Muralidhara, "Introduction to materials science for engineers," 2005.

[167] I. Hutchings and P. Shipway, Tribology: friction and wear of engineering materials: Butterworth-Heinemann, 2017.

[168] D. D. Kopeliovich, "Mechanisms of wear," Substances and Technologies. www.substech.com, mechanisms_of_wear.txt · Last modified: 2017/07/01 by dmitri_kopeliovich.

[169] T. Joyce, "Theoretical Calculation of Lubrication Regimes in a Metal-on-Metal First Metatarsophalangeal Prosthesis Evaluated against an Ex Vivo Sample," in World Congress on Medical Physics and Biomedical Engineering 2006, 2007, pp. 3315- 3318.

[170] A. Choubey, B. Basu, and R. Balasubramaniam, "Tribological behaviour of Ti-based alloys in simulated body fluid solution at fretting contacts," Materials Science and Engineering: A, vol. 379, pp. 234-239, 2004.

[171] I. Cvijović-Alagić, Z. Cvijović, S. Mitrović, M. Rakin, Đ. Veljović, and M. Babić, "Tribological behaviour of orthopaedic Ti-13Nb-13Zr and Ti-6Al-4V alloys," Tribology letters, vol. 40, pp. 59-70, 2010.

[172] L. Mohan and C. Anandan, "Wear and corrosion behavior of oxygen implanted biomedical titanium alloy Ti–13Nb–13Zr," Applied Surface Science, vol. 282, pp. 281-290, 2013.

[173] H. Attar, K. Prashanth, A. Chaubey, M. Calin, L. C. Zhang, S. Scudino, et al., "Comparison of wear properties of commercially pure titanium prepared by selective laser melting and casting processes," Materials Letters, vol. 142, pp. 38-41, 2015.

[174] K. Suresh, M. Geetha, C. Richard, J. Landoulsi, H. Ramasawmy, S. Suwas, et al., "Effect of equal channel angular extrusion on wear and corrosion behavior of the orthopedic Ti–13Nb–13Zr alloy in simulated body fluid," Materials Science and Engineering: C, vol. 32, pp. 763-771, 2012.

[175] L.-j. Xu, S.-l. Xiao, T. Jing, and Y.-Y. Chen, "Microstructure, mechanical properties and dry wear resistance of β-type Ti–15Mo–xNb alloys for biomedical applications," Transactions of Nonferrous Metals Society of China, vol. 23, pp. 692-698, 2013.

[176] F. Mamoun, A. Omar, L. Mohamed, D. Leila, and A. Iost, "Comparative Study on Tribological Behavior of Ti-6Al-7Nb and SS AISI 316L Alloys, for Total Hip Prosthesis," in TMS 2014: 143rd Annual Meeting & Exhibition, 2014, pp. 237-246.

[177] S. Li, R. Yang, S. Li, Y. Hao, Y. Cui, M. Niinomi, et al., "Wear characteristics of Ti– Nb–Ta–Zr and Ti–6Al–4V alloys for biomedical applications," Wear, vol. 257, pp. 869-876, 2004.

[178] B. Bhushan, Introduction to tribology: John Wiley & Sons, 2013.

[179] H. Dong and T. Bell, "Enhanced wear resistance of titanium surfaces by a new thermal oxidation treatment," Wear, vol. 238, pp. 131-137, 2000.

[180] A. Bloyce, P.-Y. Qi, H. Dong, and T. Bell, "Surface modification of titanium alloys for combined improvements in corrosion and wear resistance," Surface and Coatings Technology, vol. 107, pp. 125-132, 1998.

[181] A. Bloyce, "Surface engineering of titanium alloys for wear protection," Proceedings of the Institution of Mechanical Engineers, Part J: Journal of Engineering Tribology, vol. 212, pp. 467-476, 1998.

[182] M. O. Alam and A. Haseeb, "Response of Ti–6Al–4V and Ti–24Al–11Nb alloys to dry sliding wear against hardened steel," Tribology International, vol. 35, pp. 357- 362, 2002.

[183] S. Wang, F. Wang, Z. Liao, Q. Wang, R. Tyagi, and W. Liu, "Tribological behaviour of titanium alloy modified by carbon–DLC composite film," Surface Engineering, vol. 31, pp. 934-941, 2015.

[184] M. Abad and J. Sánchez-López, "Tribological properties of surface-modified Pd nanoparticles for electrical contacts," Wear, vol. 297, pp. 943-951, 2013.

[185] P. Majumdar, S. Singh, and M. Chakraborty, "Wear response of heat-treated Ti– 13Zr–13Nb alloy in dry condition and simulated body fluid," Wear, vol. 264, pp. 1015-1025, 2008.

[186] M. A. Wimmer, A. Fischer, R. Büscher, R. Pourzal, C. Sprecher, R. Hauert, et al., "Wear mechanisms in metal-on-metal bearings: The importance of tribochemical reaction layers," Journal of Orthopaedic Research, vol. 28, pp. 436-443, 2010.

[187] Alves, A.P.R.; Santana, F.A.; Rosa, L.A.A.; Cursino, S.A.; Codaro, E.N. A study on corrosion resistance of the Ti-10Mo experimental alloy after different processing methods. Mater. Sci. Eng. C 2004, 24, 693–696. [CrossRef]

[188] Alves, V.A.; Reis, R.Q.; Santos, I.C.B.; Souza, D.G.; Gonçalves, T.D.F.; Pereira-da-Silva, M.A.; Rossi, A.; da Silva, L.A. In situ impedance spectroscopy study of the electrochemical corrosion of Ti and Ti-6Al-4V in simulated body fluid at 25 ◦C and 37 ◦C. Corros. Sci. 2009, 51, 2473–2482. [CrossRef]

[189] Kumar, S.; Sankara Narayanan, T.S.N. Electrochemical characterization of β-Ti alloy in Ringer's solution for implant application. J. Alloys Compd. 2009, 479, 699–703. [CrossRef]

[190] Bai, Y.; Li, S.J.; Prima, F.; Hao, Y.L.; Yang, R. Electrochemical corrosion behavior of Ti-24Nb-4Zr-8Sn alloy in a simulated physiological environment. Appl. Surf. Sci. 2012, 258, 4035–4040. [CrossRef]

[191] G. Bolat a, D. Mareci a, R. Chelariub, J. Izquierdoc, S. Gonzálezc, R.M. Souto, Investigation of the electrochemical behaviour of TiMo alloys in simulated physiological solutions, Electrochimica Acta 113 (2013) 470–480, Elsevier.

[192] Simsek, I.; Ozyurek, D. Investigation of the wear and corrosion behaviors of Ti5Al2.5Fe and Ti6Al4V alloys produced by mechanical alloying method in simulated body fluid environment. Mater. Sci. Eng. C 2019, 94, 357–363. [CrossRef]

[193] Wang, J.C.; Liu, Y.J.; Qin, P.; Liang, S.X.; Sercombe, T.B.; Zhang, L.C. Selective laser melting of Ti-35Nb composite from elemental powder mixture: Microstructure, mechanical behavior and corrosion behavior. Mater. Sci. Eng. A 2019, 760, 214–224. [CrossRef]

[194] Chui, P.; Jing, R.; Zhang, F.; Li, J.; Feng, T. Mechanical properties and corrosion behavior of β-type Ti-Zr-Nb-Mo alloys for biomedical application. J. Alloys Compd. 2020, 842, 155693. [CrossRef]

[195] . Zareidoost, A.; Yousefpour, M. A study on the mechanical properties and corrosion behavior of the new as-cast TZNT alloys for biomedical applications. Mater. Sci. Eng. C 2020, 110, 110725. [CrossRef] [PubMed]

[196] Jawed, S.F.; Rabadia, C.D.; Liu, Y.J.; Wang, L.Q.; Qin, P.; Li, Y.H.; Zhang, X.H.; Zhang, L.C. Strengthening mechanism and corrosion resistance of beta-type Ti-Nb-Zr-Mn alloys. Mater. Sci. Eng. C 2020, 110, 110728. [CrossRef] [PubMed]

[197] A. Choubey, B. Basu, and R. Balasubramaniam, "Tribological behaviour of Ti-based alloys in simulated body fluid solution at fretting contacts," Materials Science and Engineering: A, vol. 379, pp. 234-239, 2004.

[198] Chiba, A. Pin-on-disk wear behavior in a like-on-like configuration in a biological environment of high carbon cast and low carbon forged Co-29Cr-6Mo alloys. Acta Mater. 2007, 55, 1309–1318.

[199] C. Ramos-Saenz, P. Sundaram, and N. Diffoot-Carlo, "Tribological properties of Tibased alloys in a simulated bone–implant interface with Ringer's solution at fretting contacts," Journal of the mechanical behavior of biomedical materials, vol. 3, pp. 549-558, 2010.

[200] Li, S.J.; Yang, R.; Li, S.; Hao, Y.L.; Cui, Y.Y.; Niinomi, M.; Guo, Z.X. Wear characteristics of Ti-Nb-Ta-Zr and Ti-6Al-4V alloys for biomedical applications. Wear 2004, 257, 869–876.

[201] M. Fellah, M. Labaïz, O. Assala, and A. Iost, "Comparative Tribological study of biomaterials AISI 316L and Ti-6Al-7Nb," TMS, vol. 237, pp. 237-246, 2014.

[202] T. Lee, E. Mathew, S. Rajaraman, G. Manivasagam, A. K. Singh, and C. S. Lee, "Tribological and corrosion behaviors of warm-and hot-rolled Ti-13Nb-13Zr alloys in 259 simulated body fluid conditions," International journal of nanomedicine, vol. 10, p. 207, 2015.

[203] Attar, H.; Prashanth, G.; Chaubey, A.K.; Calin, M.; Zhang, S.L.C.; Eckert, J. Comparison of wear properties of commercially pure titanium prepared by selective laser melting and casting processes. Mater. Lett. 2015, 142, 38–41.

[204] Y.H. Hon, J.Y. Wang, Y.N. Pan, Mater. Trans. 44 (2003) 2384–2390.

[205] H.S. Kim, W.Y. Kim, S.H. Lim, Scripta Mater. 54 (2006) 887–891.

[206] P. Majumdar ∗, S.B. Singh, M. Chakraborty, Elastic modulus of biomedical titanium alloys by nano-indentation and ultrasonic techniques—

A comparative study, Materials Science and Engineering A 489 (2008) 419–425,Elsevier.

[207] Wen-Fu Ho a , Shih-Ching Wu b,c , Shih-Kuang Hsu b,c , Yu-Chi Li a , Hsueh-Chuan Hsu, Effects of molybdenum content on the structure and mechanical properties of as-cast Ti–10Zr-based alloys for biomedical applications, Materials Science and Engineering C 32 (2012) 517–522, Elsevier.

[208] Xu, Y.; Gao, J.; Huang, Y.; Rainforth, W.M. A low-cost metastable beta Ti alloy with high elastic admissible strain and enhanced ductility for orthopaedic application. J. Alloys Compd. 2020, 835, 155391. [CrossRef].

[209] Zuheir Talib Khulief, Professor W. Mark Rainforth, Professor Iain Todd, Tribological, Electrochemical, and Tribocorrosion Behaviour of New Titanium Biomedical Alloys, The Department of Engineering Materials The University of Sheffield.2018

[210] Nabeel Mohammed Abdulkadhim Radhi, Jassim M. Salman Al-Murshdy (Ph.D.), Effect of Mo and Ta on Mechanical and Corrosion Behaviour of Porous Ti+5Al+2.5Fe Biomaterials, University of Babylon College of Materials Engineering Department of Metallurgical Engineering.2019.

[211] Cvijovic, A.I.; Cvijovic, Z.; Mitrovic, S.; Rakin, M.; Veljovic, D.; Babic, M. Tribological behaviour of orthopaedic Ti-13Nb-13Zr and Ti-6Al-4V alloys. Tribol. Lett. 2010, 40, 59–70.

[212] Mohan, L.; Anandan, C. Wear and corrosion behavior of oxygen implanted biomedical titanium alloy Ti-13Nb-13Zr. Appl. Surf. Sci. 2013, 282, 281–290.

[213] Luo, X.; Li, X.; Sun, Y.; Dong, H. Tribocorrosion behavior of S-phase surface engineered medical grade Co-Cr alloy. Wear 2013, 302, 1615–1623.

[214] ASTM International, 100 Barr Harbor Drive, PO Box C700, West Conshohocken, PA 19428-2959, United States. Individual reprints (single or multiple copies) of this standard may be obtained by contacting ASTM at the above address or at 610-832-9585 (phone), 610-832-9555 (fax), or service@astm.org (e-mail); or through the ASTM website (www.astm.org). Permission rights to photocopy the standard may also be secured from the

Copyright Clearance Center, 222 Rosewood Drive, Danvers, MA 01923, Tel: (978) 646-2600; http://www.copyright.com.

[215] Y.-H. Hon, J.-Y. Wang, and Y.-N. Pan, "Composition/phase structure and properties of titanium-niobium alloys," Materials transactions, vol. 44, pp. 2384-2390, 2003.

[216] Y. Hao, R. Yang, M. Niinomi, D. Kuroda, Y. Zhou, K. Fukunaga, et al., "Young's modulus and mechanical properties of Ti-29Nb-13Ta-4.6 Zr in relation to α ″martensite," Metallurgical and Materials Transactions A, vol. 33, pp. 3137-3144, 2002.

[217] R. Banerjee, S. Nag, and H. Fraser, "A novel combinatorial approach to the development of beta titanium alloys for orthopaedic implants," Materials Science and Engineering: C, vol. 25, pp. 282-289, 2005.

[218] W. Ho, C. Ju, and J. C. Lin, "Structure and properties of cast binary Ti–Mo alloys," Biomaterials, vol. 20, pp. 2115-2122, 1999.

[219] A. Almeida, D. Gupta, C. Loable, and R. Vilar, "Laser-assisted synthesis of Ti–Mo alloys for biomedical applications," Materials Science and Engineering: C, vol. 32, pp. 1190-1195, 2012.

[220] D. R. N. Correa, F. B. Vicente, R. O. Araújo, M. L. Lourenço, P. A. B. Kuroda, M. A. R. Buzalaf, et al., "Effect of the substitutional elements on the microstructure of the Ti-15Mo-Zr and Ti-15Zr-Mo systems alloys," Journal of Materials Research and Technology, vol. 4, pp. 180-185, 2015.

[221] D. R. N. Correa, P. A. B. Kuroda, and C. R. Grandini, "Structure, microstructure, and selected mechanical properties of Ti-Zr-Mo alloys for biomedical applications," in Advanced Materials Research, 2014, pp. 75-80.

[222] R. Chelariu, G. Bolat, J. Izquierdo, D. Mareci, D. Gordin, T. Gloriant, et al., "Metastable beta Ti-Nb-Mo alloys with improved corrosion resistance in saline solution," Electrochimica Acta, vol. 137, pp. 280-289, 2014.

[223] M. K. Dimah, F. D. Albeza, V. A. Borrás, and A. I. Muñoz, "Study of the biotribocorrosion behaviour of titanium biomedical alloys in simulated body fluids by electrochemical techniques," Wear, vol. 294, pp. 409-418, 2012.

[224] R. Priya, C. Mallika, and U. K. Mudali, "Wear and tribocorrosion behaviour of 304L SS, Zr-702, Zircaloy-4 and Ti-grade2," Wear, vol. 310, pp. 90-100, 2014.

[225] M. Runa, M. Mathew, and L. Rocha, "Tribocorrosion response of the Ti6Al4V alloys commonly used in femoral stems," Tribology International, vol. 68, pp. 85-93, 2013.

[226] A. Amanov and S. Sasaki, "A study on the tribological characteristics of duplextreated Ti–6Al–4V alloy under oil-lubricated sliding conditions," Tribology International, vol. 64, pp. 155-163, 2013.

[227] N. Diomidis, S. Mischler, N. More, M. Roy, and S. Paul, "Fretting-corrosion behavior of β titanium alloys in simulated synovial fluid," Wear, vol. 271, pp. 1093-1102, 2011.

[228] M.-P. Licausi, A. I. Muñoz, and V. A. Borrás, "Influence of the fabrication process and fluoride content on the tribocorrosion behaviour of Ti6Al4V biomedical alloy in artificial saliva," Journal of the mechanical behavior of biomedical materials, vol. 20, pp. 137-148, 2013.

[229] N. Diomidis, S. Mischler, N. More, and M. Roy, "Tribo-electrochemical characterization of metallic biomaterials for total joint replacement," Acta biomaterialia, vol. 8, pp. 852-859, 2012.

Appendices

Overview

Quick Details

Place of Origin:	shaanxi baoji	Brand Name:	top-ti
Model Number:	titanium bar	Application:	Industrial
Shape:	Round, Round, Round/Square/Hexagon	Length:	50-16000mm, ≤16000mm
Technique:	Forged, Rolled, Radial Forging, Rolling	Grade:	Titanium Alloy, gr1,gr2,gr5(Ti-6Al-4V),gr7,gr9,gr12,gr23,Ti15...
weight:	4.51g/cm3	Processing Service:	Bending, Cutting, polishing, Custom
Name:	titanium rod /bar	Diameter:	3-400 mm
Condition:	Annealed	Surface:	Polished surface/peeling surface/machined surface/grindin...
Materal:	titanium, titanium alloy	Standard:	ASTM B348,ASTM F67 ASTM F136,AMS 4928

Supply Ability

Supply Ability	500 Ton/Tons per Month

Packaging & Delivery

Packaging Details	wooden case, plastic foam
Port	Shanghai

Figher1: History of titanium alloy samples.

Tarbiat Modarres University

Faculty Of Sciences

X-Ray Lab.

T.M.U Analytical Lab.

Date:	Sunday, February 21, 2021
Customer:	Dr. Hamidi
Sample No:	**960**

M1	960-1	Si	S	Ti	Fe	Ni	Cu
	(%)	0.109	0.015	99.667	0.158	0.02	0.018

Sn
0.014

Traces: Cr

M2	960-2	Al	Si	Ti	Fe	Co	Ni
	(%)	6.244	0.035	93.472	0.175	0.028	0.022

Zr	Nb	Mo
0.007	0.006	0.011

Traces: Cu Sn

M3	960-3	Al	Si	Ti	V	Fe	Sn
	(%)	6.133	0.017	90.707	2.973	0.154	0.016

Traces: Ni

M4	960-4	Al	Si	S	Ti	Fe	Ni
	(%)	6.098	0.107	0.008	93.491	0.222	0.035

Zr	Nb	Mo
0.017	0.008	0.014

Traces: Cu Sn

Semi Quantitative Result
Polymer & Organic Concentrate Not Included
Trace elements should be analysis by AAS or ICP.

X-Ray Laboratory
Geology Dept.,
Faculty of Sciences,
Tarbiat Modarres University
P.O.Box: 1411-13115
Tel: +98 21 82883426
+98 21 82883427
Fax: +98 21 82883448
E-mail: Xraylab@modares.ac.ir
Tehran - I. R. Iran

Fighar2: chemical analysis of titanium alloy used in this investigation.

Tarbiat Modarres University

Faculty Of Sciences

X-Ray Lab.

T.M.U Analytical Lab.

* **Preparation procedure:** Powder press
* **Loss on Ignition (L.O.I) Method:** sample put in furnace, for 1 hour at 950 °C

* Instrument (XRF PW2404) Calibrate with Philips Analytical X-Ray B.V. standards with certificate of the secondary for the *SEMIQ*.

* **Working range elements:** Cs, Ga, Rb, Cl, Na, Ba, F, S, Mg, Cr, U, Sr, Pd, Pt, Ge, Mn, Mo, Br, La, K, Pr, Ta, Zr, Al, Fe, P, Si, Sm, Zn, Ca, In, Nb, Nd, Ti, W, Bi, Ce, Co, Hf, Th, Y, Hg, Ni, V, Pb, Sn, Ag, As, Se, Te, Sb, Cd, Cu, I, Tl.

* Detection Limit: 20ppm—100%
* Monitor system repeat every week with SRM samples.
* We are using internal method for QC, with SRM samples every month.

M. Yousefi
X-Ray Lab.

X-Ray Laboratory
Geology Dept.,
Faculty of Sciences,
Tarbiat Modarres University
P.O Box: 14117-13116
Tel: +98 21 82883426
+98 21 82883427
Fax: +98 21 82883448
E-mail: Xraylab@modares.ac.ir
Tehran - I. R. Iran

Fighar2: chemical analysis of titanium alloy used in this investigation.

Tarbiat Modarres University

Faculty Of Sciences

X-Ray Lab.

T.M.U Analytical Lab.

Date:	Tuesday, June 8, 2021
Customer:	Dr. Ahmed
Sample No:	**960**

M2		**960-2**	Zr	Nb	Ti
		(%)	11.266	12.561	76.173

Traces: Fe Ni

M4	**960-4**	Mo	Ti
	(%)	12.054	87.946

Traces: Fe Ni

Semi Quantitative Result
Polymer & Organic Concentrate Not Included
Trace elements should be analysis by AAS or ICP.

* **Preparation procedure:** Powder press
* **Loss on Ignition (L.O.I) Method:** sample put in furnace, for 1 hour at 950 °C

* Instrument (XRF PW2404) Calibrate with Philips Analytical X-Ray B.V. standards with certificate of the secondary for the *SEMIQ*.

* **Working range elements:** Cs, Ga, Rb, Cl, Na, Ba, F, S, Mg, Cr, U, Sr, Pd, Pt, Ge, Mn, Mo, Br, La, K, Pr, Ta, Zr, Al, Fe, P, Si, Sm, Zn, Ca, In, Nb, Nd, Ti, W, Bi, Ce, Co, Hf, Th, Y, Hg, Ni, V, Pb, Sn, Ag, As, Se, Te, Sb, Cd, Cu, I, Tl.

* Detection Limit: 20ppm—100%
* Monitor system repeat every week with SRM samples.
* We are using internal method for QC, with SRM samples every month.

X- Ray Laboratory
Geology Dept.,
Faculty of Sciences,
Tarbiat Modarres University
P.O.Box: 14117-13116
Tel: +98 21 82883426
+98 21 82883427
Fax: +98 21 82883448
E-mail: Xraylab@modares.ac.ir
Tehran - I. R. Iran

M. Yousef
X-Ray Lab.

Fighar2: chemical analysis of titanium alloy used in this investigation.

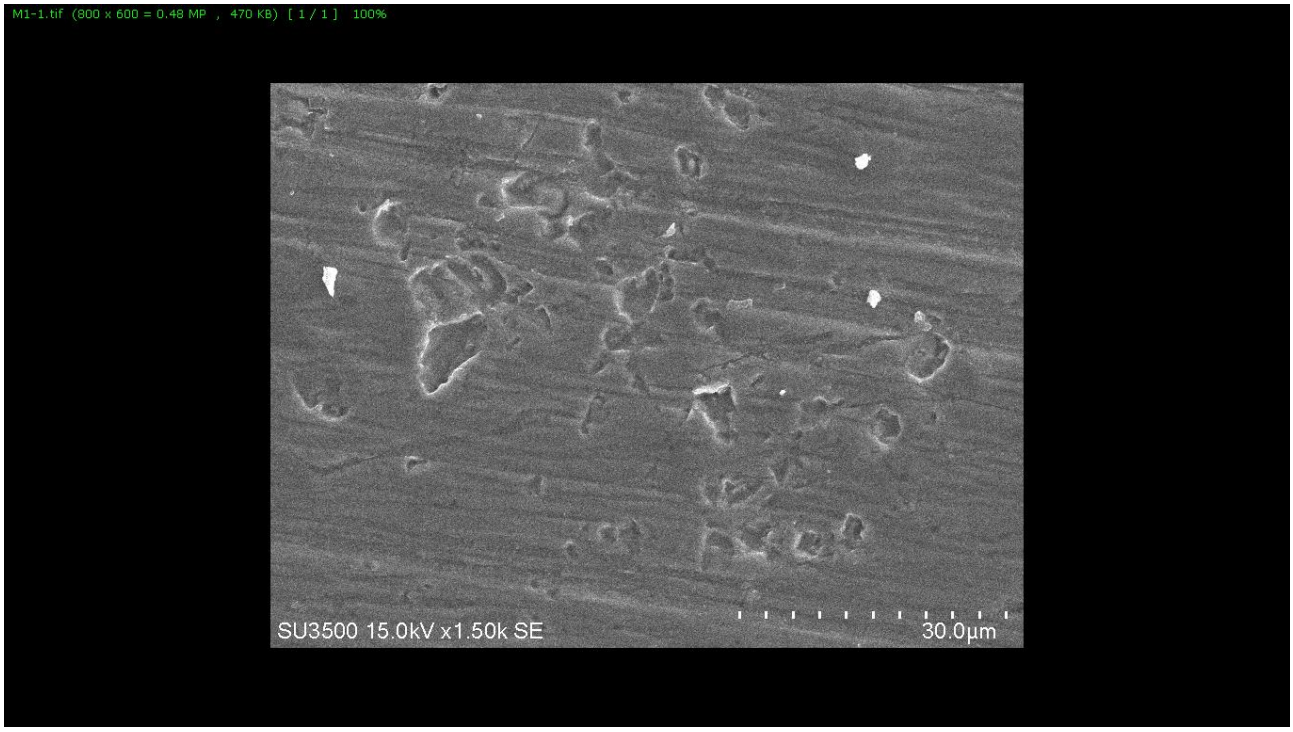

Fighar3: FESESM of Cp-Ti.

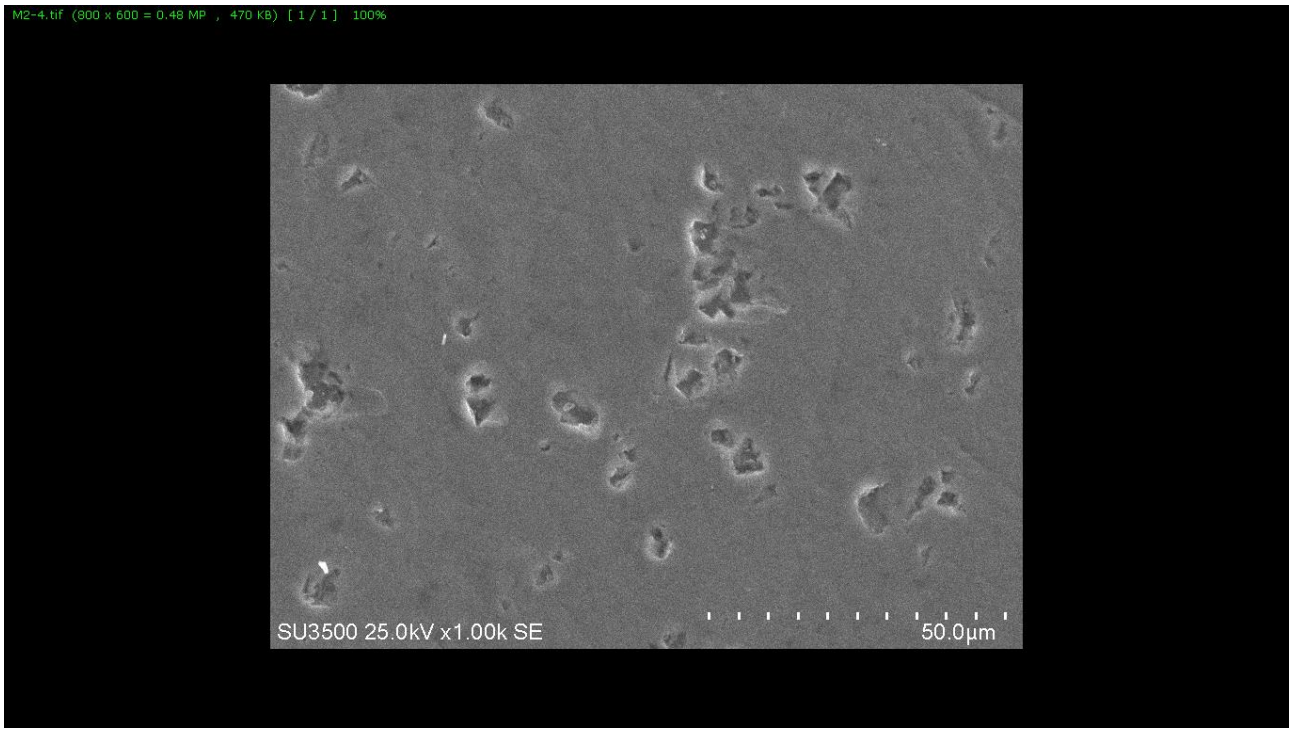

Fighar4: FESEM of Ti-6Al-4V.

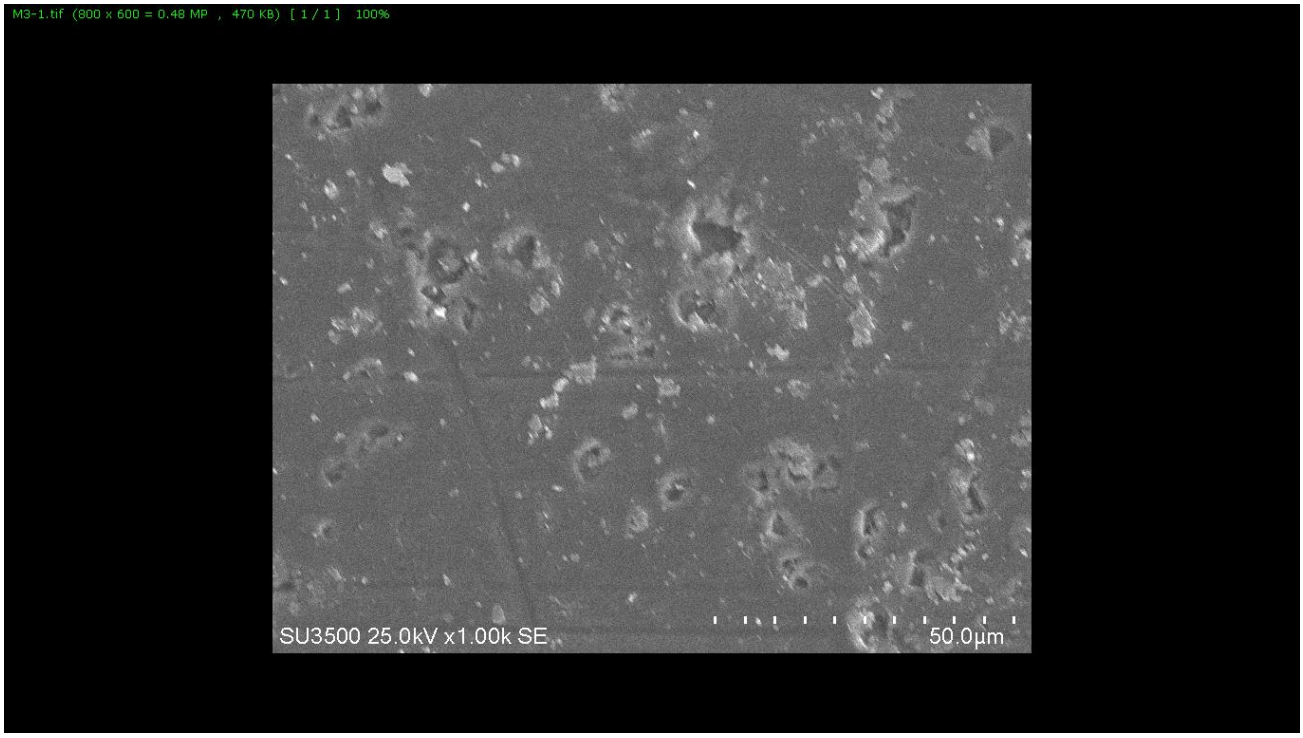

Fighar5: FESEM of Ti-13Zr-13Nb.

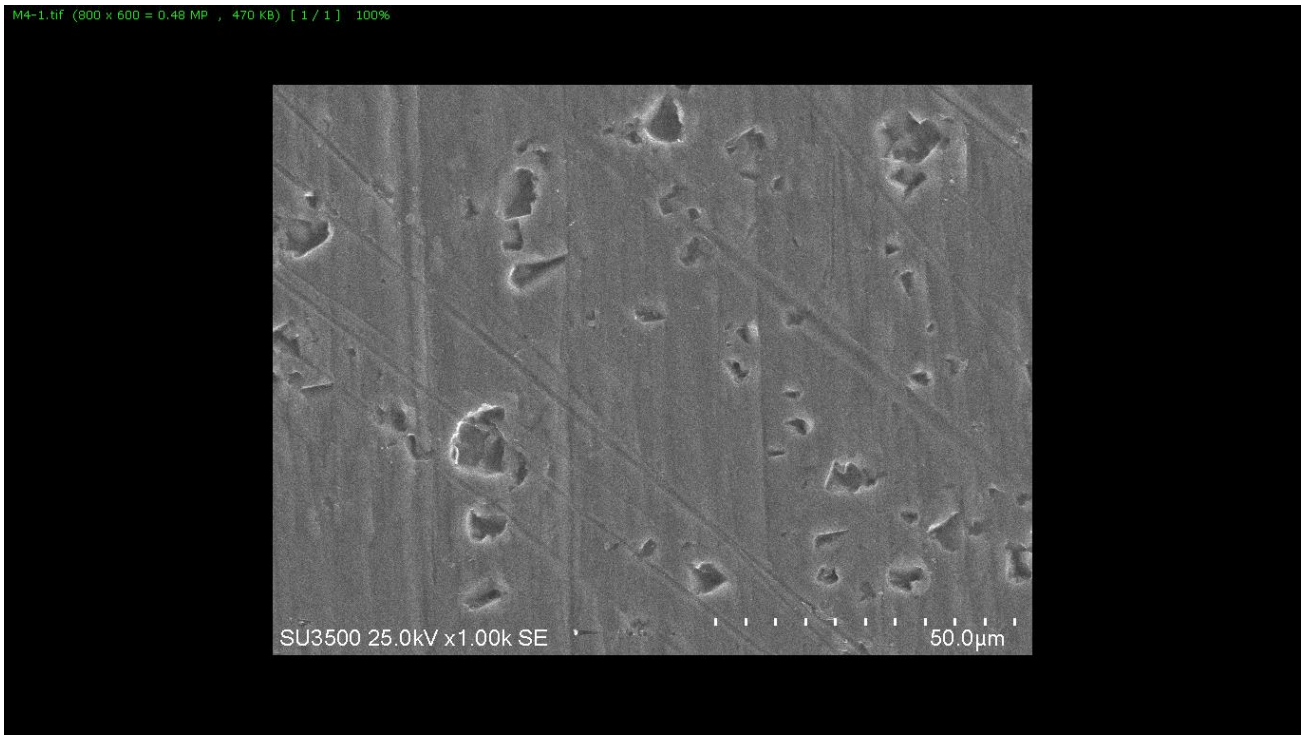

Fighar6: FESEM of Ti-15Mo.

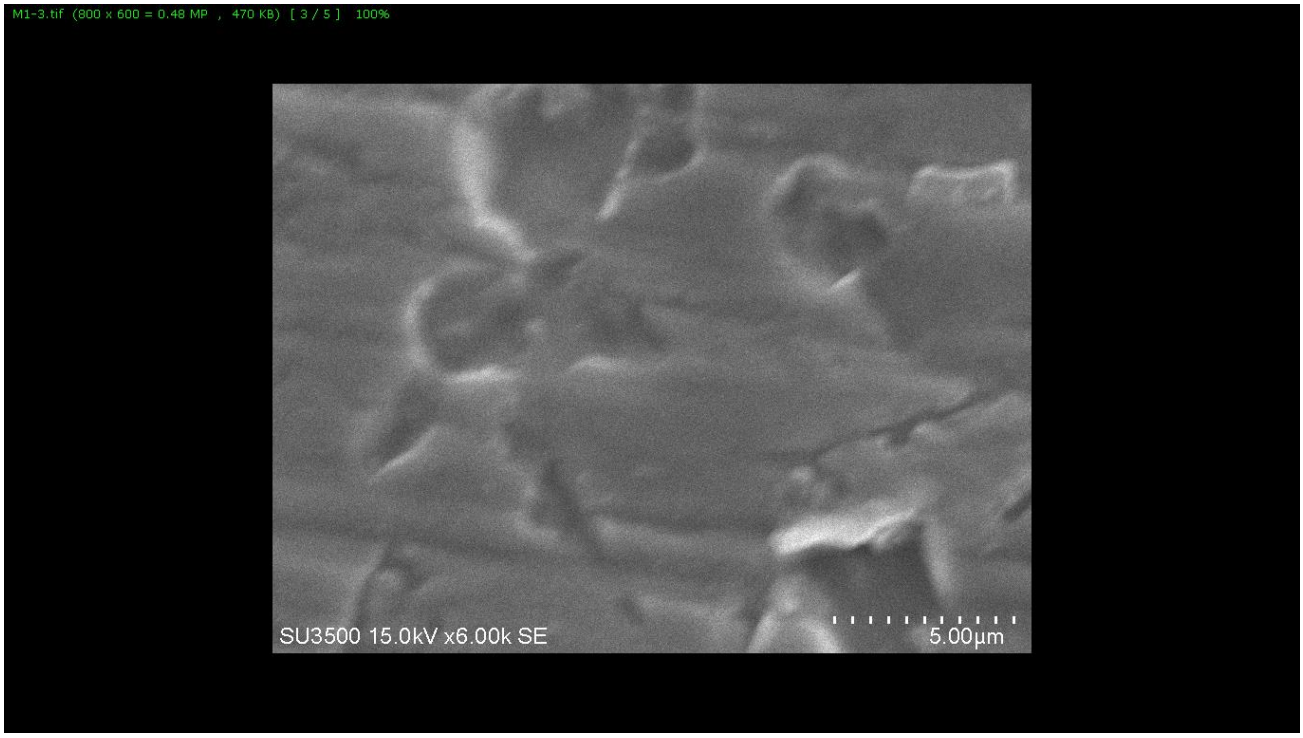

Fighar7: FESEM of Ti-8Mo-4Nb-2Zr.

(A) c:\edax32\genesis\genspc.spc

Label:

(B) peakgen.spc

Label:TiL

kV:0.0 Tilt:0.0 Take-off:36.1 Det:

Res:125 Amp.T:7.68 FS:3203 Lsec:98 8-Mar-2021 19:18:38

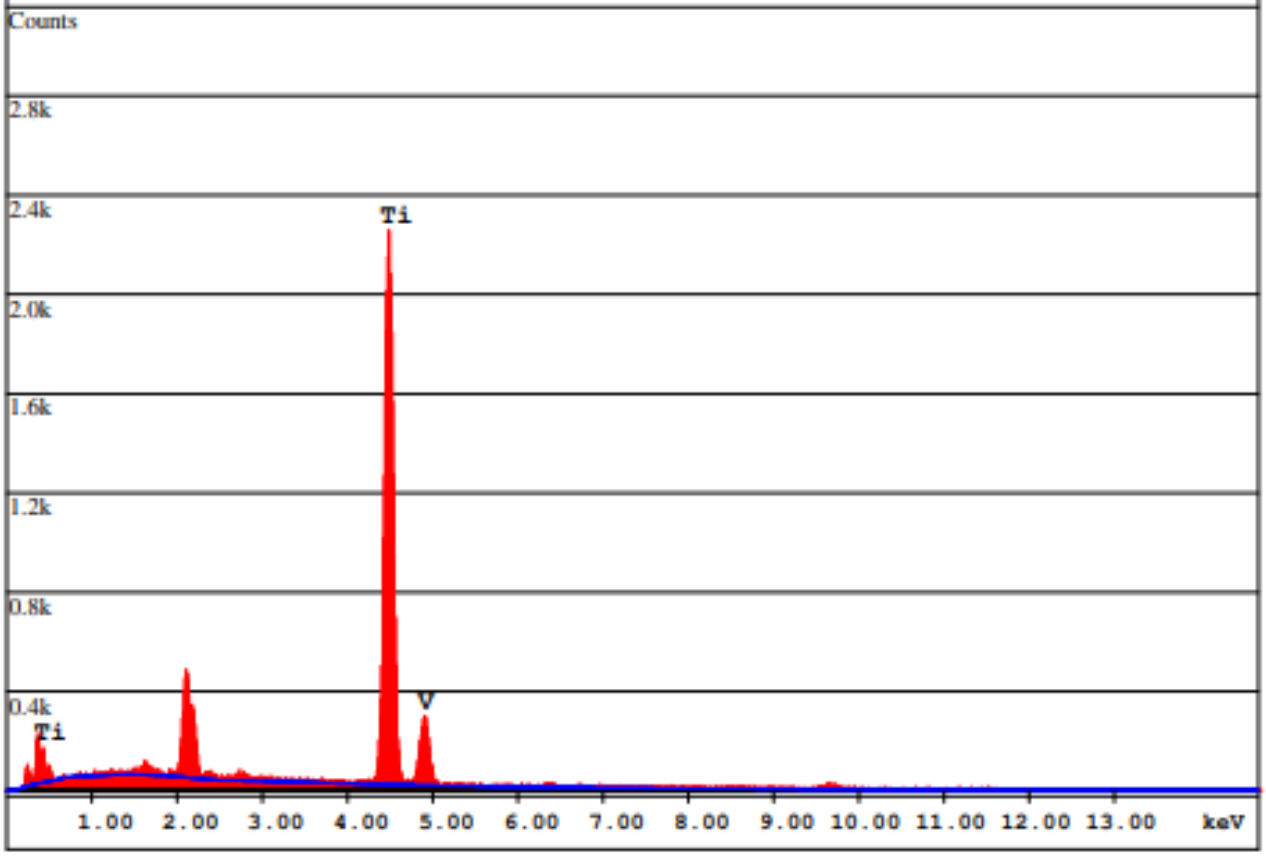

EDAX ZAF Quantification (Standardless)
Element Normalized
SEC Table : Default

Element	Wt %	At %	K-Ratio	Z	A	F
TiL	15.61	15.61	0.1561	1.0000	1.0000	1.0000
TiK	84.39	84.39	0.8439	1.0000	1.0000	1.0000
Total	100.00	100.00				

Element	Net Inte.	Bkgd Inte.	Inte. Error	P/B
TiL	3.30	1.70	7.87	1.95
TiK	178.75	2.86	0.76	62.51

Fighar8: EDX of Cp-Ti..

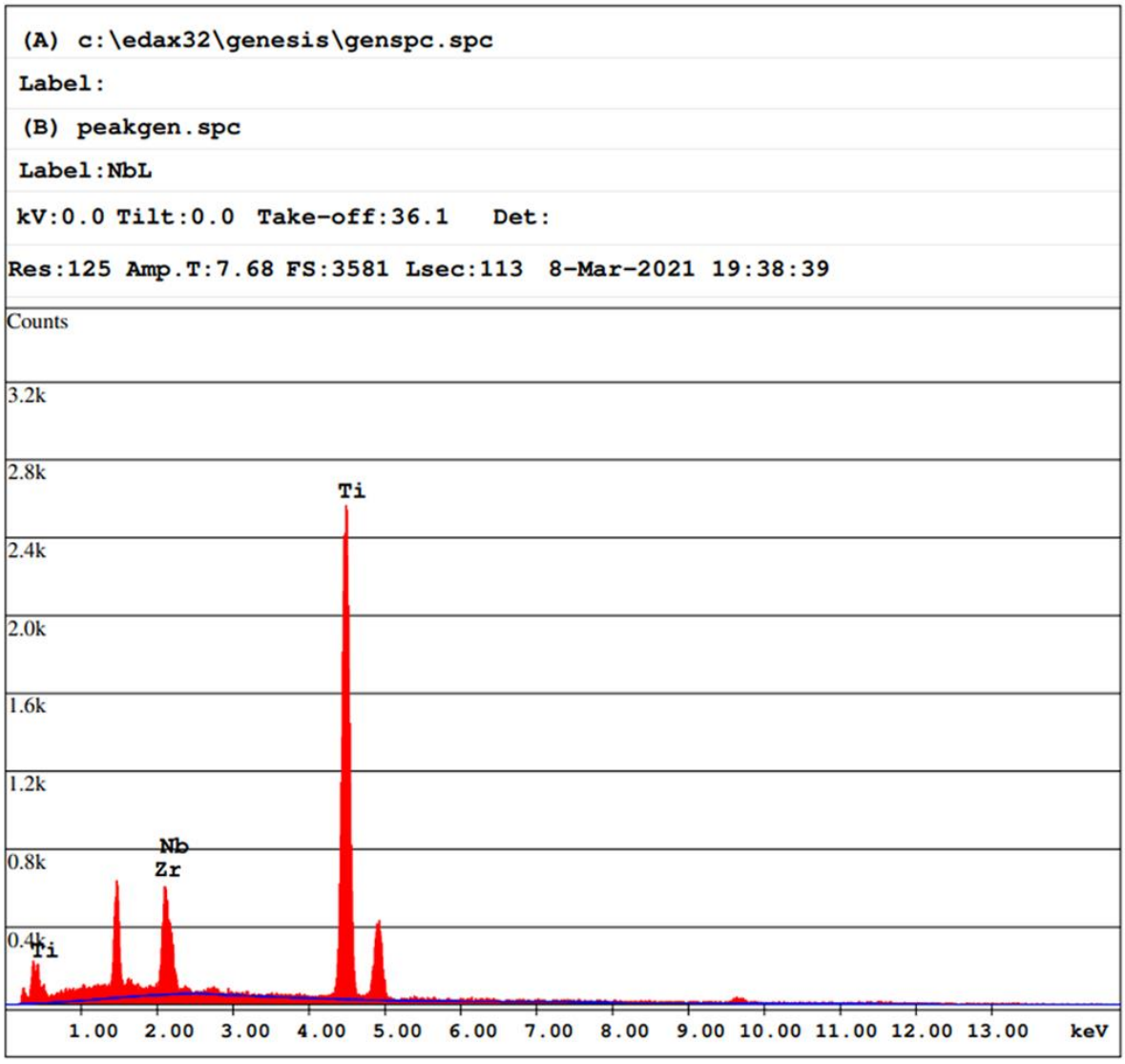

EDAX ZAF Quantification (Standardless)
Element Normalized
SEC Table : Default

Element	Wt %	At %	K-Ratio	Z	A	F
TiL	22.28	25.78	0.1377	1.0213	0.6053	1.0000
ZrK	12.65	3.59	0.1103	0.8286	1.0513	1.0013
NbL	8.35	4.98	0.0715	0.9354	0.9058	1.0103
TiK	56.72	65.64	0.5433	1.0243	0.9340	1.0011
Total	100.00	100.00				

Element	Net Inte.	Bkgd Inte.	Inte. Error	P/B
TiL	4.49	0.30	4.72	14.97
ZrK	19.95	3.51	2.44	5.69
NbL	18.73	4.13	2.60	4.53
TiK	177.11	2.71	0.72	65.25

Fighar9: EDX of Ti-6Al-4V..

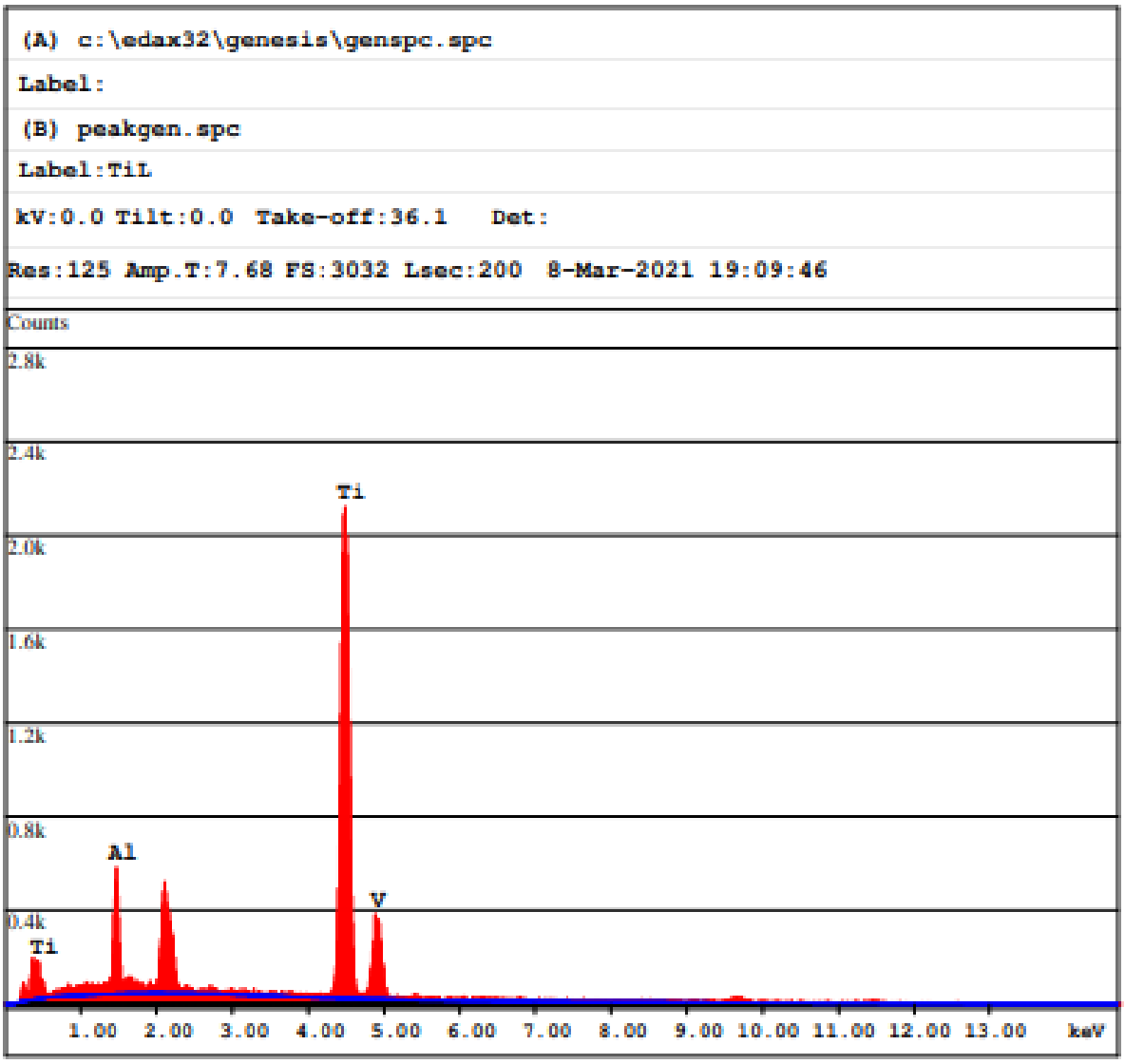

EDAX ZAF Quantification (Standardless)
Element Normalized
SEC Table : Default

Element	Wt %	At %	K-Ratio	Z	A	F
TiL	19.86	18.54	0.1710	0.9916	0.8679	1.0001
AlK	9.39	15.56	0.0498	1.0791	0.4899	1.0029
TiK	68.68	64.09	0.6758	0.9912	0.9928	1.0000
V K	2.07	1.81	0.0201	0.9708	1.0004	1.0000
Total	100.00	100.00				

Element	Net Inte.	Bkgd Inte.	Inte. Error	P/B
TiL	2.13	0.58	6.01	3.68
AlK	13.82	1.76	2.13	7.85
TiK	84.48	1.45	0.78	58.26
V K	2.21	1.36	7.09	1.63

Fighar10: EDX of Ti-13Zr-13Nb.

(A) c:\edax32\genesis\genspc.spc

Label:

(B) peakgen.spc

Label:TiL

kV:0.0 Tilt:0.0 Take-off:36.1 Det:

Res:125 Amp.T:7.68 FS:5359 Lsec:172 8-Mar-2021 19:30:49

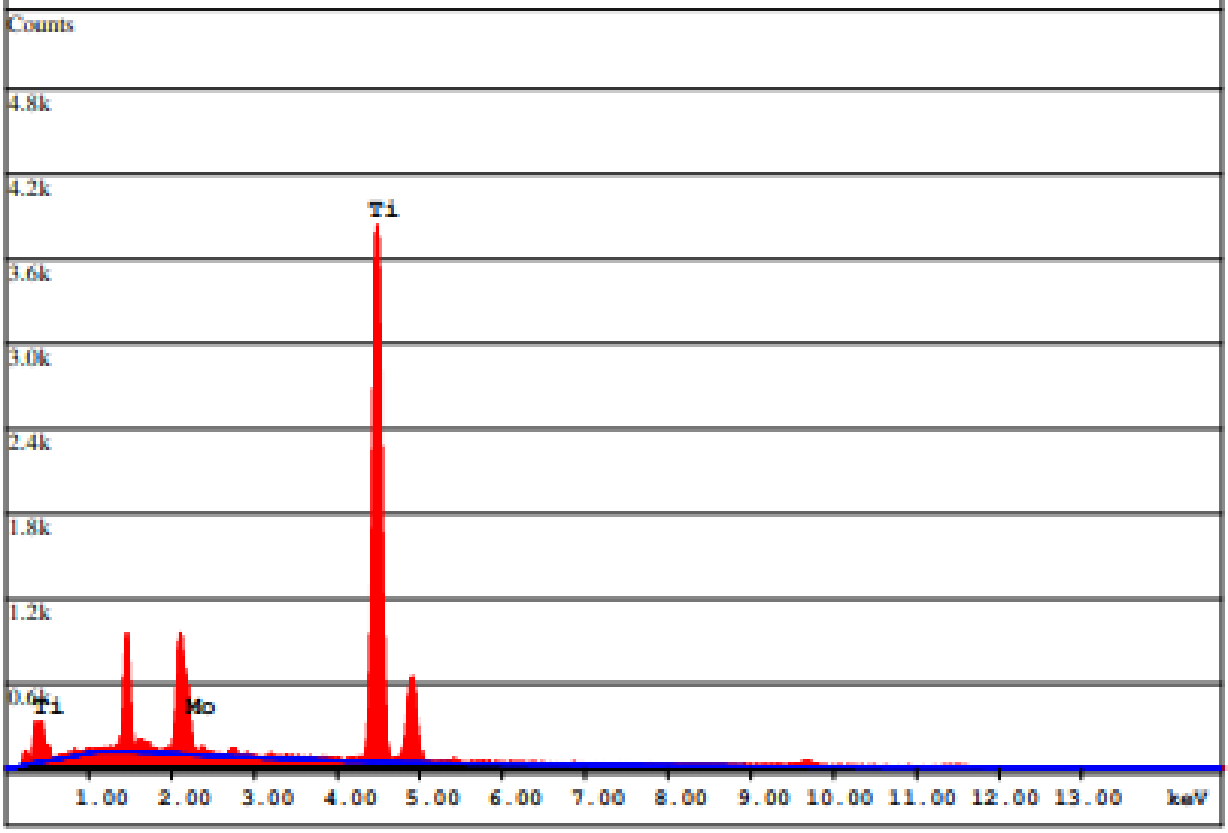

EDAX ZAF Quantification (Standardless)
Element Normalized
SEC Table : Default

Element	Wt %	At %	K-Ratio	Z	A	F
TiL	18.97	19.07	0.1809	1.0007	0.9530	1.0000
MoL	1.03	0.52	0.0092	0.8995	0.9644	1.0236
TiK	80.00	80.41	0.7981	1.0008	0.9969	1.0000
Total	100.00	100.00				

Element	Net Inte.	Bkgd Inte.	Inte. Error	P/B
TiL	4.03	1.36	4.92	2.95
MoL	1.58	4.88	16.24	0.32
TiK	177.87	2.97	0.58	59.85

Fighar11: EDX of Ti-15Mo.

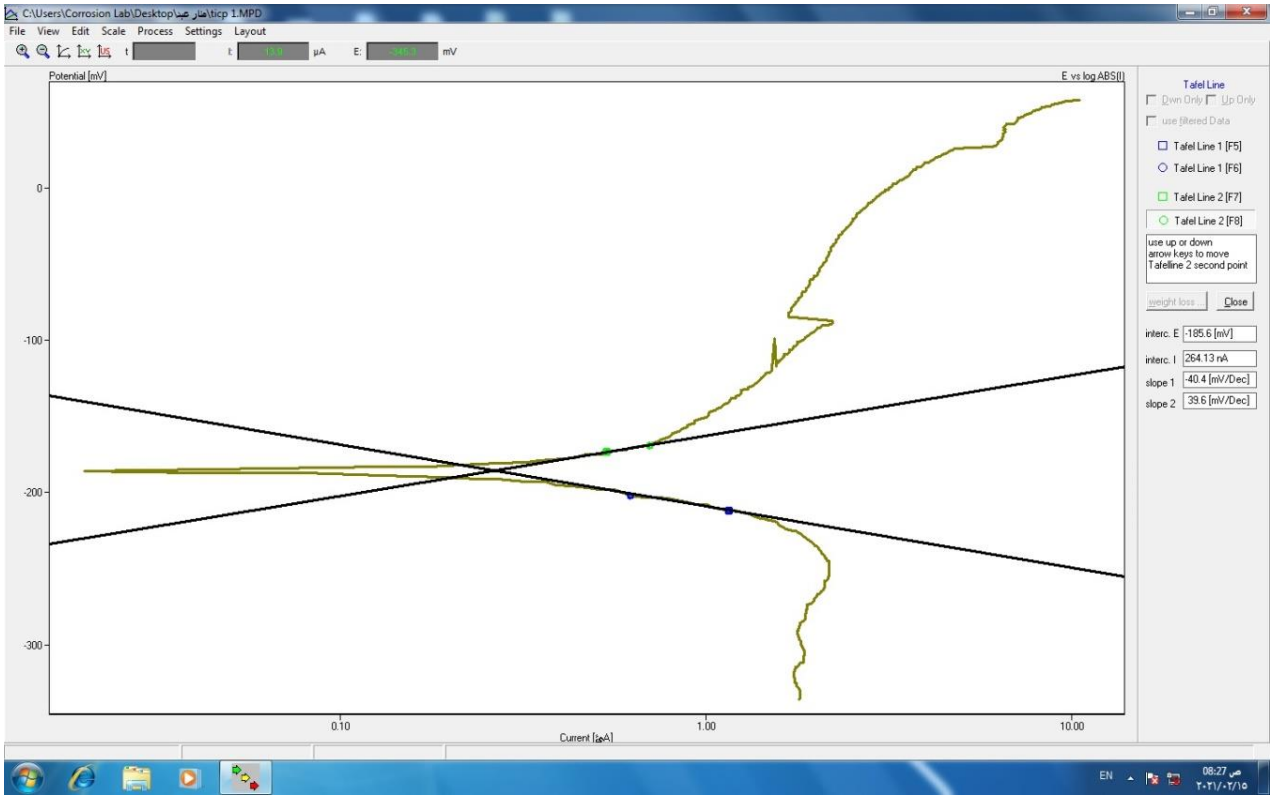

Fighar12: Potentiodynamic Polarization for Cp-Ti.

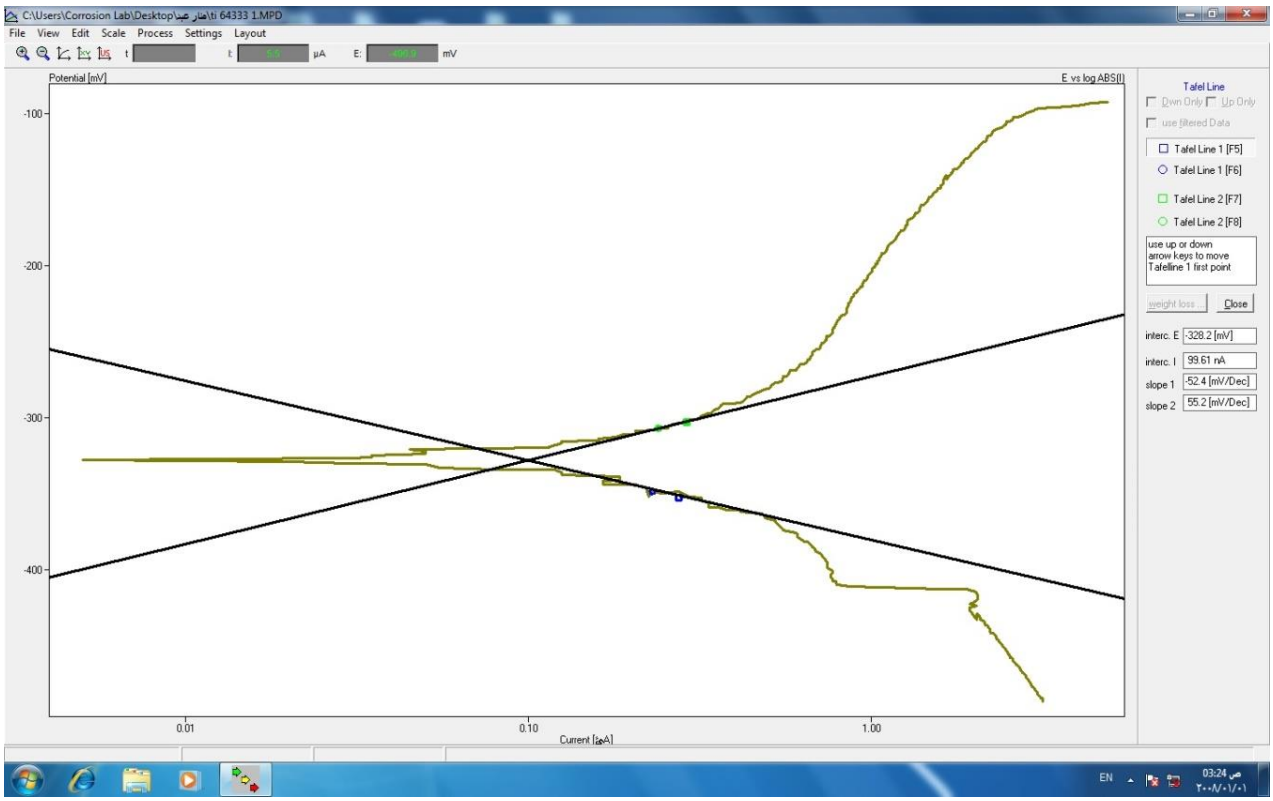

Fighar13: Potentiodynamic Polarization for Ti-6Al-4V.

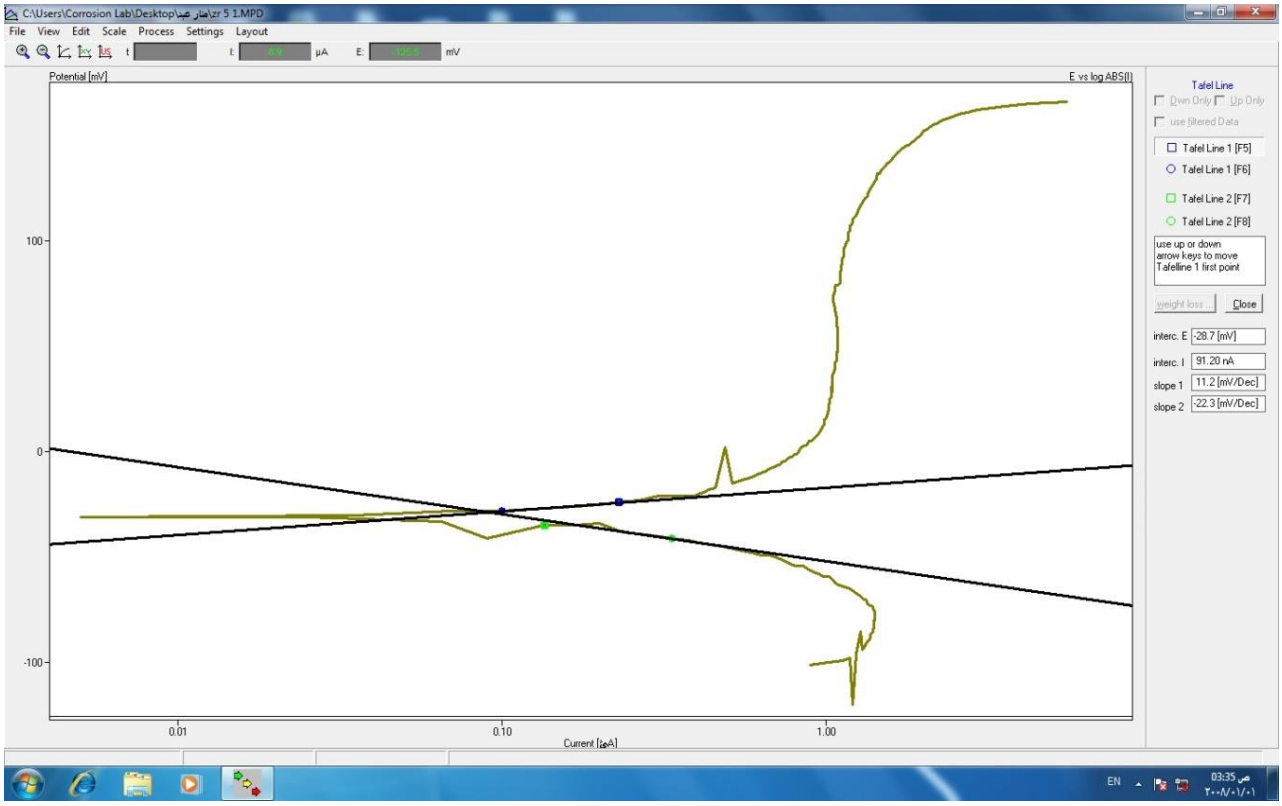

Fighar14: Potentiodynamic Polarization for Ti-13Zr-13Nb.

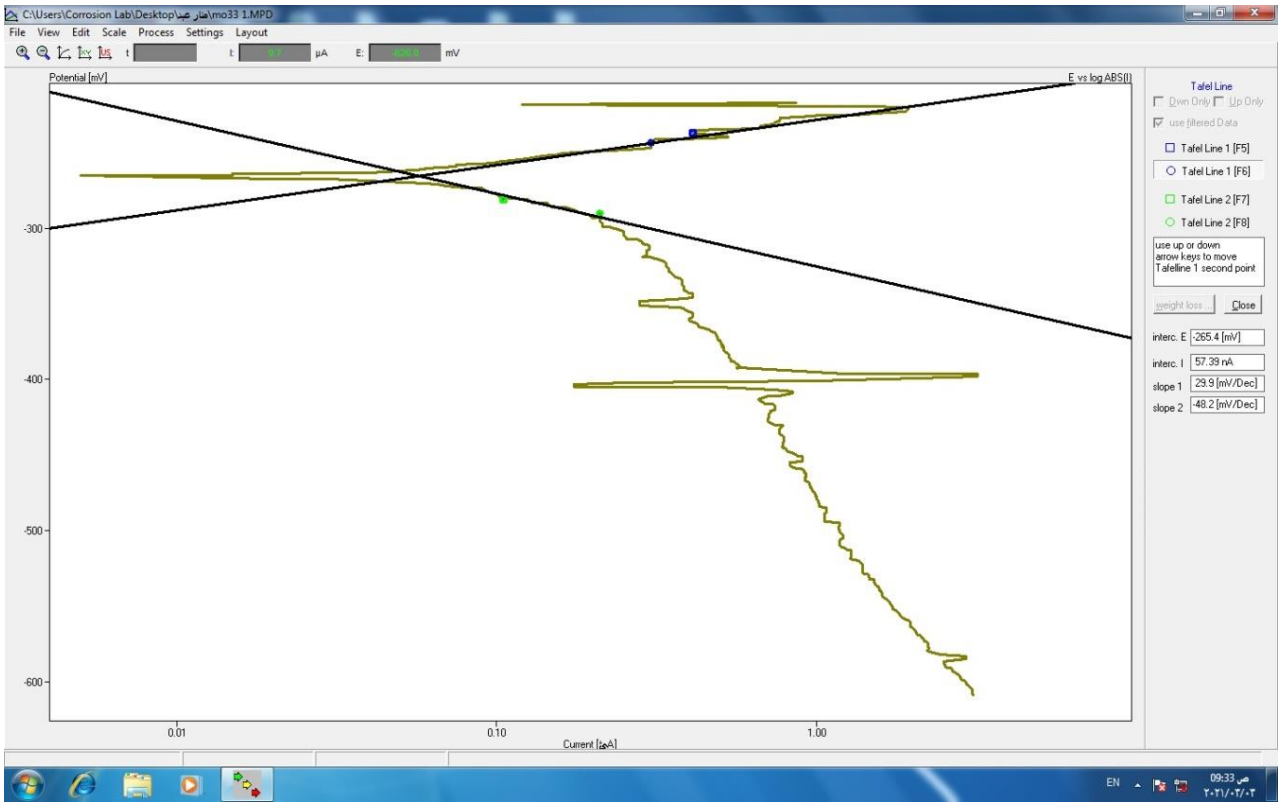

Fighar15: Potentiodynamic Polarization for Ti-15Mo.

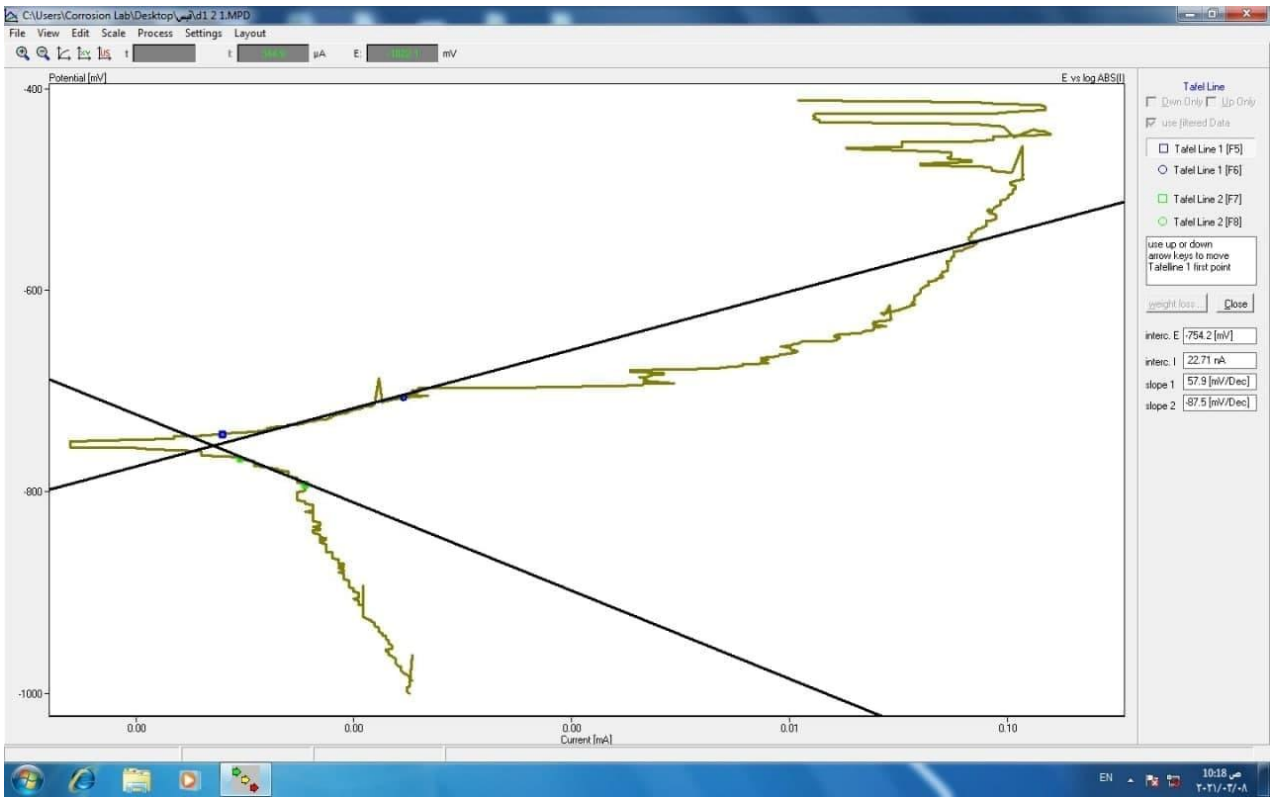

Fighar16: Potentiodynamic Polarization for Ti-8Mo-4Nb-2Zr.

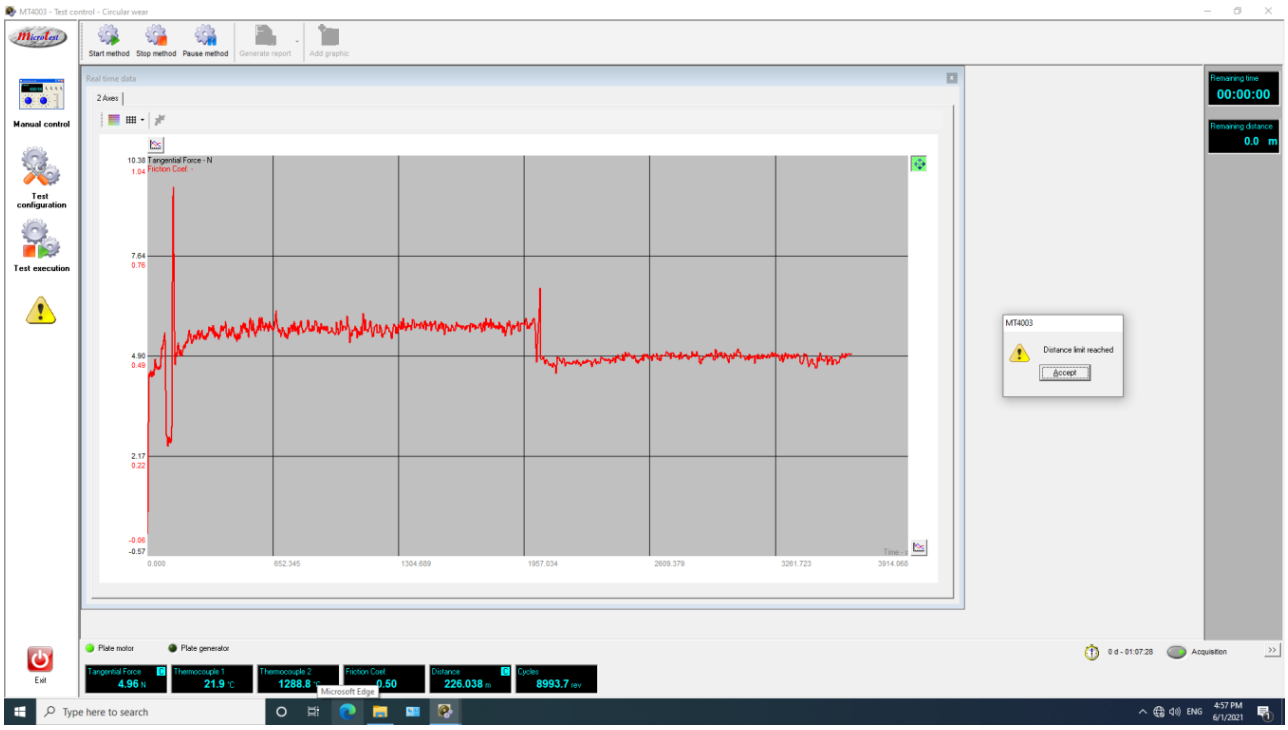

Fighar17: Lubricated sliding friction for CP-Ti alloy at 10N.

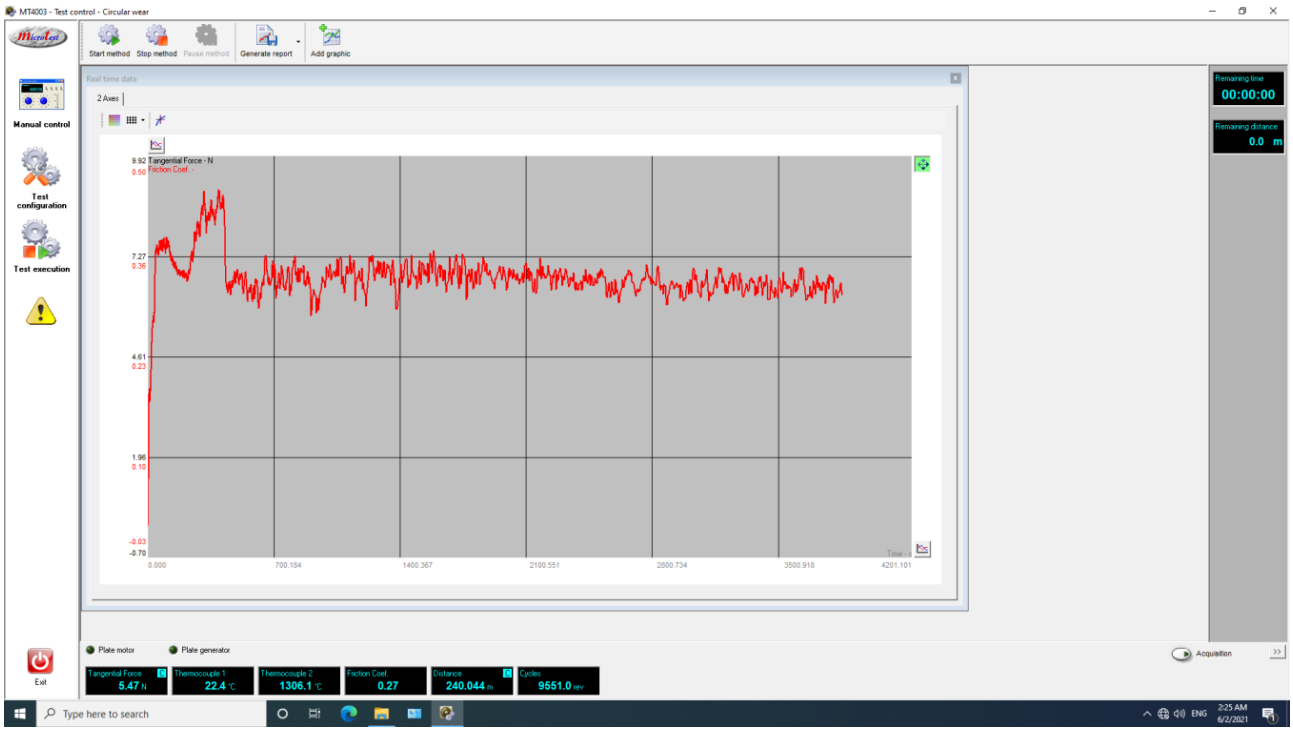

Fighar18: Lubricated sliding friction for CP-Ti alloy at 20N.

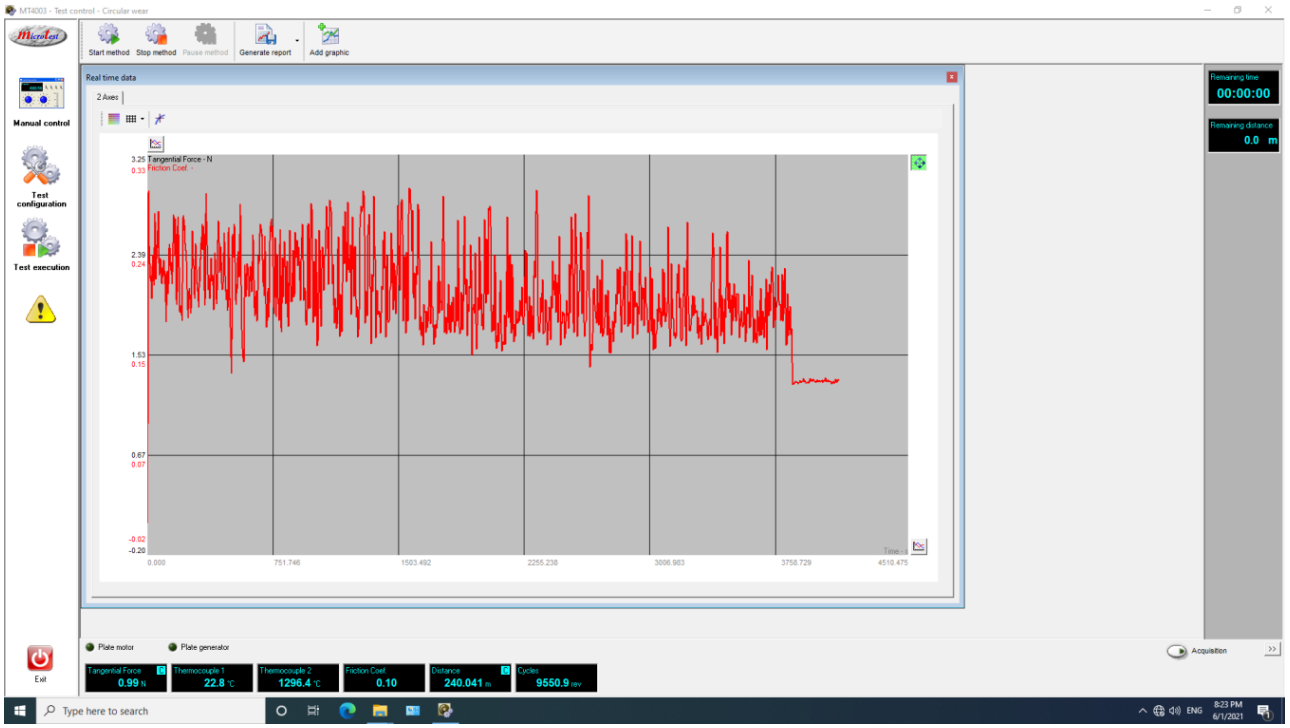

Fighar19: Lubricated sliding friction for Ti-6Al-4V alloy at 10N.

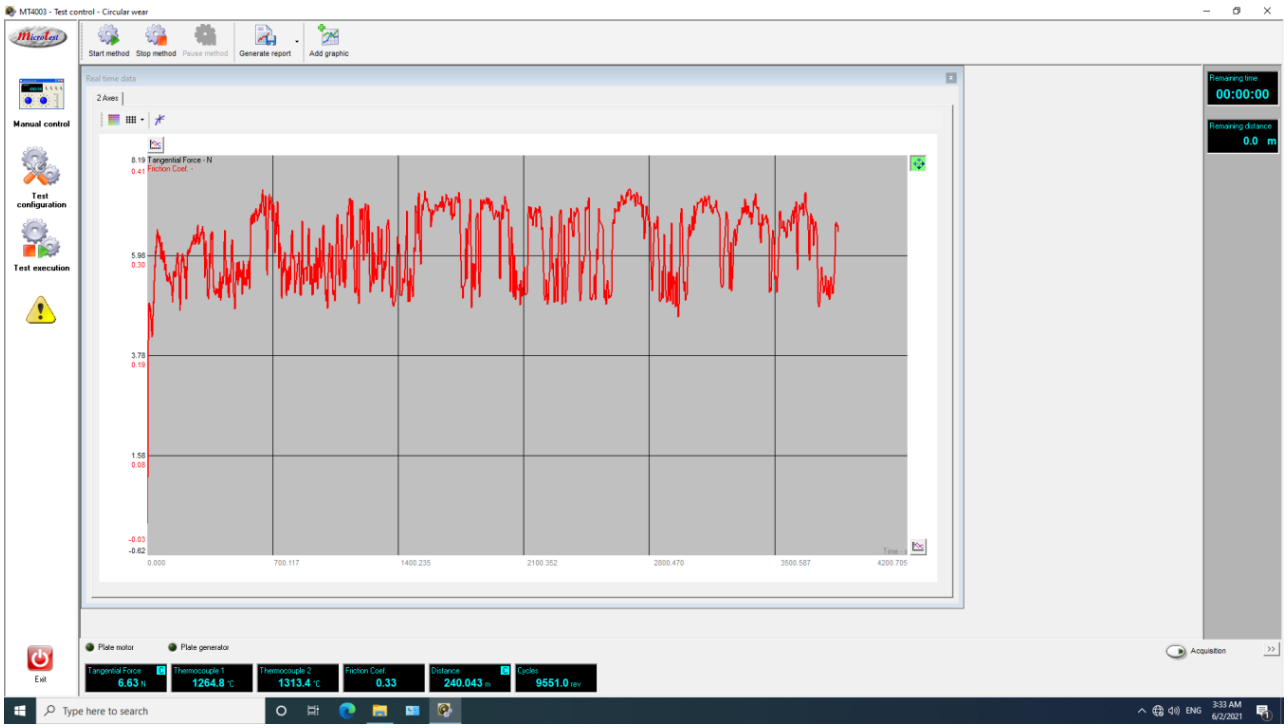

Fighar20: Lubricated sliding friction for Ti-6Al-4V alloy at 20N.

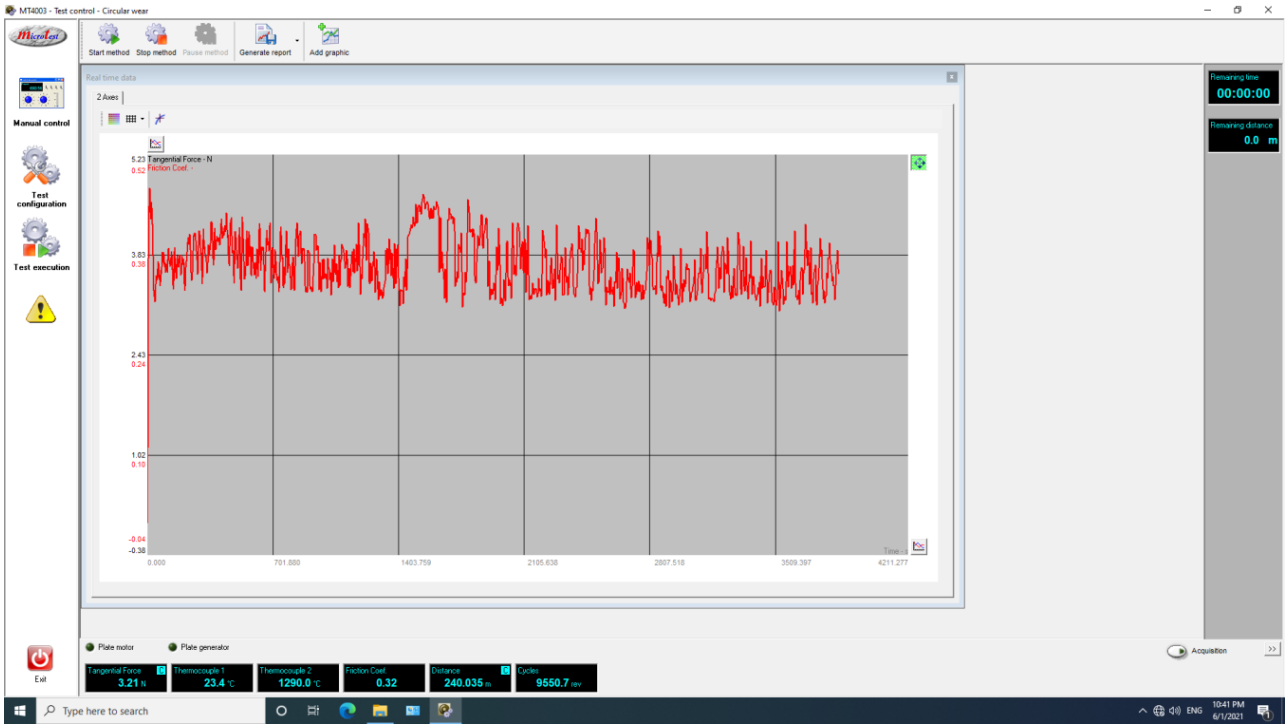

Fighar21: Lubricated sliding friction for Ti-13Zr-13Nb alloy at 10N.

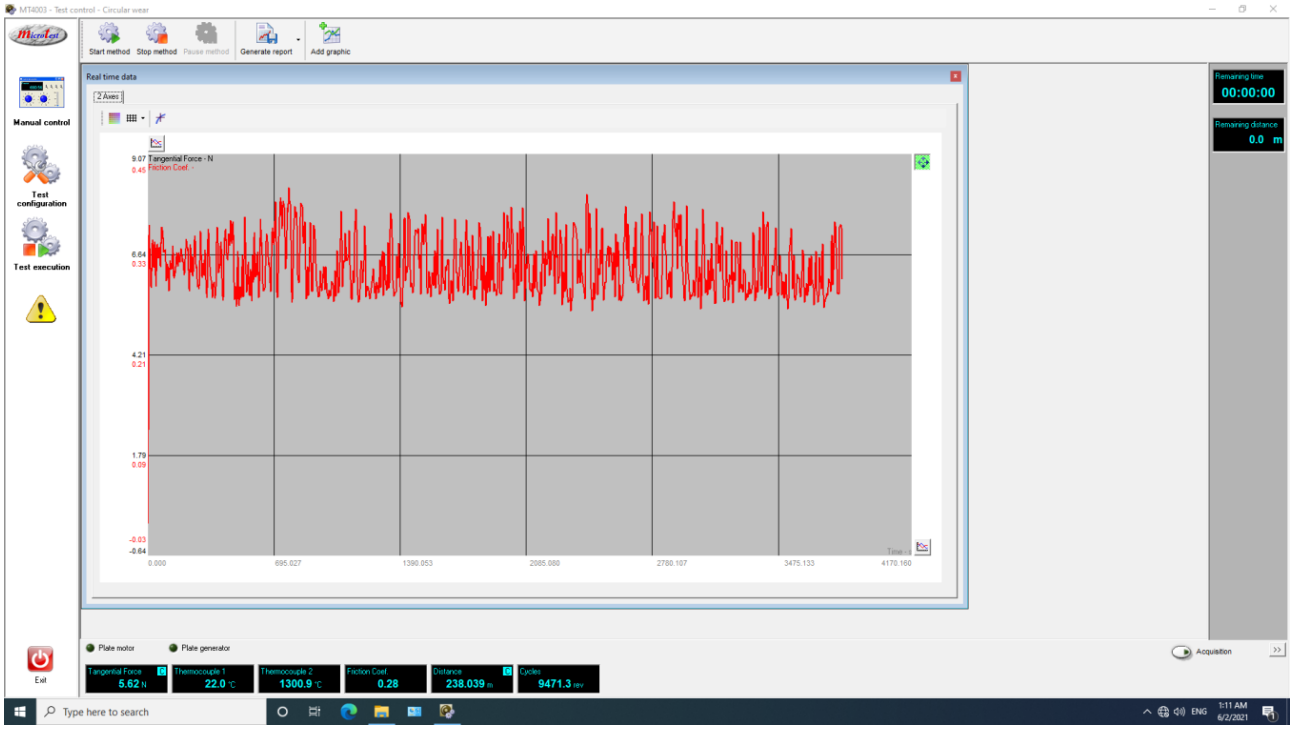

Fighar22: Lubricated sliding friction for Ti-13Zr-13Nb alloy at 20N.

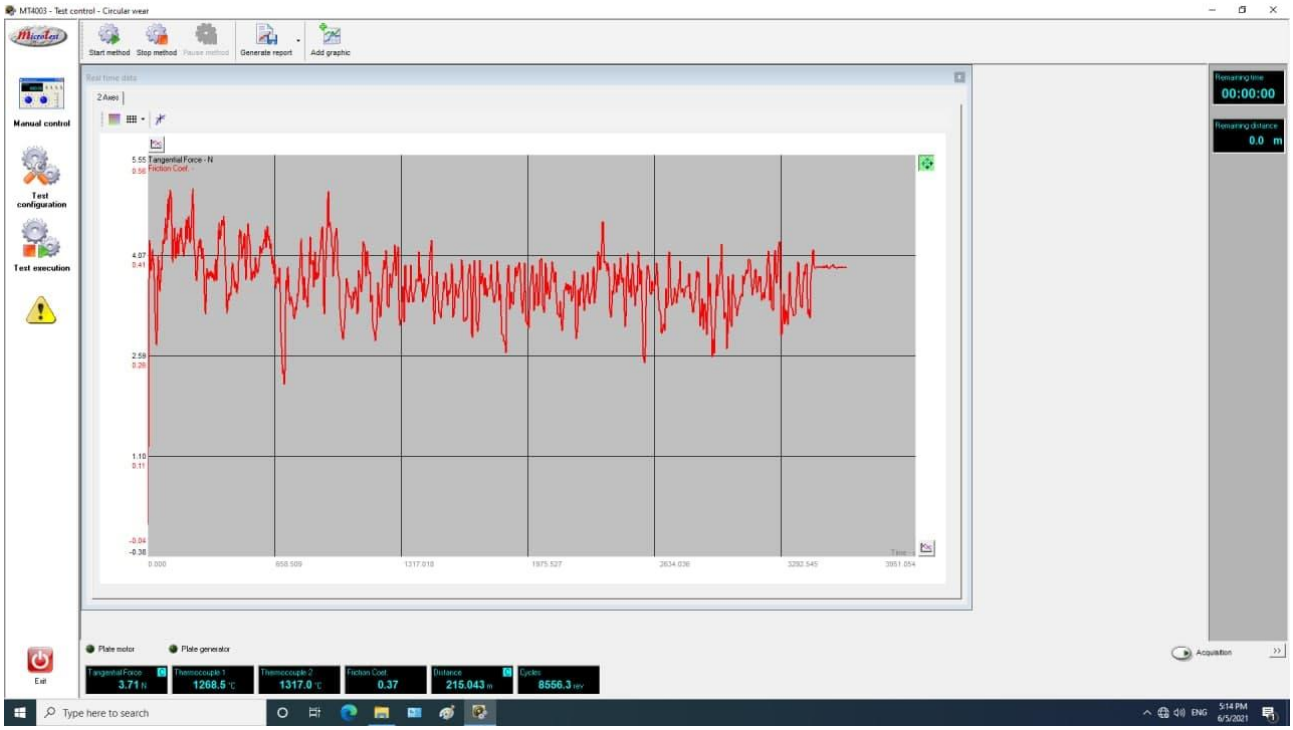

Fighar23: Lubricated sliding friction for Ti-15Mo alloy at 10N.

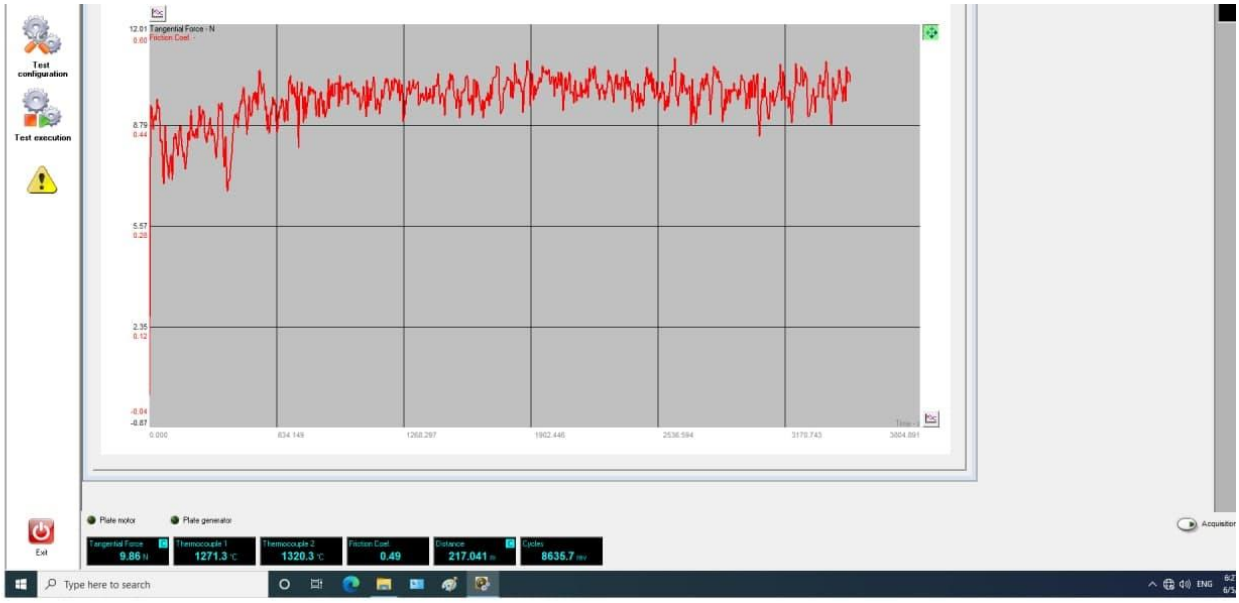

Fighar24: Lubricated sliding friction for Ti-15Mo alloy at 20N.

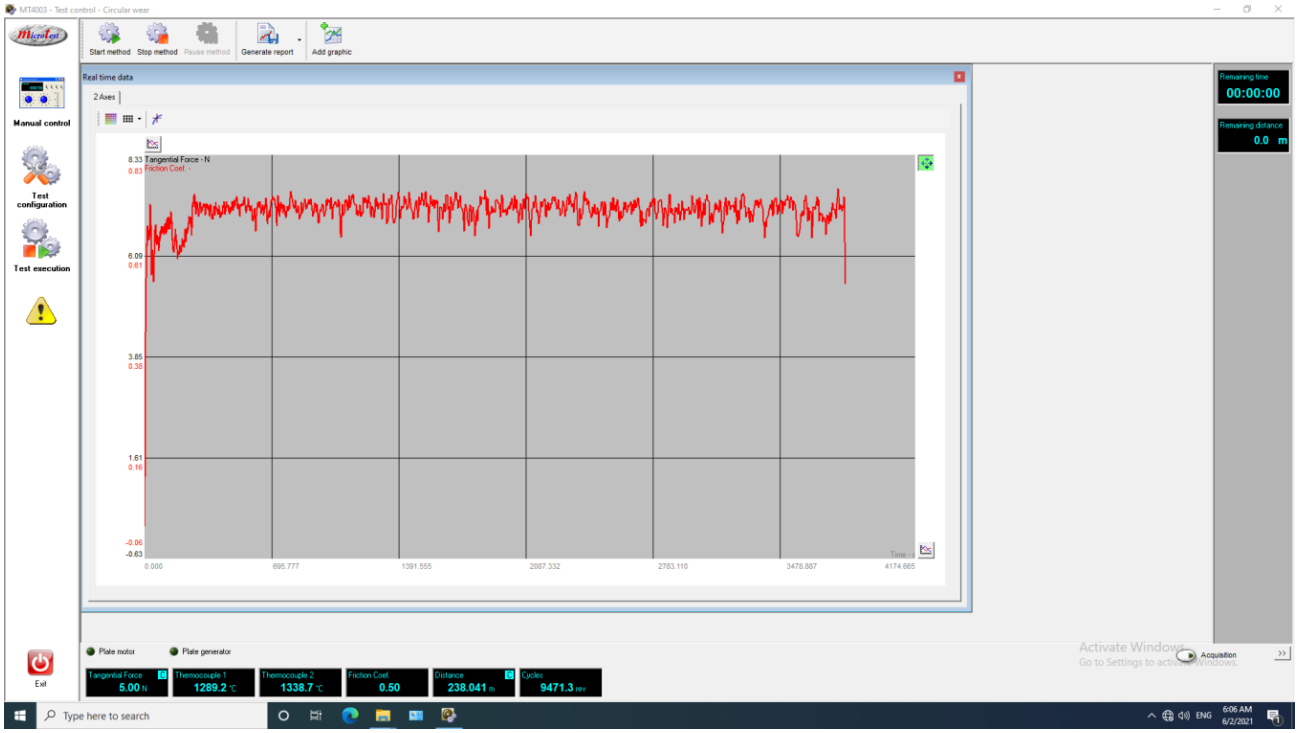

Fighar25: Lubricated sliding friction for Ti-8Mo-4Nb-2Zr alloy at 10N.

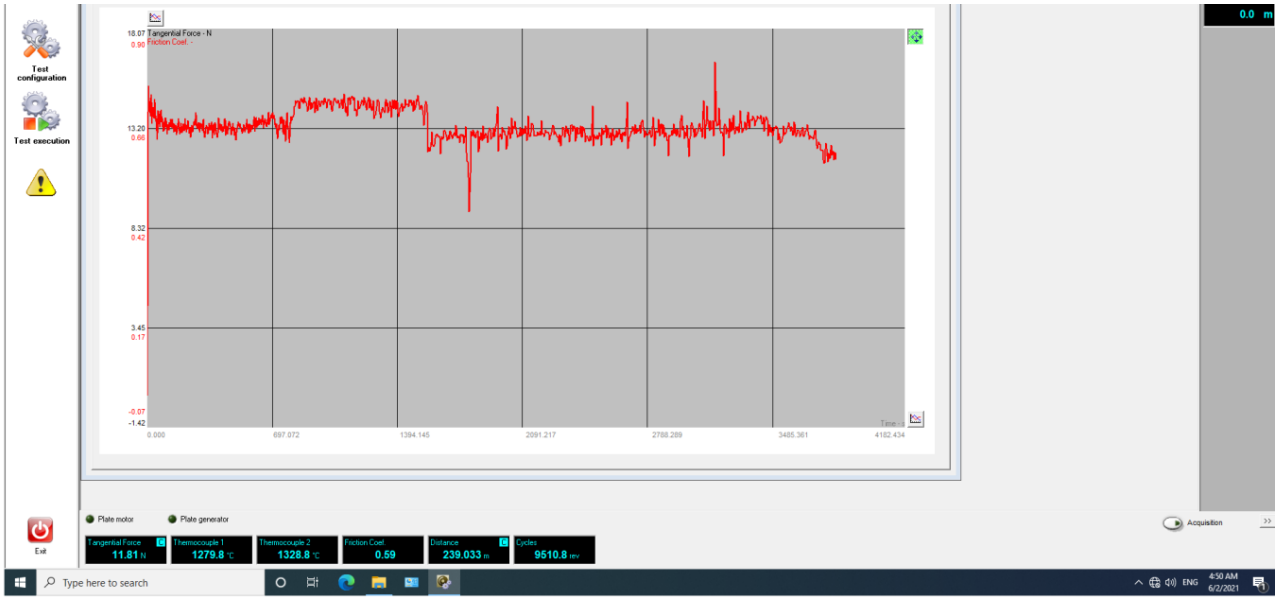

Fighar26: Lubricated sliding friction for Ti-8Mo-4Nb-2Zr alloy at 20N.

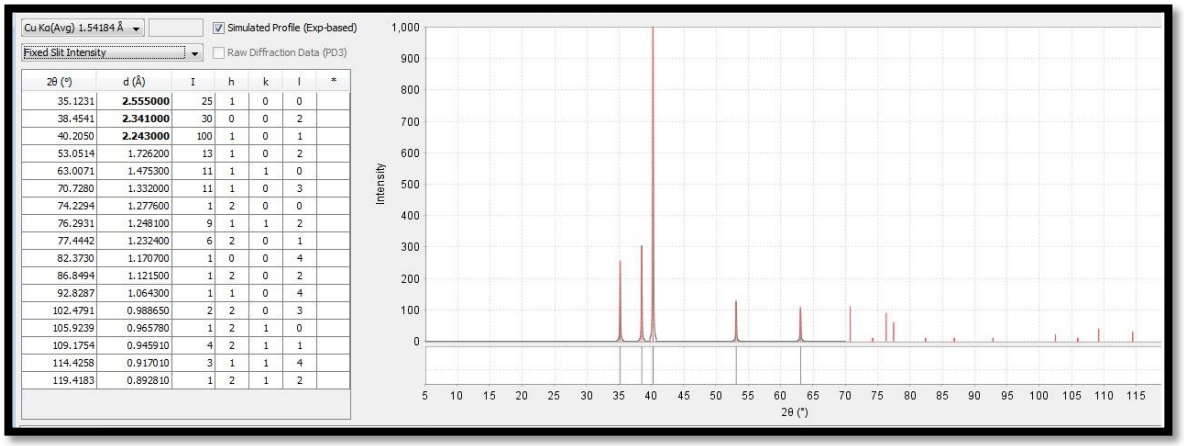

2θ (°)	d (Å)	I	h	k	l	*
35.1231	**2.555000**	25	1	0	0	
38.4541	**2.341000**	30	0	0	2	
40.2050	**2.243000**	100	1	0	1	
53.0514	1.726200	13	1	0	2	
63.0071	1.475300	11	1	1	0	
70.7280	1.332000	11	1	0	3	
74.2294	1.277600	1	2	0	0	
76.2931	1.248100	9	1	1	2	
77.4442	1.232400	6	2	0	1	
82.3730	1.170700	1	0	0	4	
86.8494	1.121500	1	2	0	2	
92.8287	1.064300	1	1	0	4	
102.4791	0.988650	2	2	0	3	
105.9239	0.965780	1	2	1	0	
109.1754	0.945910	4	2	1	1	
114.4258	0.917010	3	1	1	4	
119.4183	0.892810	1	2	1	2	

Fighar27: XRD Card for Compound α

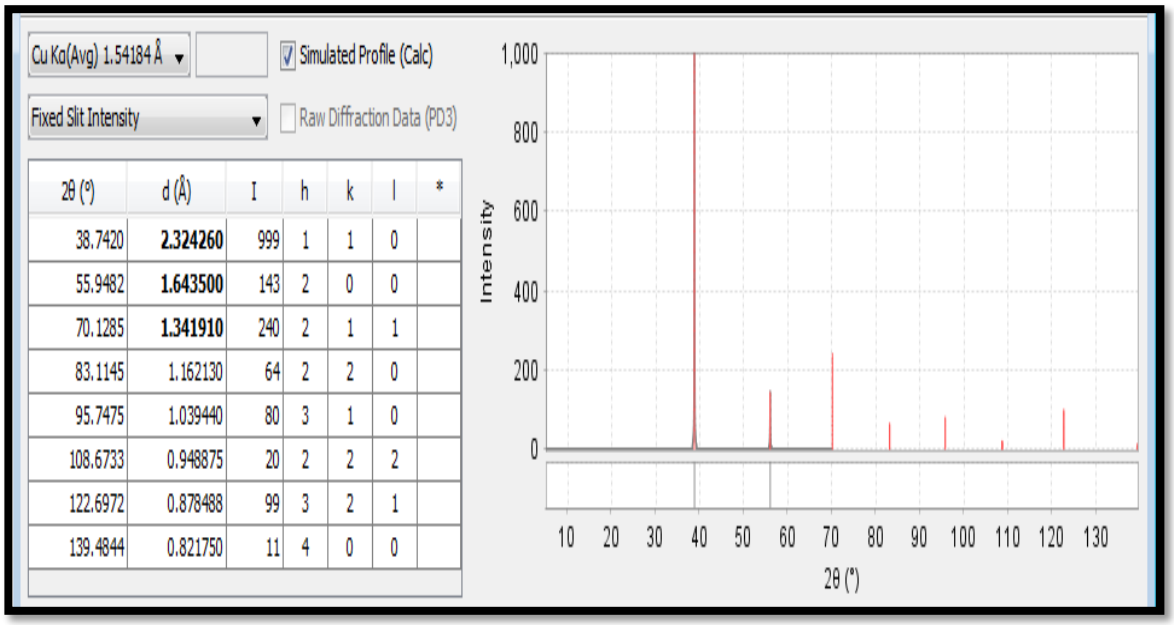

Fighar28: XRD Card for Compound β

Ministry of Higher Education and Scientific Research
Wasit University / College of Science

No: ICCPT/1/37
Date: 23/06/2021

Acceptance Letter

To: Zuheir Talib Khulief, Manar. Abdulameer. H

We delight to inform you that your manuscript entitled "Corrosion Behavior of Different Types titanium alloys for Biomedical Applications" has been accepted for participation in the First International Conference of Chemistry and Petrochemical Techniques (ICCPT) which is organized by chemistry department, college of science, Wasit university, Iraq and will be held virtually in June 26-27, 2021. The accepted manuscripts will be published in the AIP conference proceedings.

Your sincerely

Dr. Alaa Hani Alminshid
Chairman of ICCPT 2021
+9647700999557
a.hani@uowasit.edu.iq

الخلاصة :

هذه الدراسة تهدف بشكل اساسي الى دراسة البنية المجهرية والخصائص الكهروكيميائية والخصائص الترايبولوجية لسبائك التيتانيوم من الجيل الثاني. تم استخدام ثلاثة سبائك تيتانيوم الجيل الثاني : سبيكة Ti–13Zr–13Nb الغنية بالطور بيتاβ وسبيكة Ti–15Mo ذات الطور بيتا غير المستقر وسبيكة Ti–8Mo–4Nb–2Zr ذات الطور بيتا β بالكامل . وللمقارنة تم استخدام سبيكة Cp–Ti ذات طور الفا α و سبيكة تيتانيوم الجيل الاول Ti–6Al–4V ذات طور الفا وبيتا (α+β).

تم تصنيف مورفلوجية السطح والخواص الميكانيكة لسبائك التيتانيوم المستخدمة بواسطة المجهر الالكتروني الماسح FESEM , وحيود الاشعة السينية XRD , والمجهر الضوئي OM لفحص البنى المجهرية , وقد اجريت فحوصات الصلادة ومعامل المرونة لغرض الحصول على الخواص الميكانيكية لكل سبيكة ومن خلال فحوصات البنى المجهرية اتضح ان سبيكة Cp–Ti تحتوي بالكامل على طور الفا α, وان سبيكة Ti–6Al–4V تحتوي على طوري αو β, وسبيكة Ti–13Zr–13Nb غنية بالطور بيتاβ و سبيكة Ti–15Mo تحتوي على طور بيتاβ غير المستقر, اما سبيكة Ti–8Mo–4Nb–2Zr تحوي بالكامل على طور بيتا β, ومن خلال الفحوصات الميكانيكة اتضح ان السبيكة Ti–8Mo–4Nb–2Zr لديها اقل معامل مرونة واعلى صلادة بينما اظهرت سبيكة Ti–6Al–4V اعلى معامل مرونة واظهرت سبيكة Cp–Ti اقل صلادة.

تم دراسة السلوك الكهروكيميائي لجميع السبائك المستخدمة في هذه الدراسة عند درجة حرارة 37° سيليزية في محلول رينجر . في البداية تم قياس جهد الدائرة المفتوحة (OCP) قبل اختبارات التآكل .تم استدام الاستقطاب الداينمكي الفعال للتحقق من سلوك التآكل في السبائك بالإضافة الى ذلك تم استخدام اختبار الايونات المتحررة من كل سبيكة اثناء غمرها في محلول رينجر لمدة 30يوم , وذلك لقياس الايونات المتحررة . تم اثبات ان سبيكة Ti–8Mo–4Nb–2Zr الجيل الثاني ذات الطور بيتا β تحتوي على اعلى مقاومة تآكل من بين السبائك الاخرى .

تم اجراء فحص السلوك الترايبولوجي لجميع سبائك التيتانيوم المستخدمة في هذه الدراسة في محلول رينجر في درجة حرارة الغرفة عند الاحمال 10نيوتن و 20 نيوتن , بشكل عام تم ازدياد حجم التآكل الذي تم ازالته وزاد معامل الاحتكاك مع زيادة الحمل المسلط من 10نيوتن الى 20 نيوتن. ومع ذلك فان إزاله طبقه الأوكسيد الحاميه / أعاده تكوين طبقه الأوكسيد الحاميه, اثر على السلوك الترايبولوجي للسبائك. اظهرت السبيكة Ti–8Mo–4Nb–2Zr انخفاضا في حجم البلى الذي تم ازالته مع زيادة الحمل المسلط من 10 نيوتن الى 20نيوتن , واظهرت سبيكة Ti–6Al–4V اقل حجم بلى مزال واقل معامل احتكاك مقارنة بالسبائك الاخرى, ومع ذلك بالنظر الى التطبيقات الطبية الحيوية يمكن ان تكون سبيكة Ti–8Mo–4Nb–2Zr الجيل الثاني ذات الطور بيتا مرشحا جيدا مع مقاومة تآكل جيدة نسبيا ومعامل مرونة منفض وسلوك بلى قابل للمقارنة وبعناصر سبك غير سامة.

جمـهـــوريـــــة الـــــــعـراق
وزارة التعليم العالي والبحث العلمي
جـامـــــعـــــة بـــابـــــــل
كـلـيـــــة هـنـدســـة الـمـواد
قـســـم هـنـدســـة الـمـعـادن

تقصي سلوك التآكل والبلى لسبائك الجيل الاول والجيل الثاني لتيتانيوم المواد الحيوية

رســـالة
مقدمة الى قسم هندسة المعادن في كلية هندسة المواد/جامعة بابل كجزء من متطلبات نيل درجة الماجستير في هندسة المواد / المعادن

من قبل
منـــــار عبـد الاميـر حسين حسن

بإشراف
ا.م.د. زهير طالب خليف

1443هـ **2022م**